Development of a Software procedure for Curved Layered Fused Deposition Modelling (CLFDM)

Bin Huang

Master in Engineering

2009

Development of a Software procedure for Curved Layered Fused Deposition Modelling (CLFDM)

Bin Huang

A thesis submitted to

Auckland University of Technology

in partial fulfilment of the requirement for the degree of
Master in Engineering (ME)

May 2009

School of Engineering

Under the supervision of:

Dr. Sarat Singamneni

Prof. Olaf Diegel

Dr. Guy Littlefair

Contents

Abstract

Fused Deposition Modelling (FDM) is one of the most widely used Rapid Prototyping processes that uses the technique of depositing a semi-solid material in layers to build up a part and finds application in a variety of situations, be it making a mould for the rapid production of an industrial tool or the production of models for preoperative planning of complex cranial reconstructive surgery. When it comes to directly producing the end products, the process is still in its infancy, using inferior materials and flat layer deposition, bringing forth shortcomings such as poor surface quality, low strength for curved parts, and undesirably higher number of layers.

Some of these shortcomings can be overcome if material deposition is modelled in curved layers as against the traditional flat-layer slicing and deposition. While the stair case effect can be significantly minimized, mechanical properties of the parts will also be enhanced due to continuity in fibres and the elimination of the inherent weakness between laminations. However, this being a fairly new idea, there are no existing facilities for practically implementing and experimentally testing this concept of Curved Layered Fused Deposition Modeling (CLFDM). The current research is to develop both hardware and software systems to build a working FDM system and implement CLFDM.

The project involves the construction of an FDM system and then development of mathematical models for curved slicing. The numerical data generated from curved slicing algorithms is integrated with the hardware system for the practical implementation of CLFDM. Efficient

curved slicing algorithms are developed and successfully used on the FDM system built for the practical implementation of CLFDM. Several case studies involving geometrical complications of increasing complexities have been successfully modelled and physically produced using CLFDM.

Acknowledgements

I would like to express my profound gratitude to the primary supervisor, Dr. Sarat Singamneni, for his valuable support, encouragement, supervision and useful suggestions throughout this research work. His moral support and continuous guidance enabled me to complete my work successfully. I am also highly thankful to my second supervisors Prof. Olaf Diegel, Director of the Creative Industries Research Institute at Auckland University of Technology and Dr. Guy Littlefair, Program Leader, School of Engineering, Auckland University of Technology, for their valuable suggestions throughout this study.

I am also grateful for Creative Industries Research Institute and School of Engineering of Auckland University of Technology, for providing me with all the experimental and computational facilities. In particular special thanks are due to the University for funding this research through a Faculty Contestable Grant which provided partial support for me and also allowed the necessary equipment to be procured.

I am as ever, especially indebted to my parents, Mr. Zexi Huang and Mrs. Jiqing Xu for their love and support throughout my life. I am also thankful to Mr. Kevin Huang, Mr. Zhang, Mr. Adrian Law and Ms. Henna He, who guided me about the direction of my study life in New Zealand from the beginning. Moreover, my sincere thanks go to my friends, who shared their love and experiences with me.

Bin Huang

List of abbreviations

BRep: Boundary Representation

BASS: Break Away Support System (BASS)

CW: Clockwise

CCW: Counter-clockwise

CAD: Computer-Aided Design

CAGD: Computer-Aided geometric design

CAM: Computer-Aided Manufacturing

CSG: Constructive Solid Geometry

CLFDM: Curved Layer Fused Deposition Modeling

CLLOM: Curved layer laminated object manufacturing

CLSF: Cutter location Source File

EI: Extra Information

FLFDM: Flat Layer Fused Deposition Modeling

FVCP: Four Vector Cross Product Algorithm

FF: Freeform Fabrication

FDM: Fused deposition modeling

GUI: Graphical User Interface

LOM: Laminated object manufacturing

LENS: Laser Engineered Net Shaping

LM: Layered Manufacturing

MI: Multi-point Interference

MIE: Multipoint Interference elimination

MFVCP: Modified Four Vectors Cross Product Algorithm

NURBS: Non-Uniform Rational B-spline

RP: Rapid Prototyping

SI: Self Intersection

SIEA: Self intersection elimination algorithm

SLA: Stereolithography Apparatus

SLS: Selective Laser Sintering

STL: Stereo Lithography (STL)

TVCP: Two Vector Cross Product Algorithm

VSO: Vertical Surface Offsetting Algorithm

Chapter 1

Introduction

1.1 Freeform Fabrication (FF)

Freeform Fabrication (FF), as also known by another name, Solid Freeform Fabrication, is a general name of techniques for manufacturing solid objects by sequential delivery of energy and/or material to specified points in space to produce the solid part. In other words, it is an adding-materials manufacturing method, unlike the traditional way to cut the materials off. FF is often referred to as Rapid Prototyping, Rapid Manufacturing, Layered Manufacturing and Additive Fabrication. Among those mentioned, Rapid Prototyping is majorly used in the manufacturing industry as a tool to shorten the early design stage.

Rapid Prototyping (RP), 'refers to the layer-by-layer fabrication of three-dimensional physical models directly from a computer-aided design (CAD) model [1]. RP is the automatic construction of physical objects using FF additive fabrication. RP takes the virtual design from CAD or some other animation modeling software, transforms them into thin, horizontal cross-section layers and then stacks those layers together in physical space, one after another until the physical model is completed. The first technique for RP was introduced by Charles W Hull [2], and became available in the late 1980s, and was used in the manufacture of models and prototype parts. Up to date, RP is widely used in every different area apart from industry [3], as shown in Fig 1. 1.

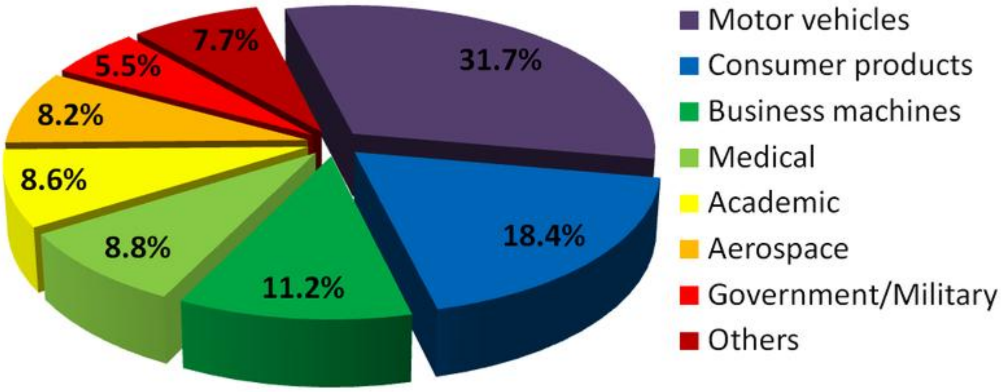

Fig 1. 1 RP applications

The primary advantage of RP is its ability to create almost any shape or geometric features, even those complex shapes that would be virtually impossible to machine. For example, RP can build intricate internal structures, parts inside of parts and very thin-wall features as shown in Fig 1. 2. With additive fabrication, the machine reads in data from a CAD model and lays down successive layers of different materials, and builds up the physical model from a series of layers. Those layers are joined together or fused automatically to create the final shape matching to the CAD model, as shown in Fig 1. 3.

RP also reduces the amount of operation time compared to that required by manually built parts. In contemporary methods of constructing a model, it normally can take from days to weeks, even months, depending on the method used and the size and complexity of the models. RP can produce the models in hours or days, depending on the machine being used and the size and number of models being produced simultaneously.

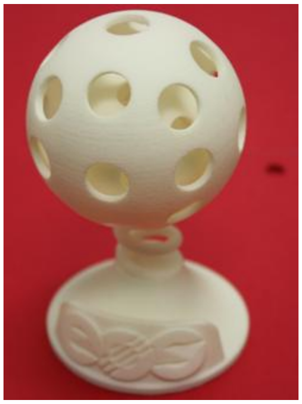

Fig 1. 2 Thin-wall features

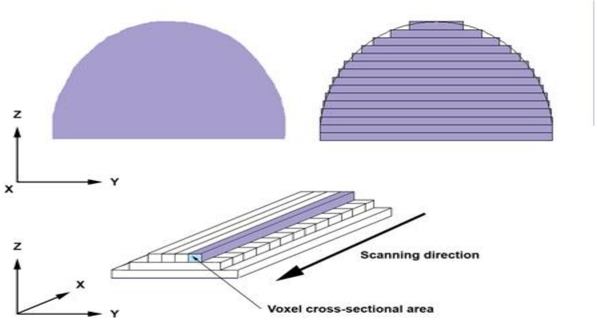

Fig 1. 3 General RP processing (Source: Wikipedia)

With the advent of stronger polymers and even metallic material being used, the advantages of RP are further extended in terms of cost-efficient, component production for not only demonstration purposes but functional prototypes.

Owing to those advantages mentioned and the fact that potential market for using RP is growing, more and more domestic and international companies are involved and getting involved into RP business. Therefore, a large number of advanced RP technologies are available in the market. The major differences are the ways layers are built to create parts. Some of them are melting or softening material to produce the layers (SLS, FDM) whereas others are laying liquid materials thermosets that are cured with laser beams (SLA). Some of the commonly used RP processes are listed in Table 1 and briefly discussed here to present the essentials features of common RP processes:

Table 1.1 Some commercial RP technologies

Prototyping technologies	**Basic materials**
Selective Laser Sintering (SLS)	Thermoplastics, metal powders
Stereolithography (SLA)	Photopolymer
Fused deposition modeling (FDM)	Thermoplastics, eutectic metals
Laminated object manufacturing (LOM)	Paper
Laser Engineered Net Shaping (LENS)	Metal

Selective Laser Sintering (SLS) [4] was developed by The University of Texas and was commercialized by DTM Corporation in 1987. SLS is a RP process that builds the models with varieties of materials using an additive fabrication method. The build materials for SLS come in powder or small particle form and a power laser, for example, carbon dioxide laser, is used to fuse the powder or small particle-like material together and form the final product. SLS has more than 10 different materials that can be used with in the same machine for a wide variety of applications, including polymers, metal and green sand. The SLS process begins with standard STL CAD file format and the STL file is sliced into a couple of thin layers. Then the slicing data and pattern are transformed to the machine and then the machine starts processing. Inside the machine, a thin layer of powder is spread across the build area by a roller from the powder delivery piston. The laser follows the tool path pattern then sinters in a raster sweep motion the cross-sectional area of the parts being built. The fabrication piston then lowers, more powder is deposited. The same processing is repeated till the model is finished, as shown in Fig 1. 4.

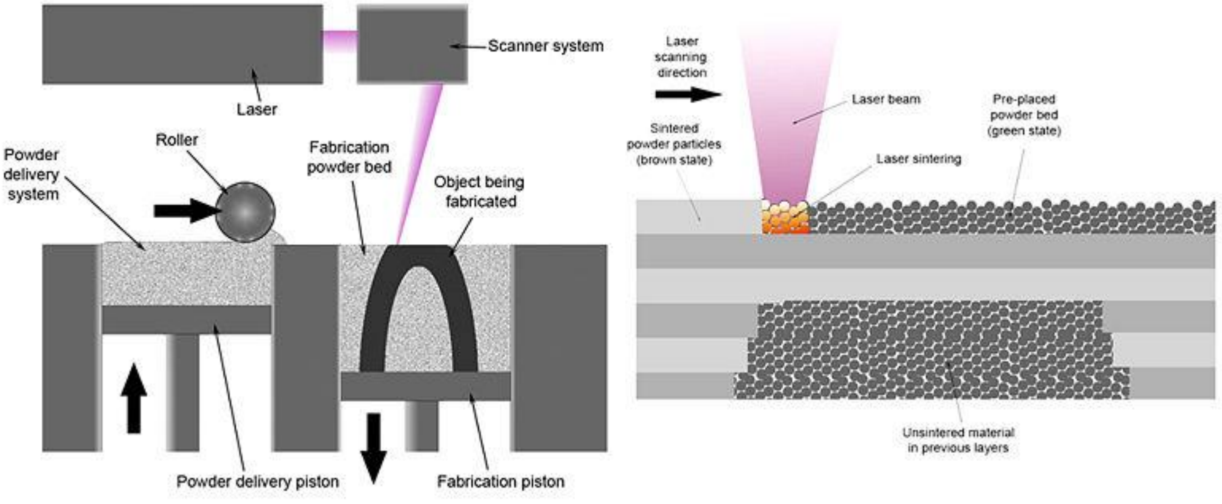

Fig 1. 4 A schematic of SLS Processing (Source: Wikipedia)

Stereolithography (SLA),[5] was the first RP process to reach the market which was introduced by 3D Systems Corporation in 1987. It was the oldest RP system, which builds the models by curing photosensitive resins with a low power laser beam. The process begins with a solid CAD model then turns it into standard STL format file. The STL is oriented into the positive octant of the Cartesian coordinate system, and then is translated up the *z* axis at least 0.25 inches to allow for the building of supports. Then the solid model is also oriented for optimum build, which involves placing complex curvatures in the x and y plane where possible, and rotating for the least *z* height as well as to where the least amount of supports are required. The UV laser light traces tool path pattern of every sliced layer of the model on the surface of the liquid photosensitive resin, curing the resin inside the sliced cross-sectional area down to the desired thickness. After a layer has been done, the SLA's elevator platform lowers down by a single layer thickness. Then, the fresh resin is recoated on the top of the harden layer by a resin-filled blade and the unfinished solid model merge into the resin. This processing continues until the entire solid model is completed. Fig 1. 5 shows the SLA processing.

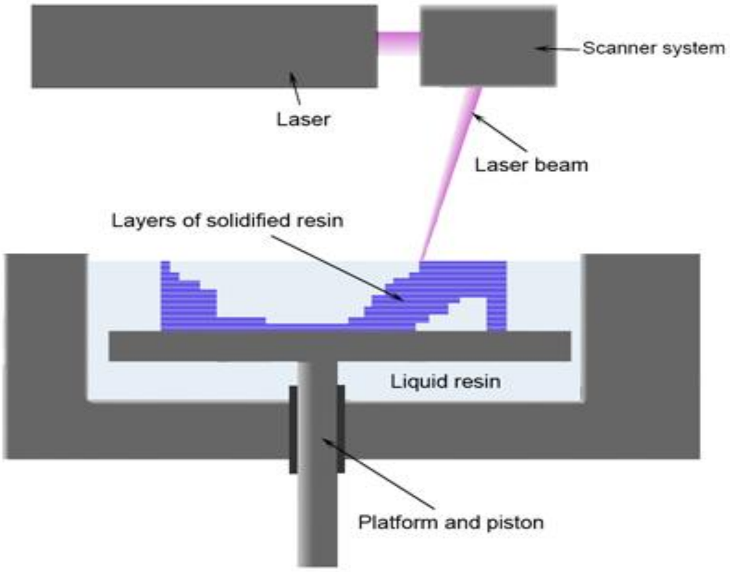

Fig 1. 5 A schematic of SLA Processing (Source: Wikipedia)

Fused Deposition Modeling (FDM) [6], is an extrusion-based rapid prototyping process by using the same additive fabrication process similar to other RP systems. FDM was developed by Stratasys Inc. in the early 1990s as a concept modeling device and now is used for direct production of end-use parts. FDM produces models from wax or plastic using motion control and extrusion nozzle. FDM will be elaborating in the following section.

Laminated Object Manufacturing (LOM)[7] is a RP techinique that produces three-dimensional models with paper, plastic, or composites. LOM was developed by Helisys Corporation. LOM is a hybrid between subtractive and additive processes. It builds up with layers of material cut individually by a laser in the shape of the cross section of the part. As layers are being added, the excess material not required for that cross section is being cut away. Fig 1. 6 shows the schematic of the LOM process. The sheet material supply roll is loaded onto the feed spindle in the bottom of the machine and the sheet material is threaded around rollers, across the platen and then back down to the take-up spindle. The material spindles turn to move new sheet material across the build plate. The build plate is lifted up until it touches the laminating roller. The roller rolls along the surface of the paper, activating the adhesive backing while simultaneously applying the downward pressure. Then the lens traces the outline of the current cross section of the part, directing the laser to cut through only that sheet material in the desired shape. After the layer is done, the old sheet material is removed and the new sheet material is brought in. The same process is repeated until the part is built.

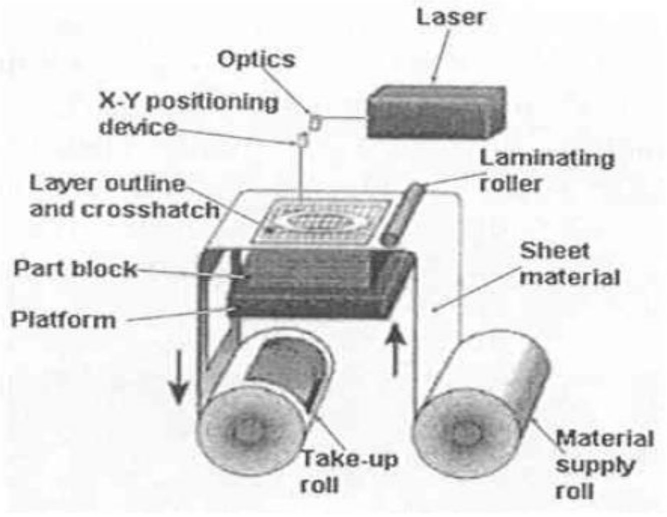

Fig 1. 6 A schematic of LOM Processing

Laser Engineered Net Shaping (LENS) [8] is the first direct-metal rapid prototyping system. Its finish parts are full strength metals. LENS was developed by Sandia National Laboratories and various industry members on Cooperative Research and Development Agreement and it was commercialized by Optomec Design Co. Like other RP processes, the LENS system uses a layered approach to manufacturing components. The STL file is sliced into horizontal cross sections and the machine builds the model from the bottom slice upwards. Metal powder is injected from feeder tubes into the focal point of a high power laser and the laser beam fuses the powder into the layer and builds models. The whole deposition device moves across the machining area following the sliced pattern and builds the layer. After one layer is built, the deposition device moves upward a layer thickness and starts working on the next layer. The same process repeats until the entire part is completed. Fig 1. 7 shows the schematic of the LENS process.

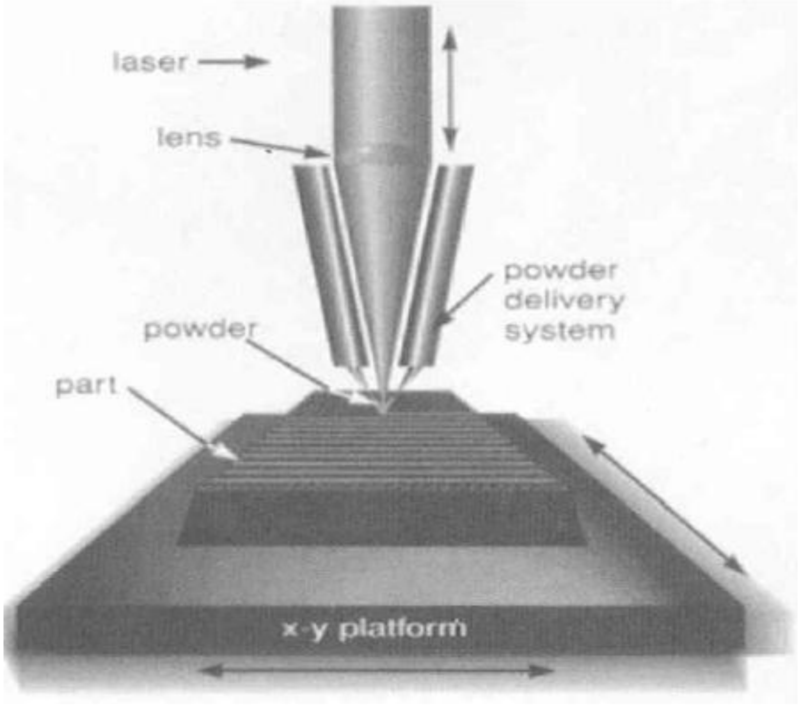

Fig 1. 7 A schematic of LENS Processing

There are some more RP technologies existing in the world, which are similar to those mentioned above but with different materials and processes. Among these, FDM is one of the most important and successful RP technology available in the market. This being the process investigated for improvement in the current research, some important aspects of the process are presented in the following section

1.2 Fused Deposition Modeling

Fused Deposition Modeling (FDM) is one of the RP technologies using an extrusion method, which is also the core technology in this project. It was developed by S. Scott Crump [9] in late 1980s and commercialized in 1990. Like other RP processing, FDM mostly utilizes the STL data as its input and works on a layer-by-layer principle. Inside a temperature-controlled chamber, a plastic filament or other metal wire is unwound from a coil and feed material to an extrusion nozzle. The nozzle with heating element is heated to melt the material, traces the slice pattern and places down the soften filament to where they are required and cling the previous layers together. Then the worktable is dropped down one step, the deposition processing is repeated until the model is completed as shown in Fig 1. 8.

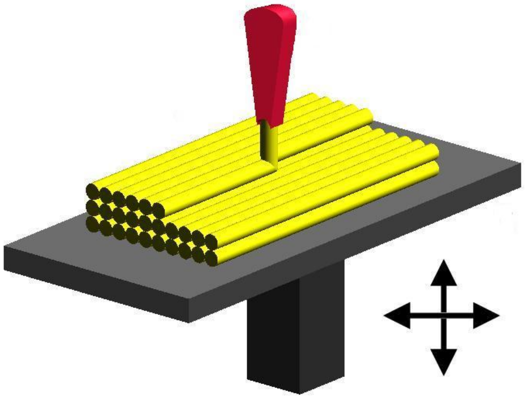

Fig 1. 8 A schematic of FDM Processing (Source: Wikipedia)

The core component of FDM is the nozzle head. The nozzle head is a movable unit in both horizontal (x and y) axis directions, and controlled by a numerically controlled system embedded in the FDM machine, whereas the worktable works in the vertical direction (z direction).

The schematic [6] of components in the extrusion head is shown in Fig 1. 9. The extrusion head is constituted with Drive Blocks, Heating Chamber and Tips. The Drive Blocks are the raw-material feeding mechanisms, which consist of two wheels and are mounted on the back of the head. They are controlled by computer and capable of loading and unloading the filament precisely. The Heating Chamber is a tube wrapped in the heating element and blend in 90-degree. It is used to change the direction of the filament flow from horizontal to vertically downward and serve as a melting area for the material, which is the major function. The tips are externally threaded and screwed up into the heating chamber outlets. They are used to reduce the extruded filament diameter for better finishing details and making the model with higher accuracies.

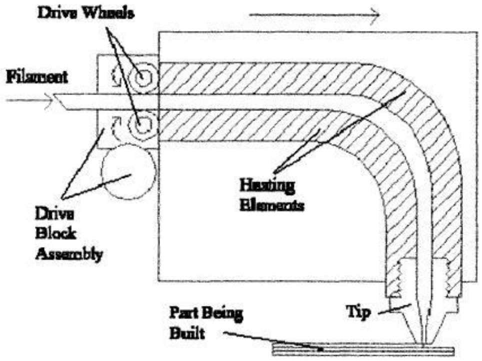

Fig 1. 9 A schematic of the Extrusion Head

Owing to the specific design of the nozzle head, the materials harden immediately after extrusion from the nozzle and models or parts are created by extruding the filament of thermoplastic materials to build the layers. Fig 1. 10 shows some parts built of ABS by FDM. Apart from the nozzle head, the temperature-controlled chamber also plays an important role in FDM processing, which offers a stable temperature environment during the processing.

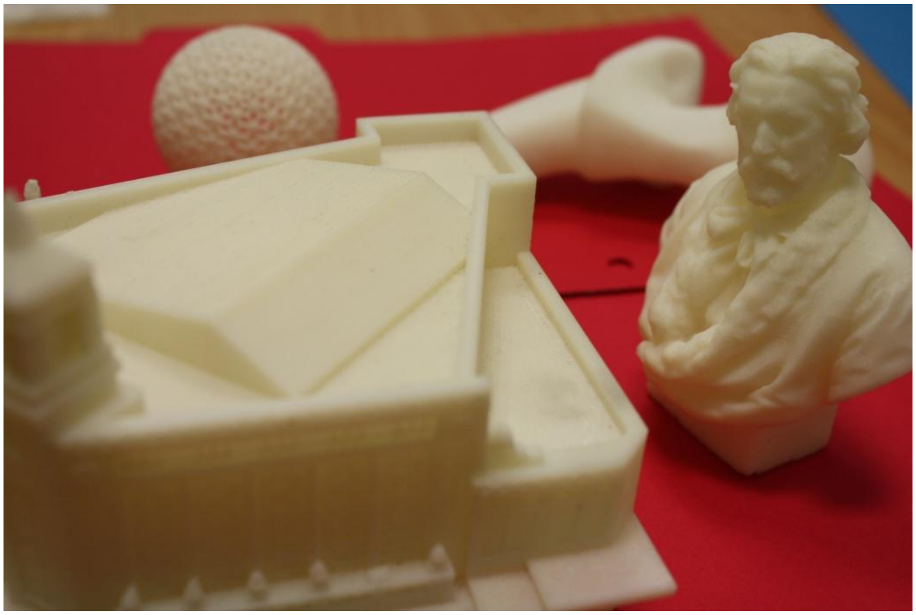

Fig 1. 10 FDM parts

The FDM machines have the capability to build parts with four different materials: Investment-casting wax (ICW06), ABS (P400), Medical Grade ABS (P500) and Elastomer (E20). Because of the high performance material properties, the FDM parts and models can be used in Concept/Design Visualization, Investment Casting and Medical Applications and production of end use parts.

The post processing of FDM parts is usually one of the easiest in RP post processing. Unlike SLA and 3DP, which need to have a heat treatment or LOM and LENS that need to cut the support material from the bottom, FDM features the Break Away Support System (BASS), which allows the support material to be peeled away easily by hand with a knife or pliers. The parts only require very little finishing before they are ready for the applications.

In terms of applications, the RP machines using FDM technology are available in the commercial market. The FORTUS 3D Production Systems Series, which is made by STRATASYS, is one of those machines popular in the world. This series of FDM machines are the “high-end” RP machines, including FORTUS 200mc, FORTUS 360mc, FORTUS 400mc and FORTUS 900mc, as shown in Fig 1. 11. These FDM machines have the highest performance capable of producing parts and models with the largest range of thermoplastic materials. They also provide the products more feature details, better surface finish and more accuracy, for instance, the latest FORTUS 900mc can produce the part up to 0.003 inch (0.0762 mm) in accuracy and 0.013 inch (0.3302 mm) in multiple layer thickness [10]. The FDM machines use production-grade thermoplastic material, such as ABS, ABSi, PPSF and PC, including PC-ABS. The FDM parts made of those materials can withstand functional testing and have high heat resistance. Unlike other RP technologies using powders or resins to simulate the thermoplastics, the FDM parts and models are produced with real thermoplastics and more versatile. They can be sanded, painted, drilled and so on. For example, Bell Helicopter used FDM machine to build the tough PC wiring conducts for the Osprey’s twin vertical stabilizers for on-the-ground testing.

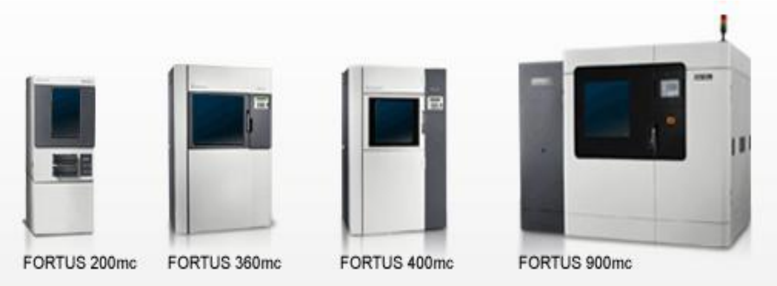

Fig 1. 11 FDM machines (Source: Stratasys Brochures)

The strength and temperature capability of the build material is the major advantage of FDM. Other advantages of FDM are safe, laser-free operation and easy post processing with the water-soluble support material. However, there are still certain shortcomings that are inherent with the FDM process.

1.3 Specific shortcomings

In FDM processing, Layered Manufacturing (LM) technology, which uses STL format files as its input data, is employed where a part is built by stacking multiple flat layers of materials. LM technology not only brings advantages to FDM process, but also unavoidable shortcomings.

"Stair-step" effect [11], is the main shortcoming of all the RP processes, particularly in FDM. It is caused by the LM technology using horizontal flat layers and the part orientation during the deposition. The faceted STL model is sliced with certain of horizontal planes, and the contour of each layer is generated. The RP machine tool, no matter whether they use a laser or a deposition head, traces the slicing pattern and builds the physical part in thin layers, which exhibit a "stair-step" effect, as shown in Fig 1. 12, and such effect becomes more obvious on curved surfaces and particularly when using the thicker layers.

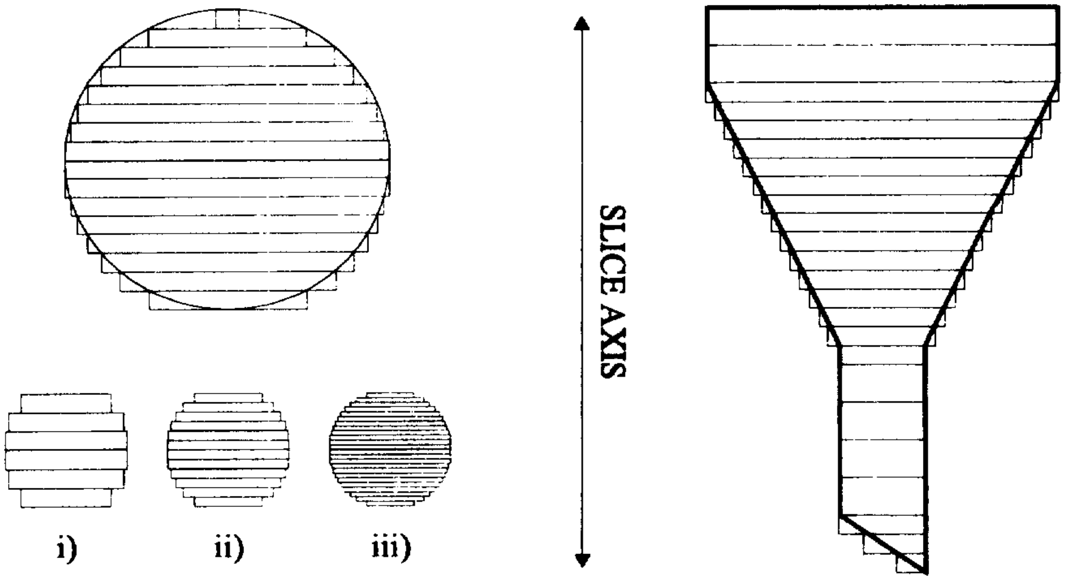

Fig 1. 12 The "stair-step" effect phenomenon

Too many layers and high time consumption to process are other shortcomings of FDM. More accuracy and higher resolution are always one of the important requirements of the RP part. To achieve the required accuracy and resolution, more layers are needed [12]. In order to build the part more accurately, the number of layers needs to be increased, whereas the thickness is reduced as shown in Fig 1. 13. However, this solution also increases the part build time, often to an unacceptable level.

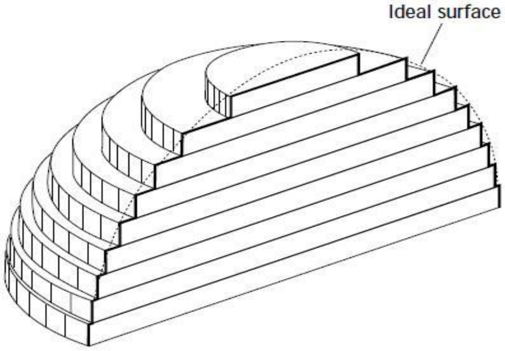

Fig 1. 13 Thin build Layers better complex surface

The anisotropy property of the final part also is a shortcoming of FDM [13]. Strength of FDM parts suffers from anisotropy and adhesive strength between layers or across filaments is weaker than the strength of continuous filaments. The air gap and raster orientation affect the tensile strength of FDM parts dramatically. In some particular cases, for example, the thin shell components, the discontinuing filament deteriorates the anisotropy phenomenon, which causes part failure as shown Fig 1. 14 [13].

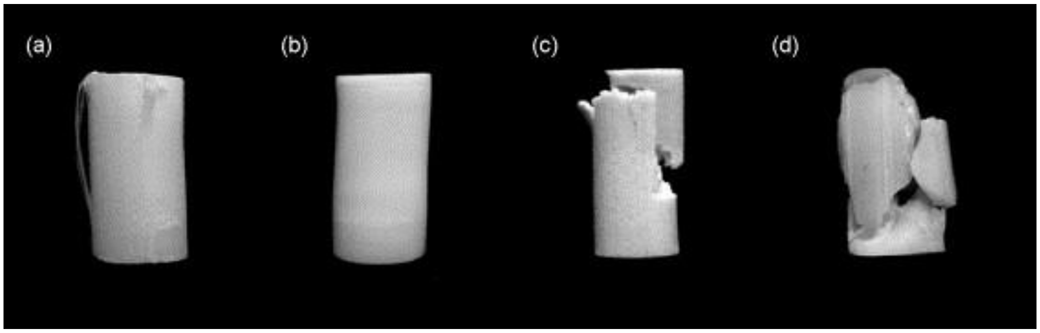

Fig 1. 14 Failure modes of the specimens: (a) FDM-axial (b) FDM-transverse (c) 3D printer-axial (d) NCDS-axial

These are some of the drawbacks that typical FDM parts suffer from. There has been research effort in different directions, attempting improvements in materials as well as deposition techniques.

1.4 Literature review

In the FDM processing, layer thickness, road width and speed are three significant parameters influencing the form and surfaces quality of prototypes [14]. It is found that the layer thickness is effective to 49.37% at 95% level of significance without pooling and the layer thickness is effective to 51.57% at 99% level of significance with pooling. The other factors, road with and speed, contribute to 15.57% and 15.83% at 99% level of significance respectively.

Several attempts have been made quantifying the several requirements of FDM. Choi et al [15] proposed a Virtual Reality system for modeling and optimization of RP processes. This system aims to reduce the manufacturing risks of prototypes early in a product development cycle, and hence reduces the number of costly design-build-test cycles. It involves modeling and simulation of RP in a virtual system, which facilitates measures of part quality, which includes accuracy, build time and efficiency with orientation, layer thickness and hatch distance. Most of the methods of improving the FDM final products are centered on two different areas: hardware and software.

In terms of hardware for FDM, several attempts have been made to better the finish of parts, and use alternative materials, like ceramic and metal materials, Allahverdi et al [16] introduced Fused Deposition of Ceramics (FDC) to prototype a variety of advanced ceramic components. In FDC, ceramic loaded polymer filaments are used to build parts. A process map, based on the compressive strength and modulus of the FDC feedstock, was developed to predict the feasibility of deposition with a variety of FDC filaments. A number of filaments such as PZT, PMN, alumina, and BiT have been successfully used in the FDC process and a high temperature silver-palladium electrode filament has been developed for the fabrication of electromechanical components. Photonic bandgap structures with alumina rods were fabricated with alumina and were used as support materials for microwave and laser applications.

Mazumder et al [17] introduced a Direct Metal Deposition (DMD) technique into RP processes. The DMD process is capable of producing three-dimensional components from many of the commercial alloys of choice. In that research, H13 tool steel was used as the deposition material and successfully built the components.

Meanwhile some systems with different nozzles, like multi-nozzle system, are brought in to implement the new materials. Khalil et al [18] developed a multi-nozzle biopolymer deposition system, which is capable of extruding biopolymer solutions and living cells for freeform construction of 3D tissue scaffold. The deposition process is biocompatible and occurs at room temperature and low pressures to reduce damage to cells. This system is capable of scaffold construction, depositing controlled amount of cells, growth factors, or other bioactive compounds with precise spatial position to form complex cell-seeded tissue constructs.

The orientation of deposition head also plays crucial rules on how the part is finally formed. Xu et al [19] found that the ability to evaluate and determine the best part build orientation for RP processes is important for building a satisfactory part/prototype within the limits of manufacturing time and build cost. Owing to the specific process characteristics of LM technology, different sets of geometric features may have critical effects on the part accuracy and build time. A proper preset of orientations of parts in FDM chamber may increase the accuracy and reduce the build time. Hu et al [20] developed an algorithm to determine the optimal direction of a hybrid rapid-prototyping process by considering both the CNC machining process attributes and the deposition process attributes.

Apart from the improvements in hardware mentioned above, internal quality of the FDM parts have had further improvement, especially for some materials like structural and functional ceramic and metal parts, which require a high degree of internal perfection. Mukesh et al [21] found that current state of FF technology and commercial FDM systems results in parts with several surface and internal defects which limits the structural properties of ceramic and metal parts. They introduced some build strategies by implementing commercial FDM systems to eliminate internal defects.

The solid models from various resources are converted into STL format files or other format files, which mostly come along with the FDM machines. Slicing procedures are implemented before the deposition. A lot of research is focused on slicing algorithms and attempting to reduce the stair-case effects and anisotropy of the final physical models. Jamieson et al [22] found that RP systems need for both tessellated and sliced data from CAD models to be input into RP machines and shown that direct slicing can be beneficial in terms of files size and in eliminating the need to slice a tessellated equivalent model. Their work also has shown that the accuracy can be enhanced, especially on rounded or tubular designs, which also benefits from reduced processing time before the build process starts.

Kulkarni et al [23] developed a procedure to develop variable thickness slices for an object by LM processes. With their procedure, the numbers of slices and cusp-height were reduced compared to the traditional RP process. Hope et al [24] developed an adaptive slicing procedure, based on surface curvature and angle of the surface normal, for improving the geometric accuracy of LM techniques which uses layers with sloping boundary surfaces that closely match the shape of the required surface. This greatly reduces the stair-step effect. This also optimizes the building of layered parts for both speed and accuracy.

Sabourin et al [12] developed an adaptive slicing method by using stepwise uniform refinement for LM. In this slicing method, the CAD model is first sliced uniformly into slabs of thickness equal to the maximum available fabrication thickness. Each slab is then re-sliced uniformly as needed to maintain the desired surface accuracy. This approach improves on past work by determining the adaptive refinement through interpolation rather than extrapolation, and it is well suited for execution in a parallel processing computer. This method has been implemented successfully and tested, where typical measured build time were reduced by approximately 50% without reducing overall surface accuracy.

The pattern of the deposition is also used to better the part quality. Yang et al [25] developed an equidistant path generation to improve scanning efficiency in LM. Experimental and simulation analyses were both performed to evaluate this path generation algorithm and it is shown this method can bring significant improvements to the present RP processes both in processing efficiency and part quality.

Luo et al [26] developed an efficient 3D model slicing algorithm for RP. This algorithm is capable of detecting the model and support features. Based on their implementation result, the model can be built without any errors during the slicing process. This slicing algorithm is a fast, accurate and reliable slicing process for applications of RP systems. Once the part is sliced, the data of flat layers is transfered to the FDM machine, and a software, like QS from Stratasys [27], generates the tool paths and builds the parts with extrusion nozzle head.

Although these improvements, especially in slicing algorithms, mentioned above lead to a great progress in FDM processing, the part surface quality and geometric accuracy are still a major concern. Reducing build time and increasing part surface quality are two factors that contradict with each other. Several different attempts have been brought forward in the literature, trying to make a better solution for curved surfaces; however, they still have their own limitations, especially for thin curved shell-type parts.

While the profound influence of RP on the product visualisation and other limited fields is quite evident, the lack of rapid prototyped engineering materials is a significant barrier to the dramatic growth of the technology and its impact on the product development endeavour. Evidently, the current processes use inferior materials and for the most part, produce a few parts suitable for limited testing. The promise of true engineering products is only slowly being realised through machine and material improvements, the progression, though, is not sufficiently advanced.

Further, the surface quality of parts produced is poor due to stair-step effect, strengths are low for certain part designs and the number of layers to make up a part is sometimes undesirably high. These problems become critical in the case of thin, slightly curved and shell-type parts. Common examples of such parts are skull bone replacements, turbine blades etc. For example, to produce the thin shell-type shape shown in Fig. 1.15 (a), the conventional FDM deposits material as shown in Fig. 1.15 (b), working on the side view of the product and resulting in a poor quality, due to stair-step effect and discontinuity of filaments across the section.

The current proposition is that the effectiveness of FDM can be improved by being able to use better materials and deposition techniques. First, while the basic process of FDM offers great potential for a range of other materials including metals and composites to be developed and used for FDM, the development of new materials based on metals and composites gets quite involving because of the specific requirement of the material to be in the feed stock form [28]. Second, building the necessary hardware and software interface to be able to deposit materials in a curved layered fashion, as shown for example, in Fig. 15(c) for the thin curved shell shape would result in reduced stair-step effect, increased strength of parts and reduced number of layers, the significance of which may be obvious in applications such as skull bone replacements as shown in Fig. 15(d).

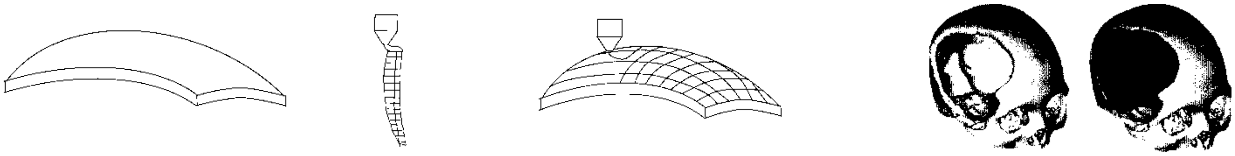

(*a) A curved model* *(b) flat layers* *(c) Curved layers* *(d) An application*

Fig. 1.15 Curved Layered FDM

Positive improvements if any in either of these directions would have a profound influence in making a further progress towards Rapid Manufacturing, the ultimate goal of the RP technology. With the development of bio-friendly materials and the use of reverse engineering, RP is becoming significantly important in medicine and in cases calling for high accuracy and plasticity, RP models are an unbeatable medical aid that foster surgical outcomes that were never possible before. Curved layered FDM could also have a significant application in the development of artefacts such as vases, statuettes and decorative pieces of complex shapes using a variety of materials.

The proposed research aims at building a FDM workstation and develops the mathematical and computational schemes necessary for the curved layered slicing and deposition. It involves the development of both hardware and software components and their integration into a working system. The most critical aspects of this would be the development of the suitable algorithms for curved layered slicing and practical implementation of the same for CLFDM.

While the proposed research is a first step towards developing a working CLFDM system together with the mathematical models, experimental investigation of the use of different materials and their combinations and the part characteristics would be topics of further research.

Klosterman et al [29] developed a curved layer process based on laminated object manufacturing (LOM) technology for efficient production of curved layer parts. This new process, based on LOM, incorporated a curved layer building style and ability to accommodate ceramic and fiber reinforced building materials. Monolithic ceramic (SiC) and CMC (SiC/SiC) article were fabricated using curved layer laminated object manufacturing (CLLOM). For making curved layer objects, the curve process afforded the advantages of eliminated stair step effect, increased building speed, reduced waste, and maintenance of continuous fibers in the direction of curvature. In other words, it meets all the advantages of the curved layer process mentioned above.

Chakraborty et al [30] developed a Curved Layer Fused Deposition Modeling (CLFDM) algorithm. It has been formulated and tested on parametric surfaces. This method is used to create slightly curved (shell-type) parts of thin-sections where traditional FDM might fail to meet the strength requirements. Higher strength is obtainable by employing longer length filament or roads and obtaining curved inter-layers of larger area per layer. This method has the potential to increase the strength of parts and to reduce the stair step effect, number of layers and build time simultaneously. The research however was only theoretical and was never attempted to be practically implemented. The current research takes off from this point and devolves into developing more practical algorithms for Curved Layered Slicing and the practical implementation of the same for CLFDM.

1.5 Research question, hypothesis and methodology

The question is whether CLFDM is practical and if so, are there any potential benefits at the end. The hypothesis is that CLFDM is practical as the basic input to any RP system is in the form of CAD files; it is essentially, processing the CAD files or the internal surface models using appropriate mathematical models. Considering the volume of the work involved, the current research is confined to developing a working CLFDM system and establishing the effectiveness of the technology is again left for the future.

The scope of the research is focused on developing a slicing algorithm for CLFDM. The methodology involves use of existing software solutions for gathering the basic data on the outer surfaces and then developing mathematical algorithms for offsetting curved slices. Existing solutions would be considered for quickly building the hardware system and necessary schemes would have to be worked for integrating the data generated from the mathematical models and the deposition system.

1.6 Objectives

The proposed research aims to develop a software-based algorithm, which consists of a series of curved offset layers with constant thickness so as to match the shape of the component accurately and implement it in the modified machine. The following are the main objectives:

1. A comprehensive state-of-the-art literature review on rapid prototyping technologies.
2. Development of mathematical models for curved layered slicing
3. Creation of deposition path patterns for stacked curved layers
4. Building and testing of the FDM platform for CLFDM
5. Practical implementation of CLFDM for parts of varying complexities

Chapter 2

Mathematical modeling and software solutions for traditional RP

2.1 General procedure of RP

In contemporary highly intense competition world, manufacturing companies in different industry areas are pushed to apply world-class manufacturing practices, which require more investment in new technological knowledge to bring high-quality and sophisticated products swiftly. Many processes of designing, testing manufacturing, even in marketing have been squeezed, in terms of time and material resources. RP, which is one of the new manufacturing practices, allows user to fabricate a real physical component directly from CAD model.

Recently, improvements of RP technologies emerged swiftly owing to the developments of computer technologies and material sciences. The advancement in computer-related areas, including CAD, CAM and CNC machining tools, and the high performance materials bring RP more close to the reality from Lab to commercial utilities. Several different procedures of RP share similar basic operating principles [31]. The basic process as shown in Fig 2. 1[31] includes the following steps:

1. Constructing the CAD model
2. Converting the CAD model to STL format
3. Checking and fixing the STL file
4. Generating support structures if needed

5. Slicing the STL file to form layers
6. Producing physical model
7. Removing support structures
8. Post-processing the physical model.

The RP input is the specified 3D data from the objects of both virtual and physical models. A virtual model, known as the computer model, is created form the CAD software, which can be a wireframe model, or surface model or solid model. A physical model can be obtained by digitizing or scanning the geometry from the physical part. Fig 2.2 shows the scanning process of an angel shape. However, the 3D data form digitizing a physical model is not always straightforward; basically the data from the physical model is saved as the point cloud data. For acquiring better resolutions, reverse engineering is required by using a coordinate-measuring machine (CMM) or laser digitizer.

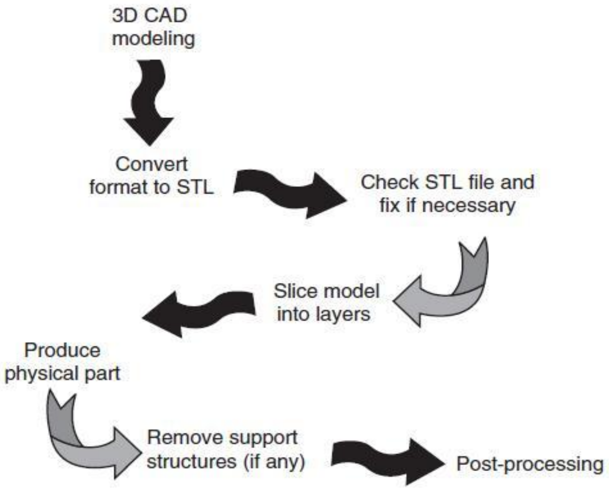

Fig 2. 1 Basic process of RP

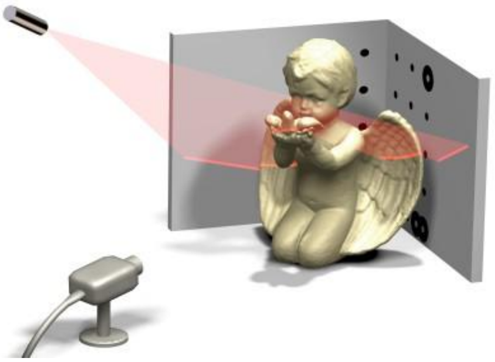

Fig 2. 2 3D scanning (Source: Wikipedia)

The 3D model, from virtual or physical model, is converted into an STL file, as will be discussed in the next section. In the STL format, the file of the model contains the x, y and z coordinates of the model in a series of triangular facets. After the 3D model is converted into an STL model, properly oriented and positioned, it is sliced into layers with a series of horizontal planes. The distance between every two adjacent planes is equal to the thickness of the layer. Then the support structure is generated based on the bottom surface of the STL model. After the orientation and the support decisions have been made, the tool paths that the machine will use to build each layer will be determined.

Once the STL file is sliced, the contour of each layer is transferred to the RP machine. The RP machine starts to build the model and the build process is fully automated. The tool head, depending on Liquid-Based or Solid-Based or Powder-Based RP processes, traces the points from the tool paths, curing the photo sensitive epoxy resin as in SLA, or depositing the material in solid state as in FDM, or sintering the powders as in SLS to form the layers. Once the build process is completed, the support is being removed from the build material, while methods of removal can vary from process to process.

Having identified the essential stages of a general RP process, the reminder of the chapter presents how some of the critical aspects like solid modeling, tessellation and slicing are handled in traditional RP. Some of the aspects presented here allow the basic understanding of underlying principles for the solutions to be developed and presented in subsequent chapters in the context of CLFDM

2.2 Solid modeling

2.2.1 Geometric models

The RP process begins with the development of a CAD model. Geometric modeling, also known as computer-aided geometric design (CAGD), is a branch of computational geometry and comes in handy in the development of virtual models. It deals with the construction and representation of free-form curves, surfaces or volumes [32]. The geometric model can be either two dimensional or three dimensional in terms of space [33].

Two dimensional geometric models are geometric models of objects as two-dimensional figures, which were the first ones to be developed in view of their relatively lesser complexity, usually on the Euclidean or Cartesian plane. Even though the objects are three-dimensional, the 2D geometric models are often adequate for certain flat objects. However, the 2D geometric models have their limitations because they are inherently difficult to represent the complex objects and definitely not suitable in the context of RP.

Three dimensional geometric models, often known as 3D models, are the collection of point data of 3D objects in 3D space, connected by various geometric entities such as lines, triangles, curved surfaces, etc. Several 3D graphic software packages developed during the past few years have the ability to provide all the information required for manufacturing applications and have also been gradually equipped with modules needed for tessellation and slicing as required for RP.

Solid models in 3D are again constructed using line, surface and volume models [33]. Line model, also called wireframe model, represents objects by lines with their endpoint coordinates and their connectivity relationships. Although simple and not taking huge computer storage space, it may get ambiguous for end users to understand. Also, it is essential to store further information, in addition to the vertex data to describe the nature of a solid.

The surface model, also known as shell/boundary model, is constructed essentially from surfaces such as planes, rotated curved surfaces and even more complex surfaces [33]. The surface model is capable of representing the solid clearly from the manufacturing point of view. However, the interior information of the solid models would not be available for generating the CNC cutter tool paths. Apart from that, the calculation of properties such as mass and inertia would be difficult. Therefore, a surface model for constructing the solid is tedious and not generally attempted. But it would be available as part of the modeling technique, and used to present the product in terms of design.

The solid/volume model, which is consisting of the complete description of the solid in a certain form, is the most ideal representation although more difficult to build. In other words, all the information needed for manufacturing can be obtained from models developed using this technique. The solid/volume model has been widely used in engineering software. As the CAD model used for processing in an RP system is usually built using the solid modeling method, some of the underlying principles are briefed in the following section.

2.2. 2 3D Geometric solid model construction

Geometric representation of a 3D solid model consists of a lot of information, like dimensions, tolerances, material specifications, and the processing requirements, etc. There are different ways of making 3D models: Sweeping, Constructive Solid Geometry (CSG) and Boundary Representation (BRep).

Sweeping can be divided into three sub-divisions: Extrude, revolve and sweeping along guide lines.

Extrude

In the extrusion, a 2D surface or a section is extruded along a vector then generating the 3D model, as shown in Fig 2. 3. The extrusion models are possible to have the taper along the linear direction. It is also possible to sweep a profile through a three dimensional direction. However, not all types of models can be modeled by extrusion; for example, any variations in directions transverse to the direction of extrusion cannot be created.

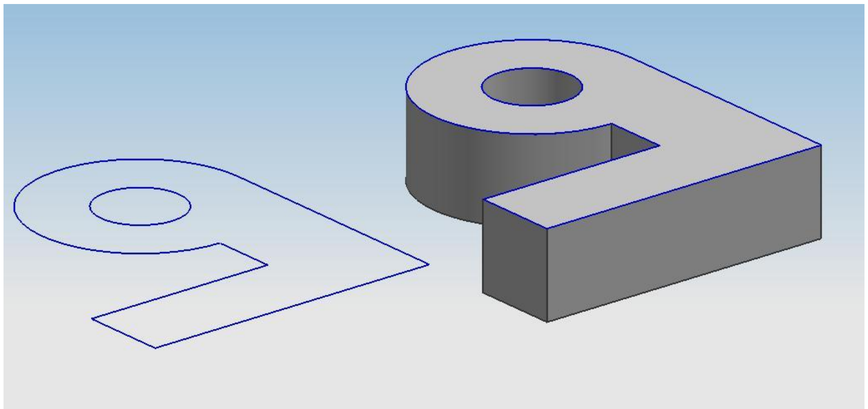

Fig 2. 3 Extrusion

Revolve

Revolve is another type of construction technique and works by revolving a section about an axis. However, it is just suitable for axis-symmetric models, as shown in Fig 2. 4.

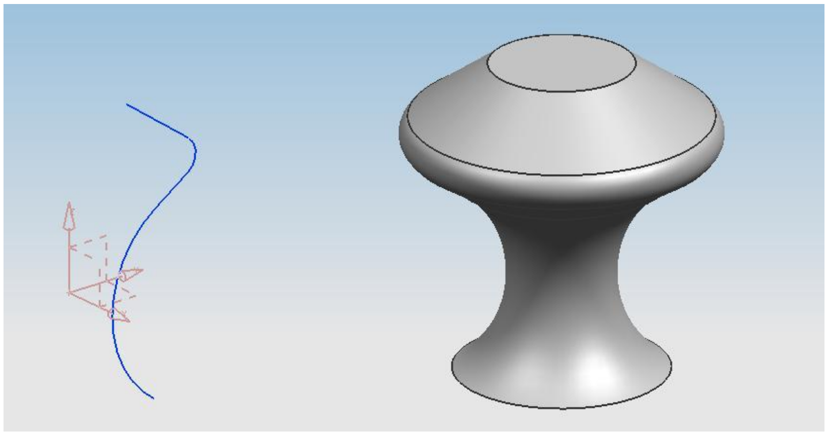

Fig 2. 4 Revolving

Sweeping along the guide

Sweeping along the guide is an extension of extrusion, which creates a solid body by sweeping a section along one or more guides using various options to control the shape along the guide, as shown in Fig 2. 5.

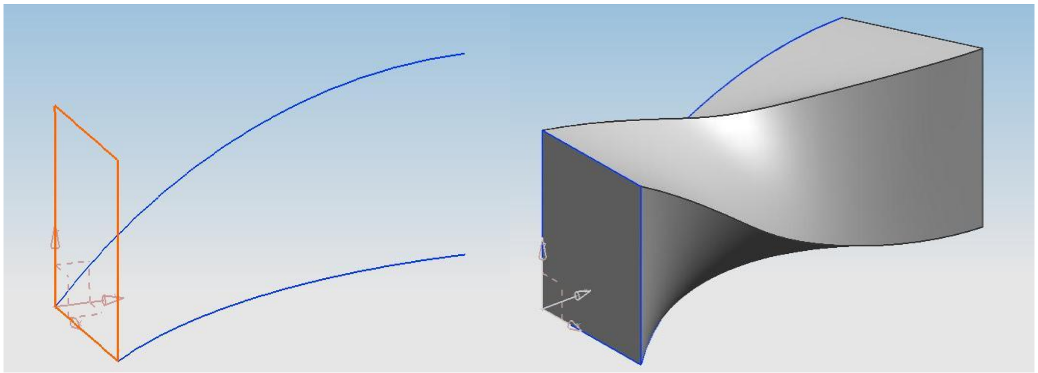

Fig 2. 5 Sweeping along the guides

Constructive solid geometry (CSG)

Although the swept technique is capable of generating reasonably complex surfaces, they are not suited for the purpose of inputting geometry. One of the best techniques for solid modeling is Constructive Solid Geometry (CSG), which is often but not always a procedural modeling technique used in CAD, and is based on the primitives. The primitives are the simplest solid objects such as blocks, cylinders, sphere and cones. CSG allows a complex solid model to be created by using Boolean operators to combine objects. A model is constructed from primitives by means of allowable operations, typically, Boolean operations on sets: union, intersection and difference. A primitive can be described by a procedure accepting some parameters. A sphere can be described by its center point whereas a block by end points. These two primitives can be combined into a compound object, as shown in Fig 2. 6.

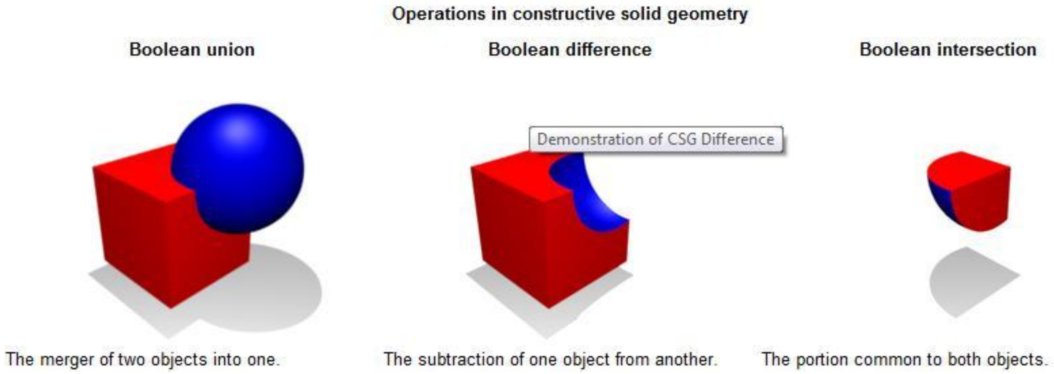
Operations in constructive solid geometry
Boolean union
Boolean difference
Boolean intersection
Demonstration of CSG Difference
The merger of two objects into one.
The subtraction of one object from another.
The portion common to both objects.

Fig 2. 6 Boolean operators

Boundary Representation (BRep)

In solid modeling, Boundary representation (BRep) is a method of representing shape by using the limits. A solid is represented as a collection of connected surface elements, the boundary between solid and non-solid. BRrep models are composed of two parts: topology and geometry. The main topological items are faces, edges and vertices and faces are the mostly used in the actual cases. Compared to the CSG, BRep representation is more flexible because it not only can use the operation sets but also the surface modeling, especially Freeform Surface Modeling.

A 3D surface can be obtained by traversing an entity, e.g., a line, polygon or curve, along a path in space and such surfaces are called sweep surfaces [34], as shown in Fig 2. 7. It also can be obtained from revolving a 2D entity about an axis in space, resulting the surfaces of revolution [34], as shown in Fig 2. 8. However, there are some surfaces, which cannot be described by any of the analytical techniques available, e.g. car bodies, ship hulls, airplane cockpits and some decorative surfaces for aesthetics.

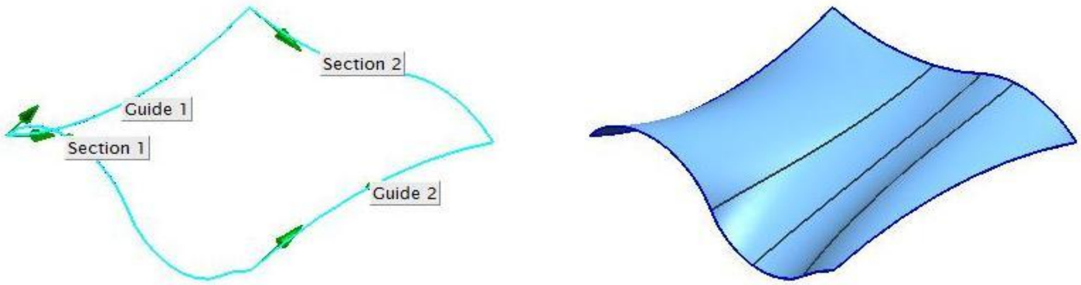

Fig 2. 7 Sweep surface

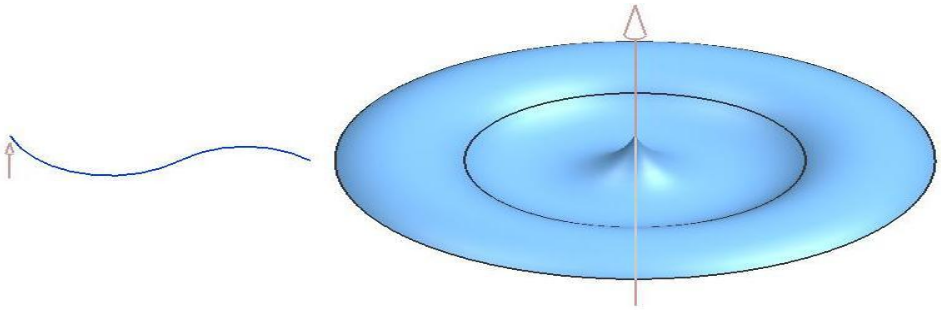

Fig 2. 8 Surface of Revolution

In order to represent those more complex surfaces, freeform surfaces, which can be modeled through a series of control points and other boundary conditions were introduced. A freeform surface, or freeform surfacing, is used to describe the skin of a 3D geometric element. Unlike regular surfaces such as plane, cylinders, conic and quadric surfaces, freeform surfaces do not have rigid radial dimensions. The forms of freeform surfaces are not stored or defined by polynomial equations, but by their poles, degree and number of patches. There are many mathematical models used to describe the free form surfaces, one of the widely used being Non-Uniform Rational B-spline (NURBS), which is a special case of rational B-splines. NURBS curves and surfaces are defined by their order/degree, weighted control points and knot vector. For simplicity, Bezier surfaces are modeled for the purpose of validating CLFDM in solids enveloped by freeform surfaces,

Bézier curve

Bézier curve, which was developed by the French engineer Pierre Bézier in 1962, is a method of shape description suitable for freeform curves and surfaces [34]. It is determined by a defining polygon, as shown in Fig 2. 9. The mathematical equation of Bézier curve is defined by:

$$P(t) = \sum_{i=0}^{n} B_i J_{n,i}(t) \qquad 0 \leq t \leq 1 \tag{2 - 1}$$

Where the Bézier or Bernstein basis or blending function is

$$J_{n,i}(t) = \binom{n}{i} t^i (1-t)^{n-i} \tag{2 - 2}$$

With

$$\binom{n}{i} = \frac{n!}{i!\,(n-i)!} \tag{2 - 3}$$

The Bézier curve generally follows the shape of the defining polygon. Its first and last points are coincident with the first and last points of the defining polygon, whereas the tangent vectors at the end points have the same directions as the first and last polygon spans respectively.

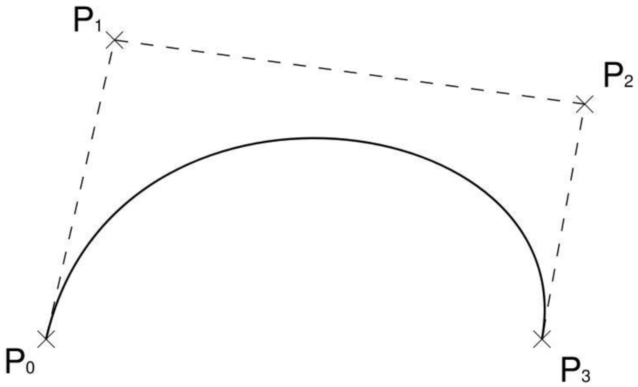

Fig 2. 9 Bézier curve

Bézier surface

A given Bézier surface of order (n, m) is defined by a set of (n+1), (m+1) control points [34]. A Cartesian or tensor product Bézier surface, as shown in Fig 2. 10, is given by

$$Q(u,w) = \sum_{i=0}^{n}\sum_{j=0}^{m} B_{i,j} J_{n,i}(u) K_{m,j}(w) \qquad \text{(2 - 4)}$$

Where $J_{n,i}(u)$ and $K_{m,j}(w)$ are the Bernstein basis functions in the u and w parametric directions. The Bézier or Bernstein bases are

$$J_{n,i}(u) = \binom{n}{i} u^i (1-u)^{n-i}$$
$$K_{m,j}(w) = \binom{m}{j} w^j (1-w)^{m-j} \qquad \text{(2 - 5)}$$

With

$$\binom{n}{i} = \frac{n!}{i!\,(n-i)!}$$
$$\binom{m}{j} = \frac{m!}{j!\,(m-j)!} \qquad \text{(2 - 6)}$$

A Bézier surface will transform in the same way as its control points under all linear transformations and translation. It also will completely lie within the convex hull of its control points. All u=constant and v=constant lines in the space, especially four edges of the deformed unit square are Bézier curves. The points in the patch corresponding to the corners of the deformed unit square coincide with four of the control points. However, the Bézier surface does not pass through all other control points.

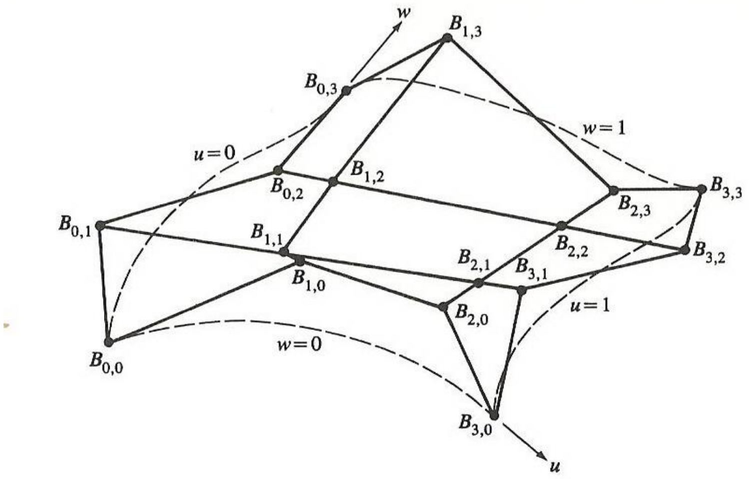

Fig 2. 10 Bézier surface

In the current research, Bezier surfaces are modelled in MATLAB for the purpose of testing the curved layered algorithms in the case of solids formed by freeform surfaces. Whichever way the CAD models are developed, they are not directly suitable for processing on an RP machine as traditional RP software recognise and process STL file formats only.

2.3 STL format

STL (Stereo lithography) file, as the de facto standard, has been used as a connection linking CAD model design and prototype fabrication in many systems [35] as shown in Fig 2. 11. The STL file, conceived by the 3D Systems, USA, is created from the CAD database via an interface on the CAD system. It consists of a mesh of triangular facets representing the outside shell of the solid object, where each triangular facet shares the sides with adjacent elements and the vertices are ordered by the right-hand rule. It also consists of the x, y and z coordinates of the three vertices of each surface triangle, with an index to describe the orientation of the surface normal [31]. However, the representations of color, texture or other common CAD model attributes are not available in the STL files.

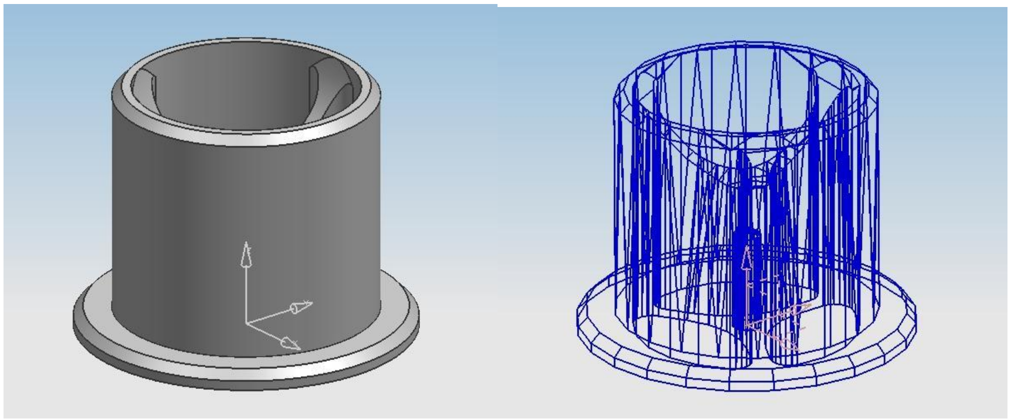

Fig 2. 11 A CAD model in CAD format and STL format

The STL file format specifies in two representations: ASC II and Binary. Binary files are more common, because they are more compact compared to ASCII files [36].

ASCII STL

An ASCII STL file starts with a comment line, and then continues with the number of triangles, the general structure of which is as shown in Fig 2. 12.

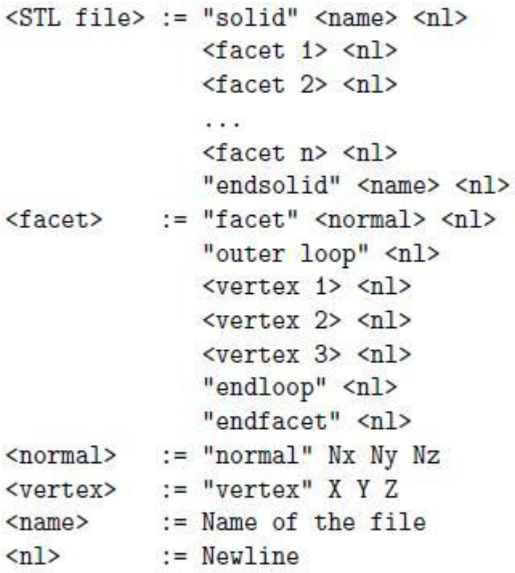

```
<STL file> := "solid" <name> <nl>
              <facet 1> <nl>
              <facet 2> <nl>
              ...
              <facet n> <nl>
              "endsolid" <name> <nl>
<facet>    := "facet" <normal> <nl>
              "outer loop" <nl>
              <vertex 1> <nl>
              <vertex 2> <nl>
              <vertex 3> <nl>
              "endloop" <nl>
              "endfacet" <nl>
<normal>   := "normal" Nx Ny Nz
<vertex>   := "vertex" X Y Z
<name>     := Name of the file
<nl>       := Newline
```

Fig 2. 12 ASCII STL format

An example of the ASCII STL file of a part is shown in Fig 2. 13.

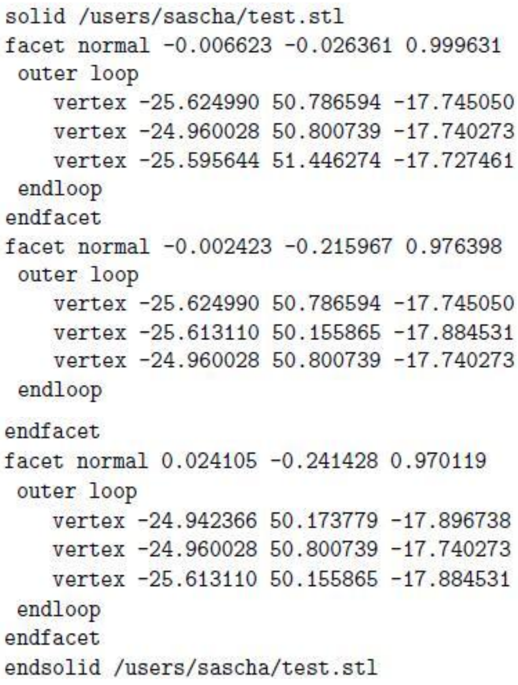

```
solid /users/sascha/test.stl
facet normal -0.006623 -0.026361 0.999631
 outer loop
    vertex -25.624990 50.786594 -17.745050
    vertex -24.960028 50.800739 -17.740273
    vertex -25.595644 51.446274 -17.727461
 endloop
endfacet
facet normal -0.002423 -0.215967 0.976398
 outer loop
    vertex -25.624990 50.786594 -17.745050
    vertex -25.613110 50.155865 -17.884531
    vertex -24.960028 50.800739 -17.740273
 endloop
endfacet
facet normal 0.024105 -0.241428 0.970119
 outer loop
    vertex -24.942366 50.173779 -17.896738
    vertex -24.960028 50.800739 -17.740273
    vertex -25.613110 50.155865 -17.884531
 endloop
endfacet
endsolid /users/sascha/test.stl
```

Fig 2. 13 An example ASCII STL format file

Binary STL

A Binary STL file has an 80 character header. Following the header is a 4 byte unsigned integer indicating the number of triangular facets in the file. And then, the data describing each triangle is written after the unsigned integer. The file ends after the last triangle, as shown in Fig 2. 14. Each triangular facet is described by 32-bit-floating point numbers, three for the normal and other three for the x, y and z coordinates of each vertex.

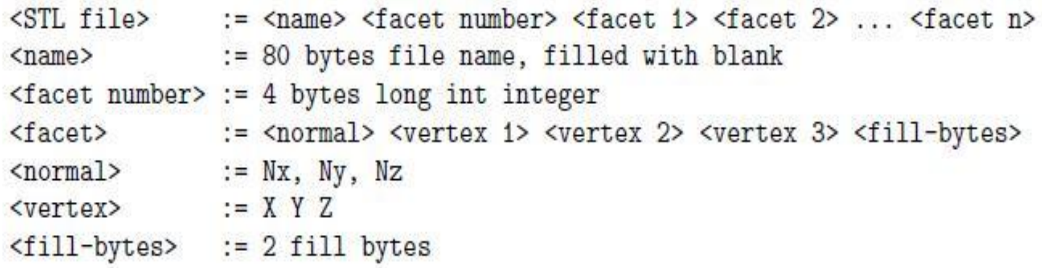

```
<STL file>     := <name> <facet number> <facet 1> <facet 2> ... <facet n>
<name>         := 80 bytes file name, filled with blank
<facet number> := 4 bytes long int integer
<facet>        := <normal> <vertex 1> <vertex 2> <vertex 3> <fill-bytes>
<normal>       := Nx, Ny, Nz
<vertex>       := X Y Z
<fill-bytes>   := 2 fill bytes
```

Fig 2. 14 Binary STL format

The advantage is, slicing the STL file is much easier compared to slicing models developed by other methods like B-rep and CSG. It can also make the process robust and reliable to get the correct result the first time. However, several problems still plague STL to date [35], owing to the very nature of STL files as they contain no topological data. Many commercial tessellation algorithms used by CAD vendors today are also not robust, and as a consequence, they tend to create polygonal approximation models which exhibit the following types of errors:(1) Gaps; (2) Degenerate facet; (3) Overlapping; (4) Non-manifold topology conditions. Additionally, STL files are not compatible for all the RP devices, in terms of solid model construction, programs may vary from business to business. Some systems can accept the STL files directly, whereas others require pre-processing. Although STL format is not perfect for the RP, it is still being widely used around the world.

2.4 Slicing method

Once the CAD model is converted into the STL format, it needs to be sliced at a particular orientation. The STL model slicing procedure is to generate a series of closely spaced 2D cross-sections of a 3D model. The distance between every two cross-sections or layers is Z-thickness, which can be specified. The actual thickness varies, and depends on the accuracy requirements and the properties of different materials. The slicing the STL file is an approximate procedure. The main error, which is known as stair-case effect, occurs in this stage and also leads to rough surfaces.

At the beginning of the slicing process, a model in the STL format file is properly oriented and positioned. A series of parallel flat planes are introduced directly to slice the STL file, as shown in Fig 2. 15. The distance between every adjacent plane is equal to the thickness of the filament or the curing depth of the photo/heat-sensitive resin or powder layers. As the STL file is a triangular-facet model, contains no extra information about the inner details of the model. The parallel planes cut through the triangulated surfaces of the model, getting the layer contour information. The outcome of the slicing process is a series of contour curves, formed by connecting the intersection points, as shown in Fig 2. 16. Since all the facets are planar triangles and all the curves are made of line sections, the slicing process is to get the intersection points. The coordinates of the intersection points are recorded down for the tool path generation. However, it is a time-consuming task, and might waste a great deal of time while dealing with redundant or erroneous information.

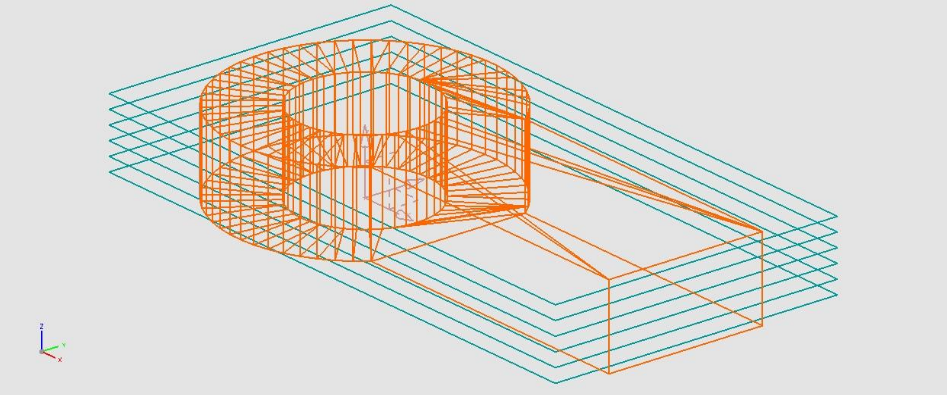

Fig 2. 15 STL files slicing

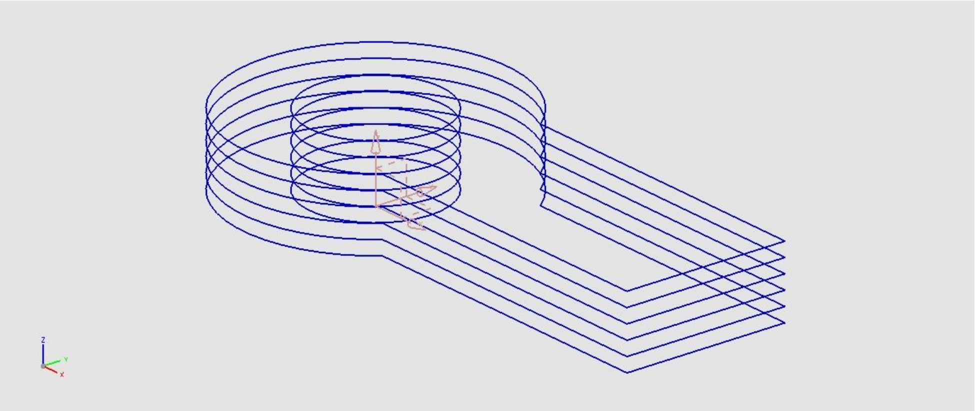

Fig 2. 16 Contour curves accquiring

Because the intersections are just a couple of lines and the RP machine cannot identify which part is the solid, a definition of solid part is introduced. Conventionally, the clockwise (CW) and counter-clockwise (CCW) directions indicate the inner and outer loops respectively [37]. In other words, for or every layer, the RP machine works on the contours of the layers, the positive direction of the contours follow the counter-clockwise direction, and the left hand side of the contour curve is defined as solid. Once the solid part is identified, it is ready for the tool path generation and processing.

2.5 Creation of tool pathway

After the part is sliced, most of the RP software automatically generates the support structures, located under the base of the part. After the orientation and the support decision have been made, the users can then determine the tool path that the machine will use to build each layer. The tool path allows a great variety of options to the user depending on finished part strength, build time, or weight and surface finish.

At the start of the tool path generation, a set of unsorted vectors is available in every z increment [38]. Those vectors are not connected and are not in sequence. Hence, the RP machine cannot identify the layers. In order to run these sliced layers in the RP machine, these vectors should be arranged in a proper form. The vectors on the same triangular facet are connected with straight lines, as shown in Fig 2. 17.

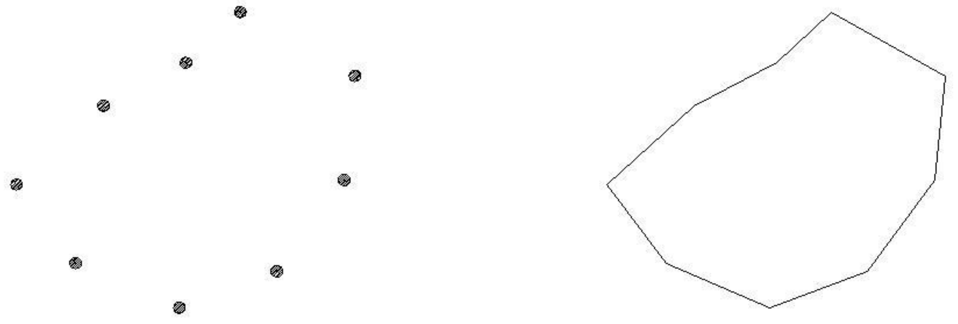

Fig 2. 17 Contour Construction

As all the triangular facets in the STL file are sharing edges with three adjacent triangular facets, all the section points are connected by lines and the resulting contour becomes the tool path of the slice, making the outer surface smoother. Inside the contour tool path, the tool path pattern is mostly set at ±45 ° zigzag pattern automatically in every layer, unless the users define other pattern options. The tool path patterns are perpendicular between two adjacent layers, as shown in Fig 2. 18. If the parts are hollow inside, the tool path is created with larger air gaps in the middle.

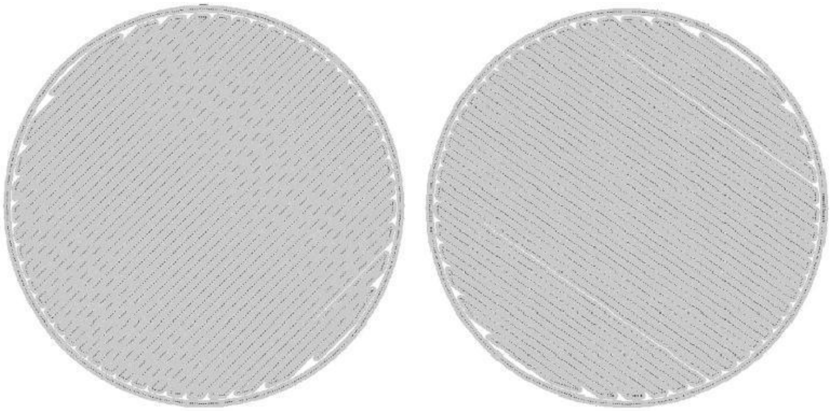

Fig 2. 18 Different tool paths of two adjacent layers

The output condition is set to be "on", when the laser beam or deposition nozzle tracing the tool path contours or the filling patterns, or "off" when the laser been or deposition is working on the transitional motion, like from one tool path move to another tool path, as shown in Fig 2. 19.

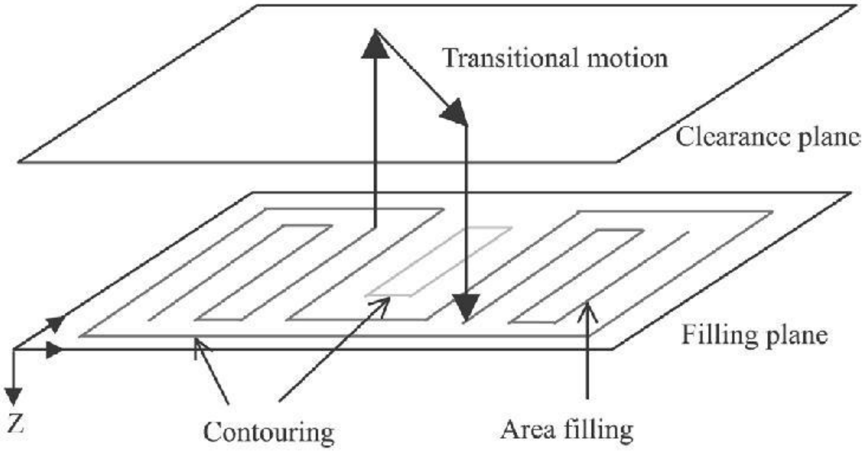

Fig 2. 19 Tool path of RP motions

When the tool path for the part is finished, the tool path for support structure is created, whose processing is similar to the generation of the tool path of the part.

The output of the tool path generation is transferred to the RP machine, which is based on a three-axis movable platform driven by servo motors and stepper motors. When all the data from the tool path output loaded into RP machine, the part is ready to be built.

2.6 Software and hardware integration

The RP machine is a CNC-like machine, which has three stepper motors running in X, Y and Z axis. The motion of RP machine is similar to an ordinary three axis CNC machine. However, instead of having a cutter head, the RP machine has the tool holder, which is for the operating device, mostly is laser beam device or deposition nozzle. Unlike the CNC machine, the tool holder only works on X and Y axis whereas the work platform works on Z axis like an elevator. The RP machines mostly have their own drivers, which control the motors to implement different motions.

Once the STL file is sliced and the tool paths have been generated, the coordinates of the tool path will be recorded down. The data of coordinates and the output conditions are transferred to RP machine. The operating device traces the coordinates of every single point on the tool path, including the operating motions and the transitional motions, from the first layer to the last layer. Meanwhile, the operating device starts to build the part, following the output conditions of the points. Once the lower layer is completed, the work platform drops to next level by one increment, and then the RP machine repeats the build processing again until the entire model finished.

The graphical user interface (GUI) software program, which makes the RP processing visual to users, is coming along with the machine. It displays the build process simulation in CAD environment on the computer monitor as well as other useful information, for example, build time and tool paths, from beginning of the process.

Having identified the procedures and mathematical formulations used for the processes in traditional RP, the next task is to use this knowledge and develop software and hardware solutions for the application of CLFDM. Some of the mathematical models and other procedures discussed here are used in the procedures developed for the practical implementation of CLFDM, as presented in the next chapter.

Chapter 3

Mathematical algorithms for CLFDM

3.1 General considerations for CLFDM

Flat Layer Fused Deposition Modeling (FLFDM) was made commercially available since early nineties and had undergone a continuous improvement in materials and product quality. Hardware and software for FLFDM have evolved over time to be able to generate various prototype models and parts with a few materials. Current slicing algorithms can handle all models of any complexity, in any orientation. Even today, many researchers and engineers are still developing new methods and mathematical algorithms to slice the models with flat layers for FLFDM.

Although there is a considerable amount of research work done on FLFDM, there is no solution readily available for slicing a 3D model with curved layered slices. At the time this work was started, there was only one report in the existing literature [30] that brought forward the concept of curved layered slicing algorithm. They only talked about the theoretical approaches, with no practical application whatsoever.

The implementation of curved layered slicing requires an understanding and subsequent modeling of the 3D surface, setting data points and fitting a surface model. The curved layered slicing algorithm subsequently needs integration with a hardware system for the practical implementation of CLFDM.

3.2 Surface data generation

Gathering the key point data from the surface is the fundamental task in a curved layered slicing algorithm. Appropriate construction of subsequent curved layers is based on the accuracy of data points from the surface. In this research, three different methods of acquiring surface data are developed and used. They are surface data generation by G&M codes, surface modeling and STL file.

3.2.1 G&M code method

A 3D virtual solid CAD model of any complex shape can be created using any 3D engineering (SolidWorks, Unigraphics NX, etc) or animation software (3ds Max, etc) with built-in modeling functions. It also can be obtained by scanning a physical model using a 3D laser scanning machine. A 3D virtual solid model is shown in Fig 3. 1.

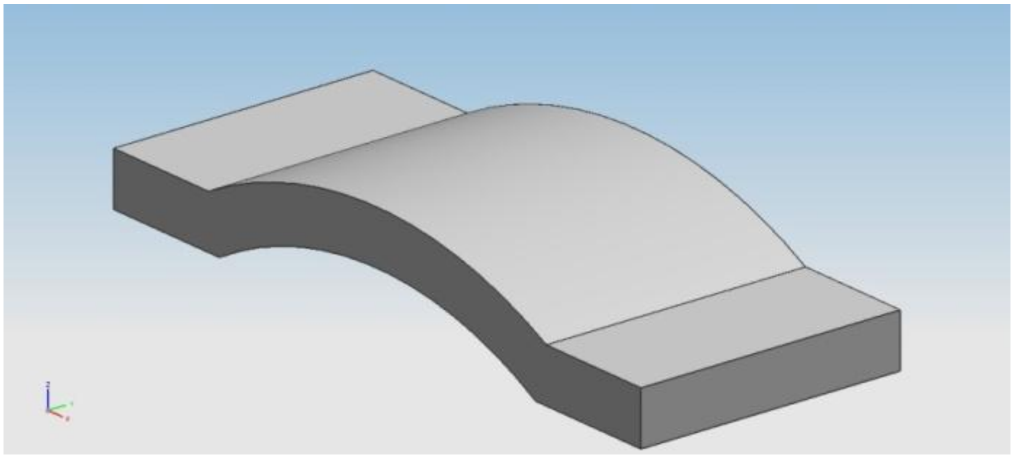

Fig 3. 1 A 3D CAD model

The CAD model is transferred to any available CAM software (SolidCAM, Manufacturing Module in UGNX) directly. Then the CAM software generates the G&M codes automatically by following the shape of the top surface of the part with its own or user defined patterns, mostly in the zigzag pattern. In order to replicate the motions of the deposition nozzle when run on the RP machine, the

G&M codes for the cutter path data are generated based on the three-axis milling with the ball cutter. The size of the ball cutter is equal to the diameter of the nozzle head. Fig 3. 2 shows the cutter paths developed using the G and M code data generated by the Manufacturing Module in UGNX for the top surface of the model.

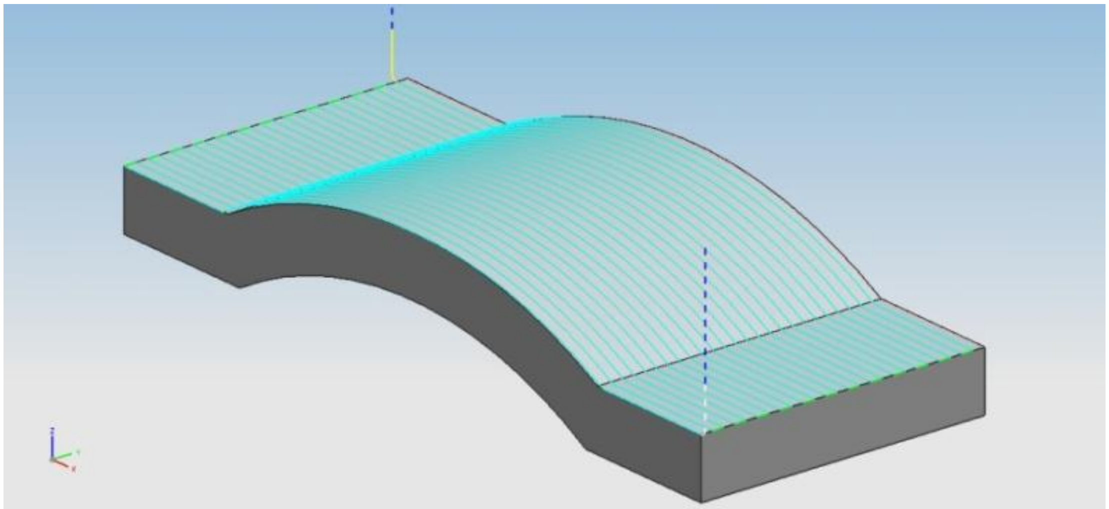

Fig 3. 2 G&M code of top surface

When using different CAD software, the formats of the CAD models may vary from one software to the other. Further, when they are transferred to the CAM software, the mathematical equations or descriptions might be lost. It is necessary to exercise caution while gathering the data points from the surfaces, especially the ones required to be machined or deposited in this case. The CAD files may be stored in the IGES format, for compatibility between different platforms. The reason for using G&M codes here is to record the x, y and z coordinates of the points defining the surface topology. When the G&M codes are generated, the x, y and z coordinates of the surface points are recorded by the computer and saved as a text file. Fig 3. 3 shows a raw text file of G&M codes generated by the Manufacturing Module of UGNX.

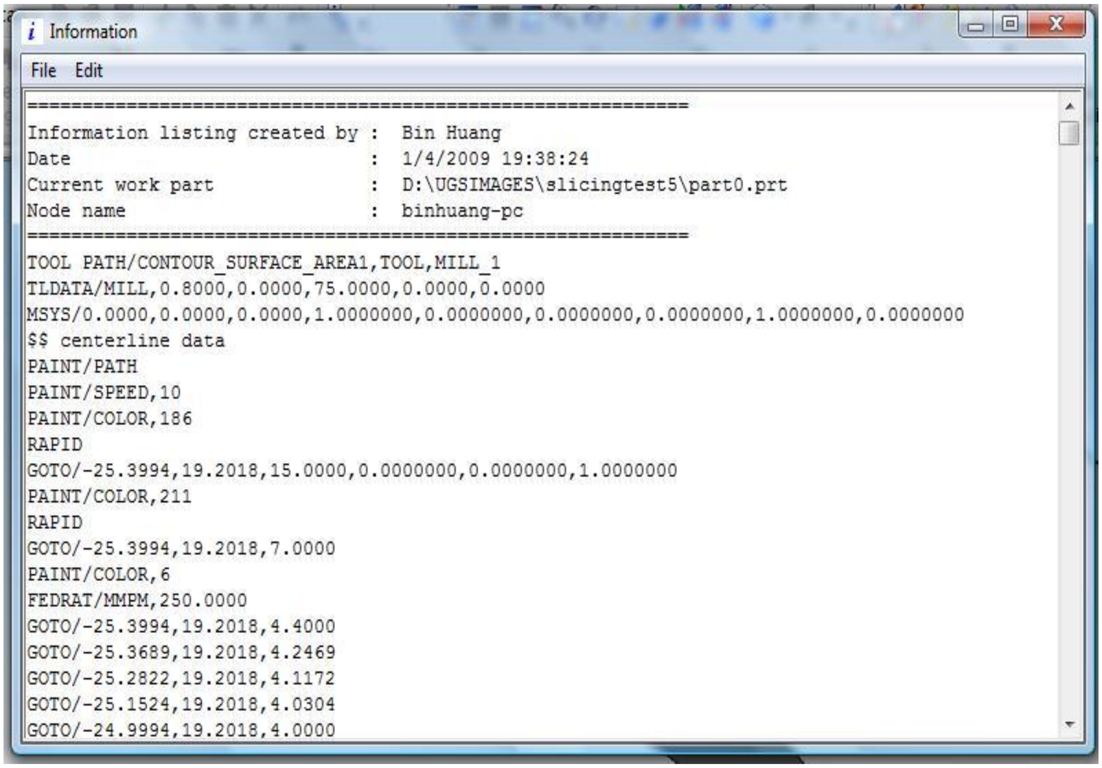

```
============================================================
Information listing created by :  Bin Huang
Date                           :  1/4/2009 19:38:24
Current work part              :  D:\UGSIMAGES\slicingtest5\part0.prt
Node name                      :  binhuang-pc
============================================================
TOOL PATH/CONTOUR_SURFACE_AREA1,TOOL,MILL_1
TLDATA/MILL,0.8000,0.0000,75.0000,0.0000,0.0000
MSYS/0.0000,0.0000,0.0000,1.0000000,0.0000000,0.0000000,0.0000000,1.0000000,0.0000000
$$ centerline data
PAINT/PATH
PAINT/SPEED,10
PAINT/COLOR,186
RAPID
GOTO/-25.3994,19.2018,15.0000,0.0000000,0.0000000,1.0000000
PAINT/COLOR,211
RAPID
GOTO/-25.3994,19.2018,7.0000
PAINT/COLOR,6
FEDRAT/MMPM,250.0000
GOTO/-25.3994,19.2018,4.4000
GOTO/-25.3689,19.2018,4.2469
GOTO/-25.2822,19.2018,4.1172
GOTO/-25.1524,19.2018,4.0304
GOTO/-24.9994,19.2018,4.0000
```

Fig 3. 3 The raw G&M code data in a text format file

Apart from the coordinates of the surface points, the raw G&M code text format file includes a lot of other data, such as the manufacturing information, and other instructions for the motion of the milling cutter etc. The unnecessary data needs to be removed before the text file is transferred to the RP machine, as the machine gets into a dull loop once reaching the unintelligible portions. In this research, the unnecessary information in the text file is deleted manually, as it gets quite involving to alter the file programmatically. In Fig 3. 4, a modified text file is presented with the header and footer, as well as other unnecessary information removed and only the x, y and z coordinates remaining. This modified file will be the input to the slicing program.

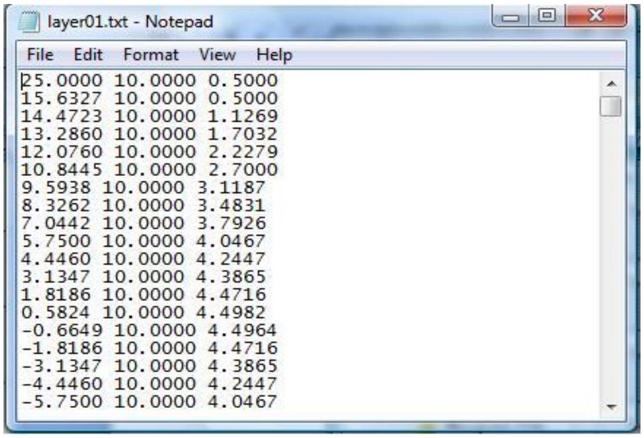

```
25.0000 10.0000 0.5000
15.6327 10.0000 0.5000
14.4723 10.0000 1.1269
13.2860 10.0000 1.7032
12.0760 10.0000 2.2279
10.8445 10.0000 2.7000
9.5938 10.0000 3.1187
8.3262 10.0000 3.4831
7.0442 10.0000 3.7926
5.7500 10.0000 4.0467
4.4460 10.0000 4.2447
3.1347 10.0000 4.3865
1.8186 10.0000 4.4716
0.5824 10.0000 4.4982
-0.6649 10.0000 4.4964
-1.8186 10.0000 4.4716
-3.1347 10.0000 4.3865
-4.4460 10.0000 4.2447
-5.7500 10.0000 4.0467
```

Fig 3. 4 A modified G&M code text format file

3.2.2 Surface modeling method

A curved surface can be defined not only by a series of data points but also by using one of the mathematical models reviewed in Chapter 2. Surface point data can be computed by solving the appropriate mathematical models. Surfaces generated like these are unrestricted other than that they follow the key point format and are known as freeform surfaces. The mathematical models allow computation of coordinates of any number of surface points, based on the key point data.

A freeform surface in whatever shape can be created by modeling the constitutive models in any programming system such as C or MATLAB. For the purposes of the current investigation, the Bezier surface is modeled using MATLAB (chapter 2). The program outputs the Bezier surface for any set of key points interactively input by the user. The quality of the surface depends on the number of points computed on the surface. The more the points used to describe the surface; the better is the quality of the surface. Although the number of points could be infinite mathematically, there still has some limit in the actual case, considering the difficulties, handling too large data files. In this research, the number of points in x and y directions is affected by the diameter of the deposition filament. In other words, the distance between two adjacent points in the Y-direction will be equal to the diameter of the deposition filament. A freeform Bezier surface created in MATLAB is shown in Fig 3. 5.

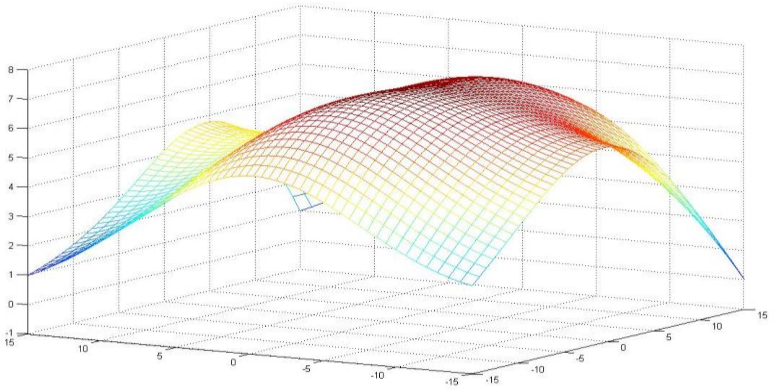

Fig 3. 5 A freeform surface

When the freeform surface is created, the x, y and z coordinates of every topology point are stored into three different matrices, which in this case are Px, Py and Pz matrices respectively. The coordinate data presented in Fig 3. 6 gives the sequence of points from the first column to the last column while each row represents points along an iso-parametric line. For example, X, Y and Z coordinates of the first point on the first iso-parametric line are (-15 15 1).

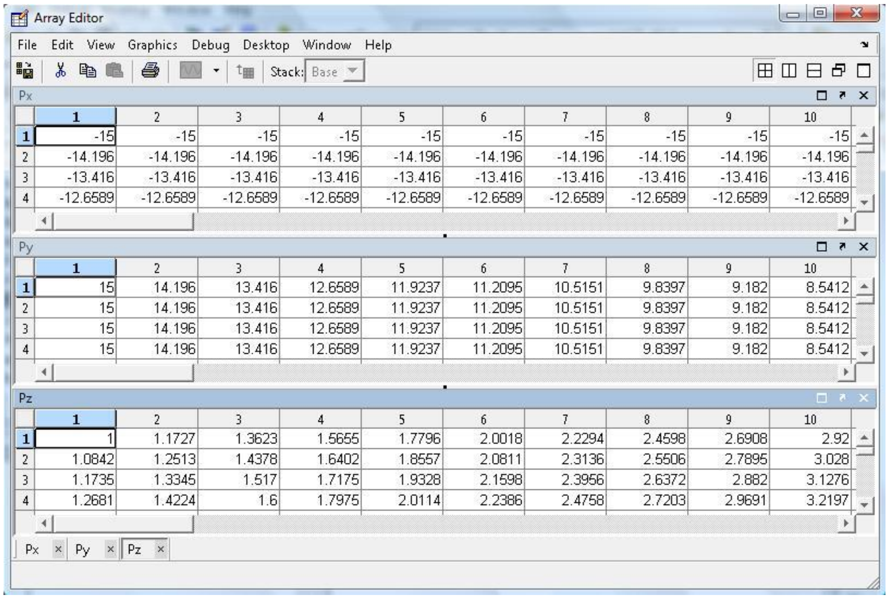

Px

	1	2	3	4	5	6	7	8	9	10
1	-15	-15	-15	-15	-15	-15	-15	-15	-15	-15
2	-14.196	-14.196	-14.196	-14.196	-14.196	-14.196	-14.196	-14.196	-14.196	-14.196
3	-13.416	-13.416	-13.416	-13.416	-13.416	-13.416	-13.416	-13.416	-13.416	-13.416
4	-12.6589	-12.6589	-12.6589	-12.6589	-12.6589	-12.6589	-12.6589	-12.6589	-12.6589	-12.6589

Py

	1	2	3	4	5	6	7	8	9	10
1	15	14.196	13.416	12.6589	11.9237	11.2095	10.5151	9.8397	9.182	8.5412
2	15	14.196	13.416	12.6589	11.9237	11.2095	10.5151	9.8397	9.182	8.5412
3	15	14.196	13.416	12.6589	11.9237	11.2095	10.5151	9.8397	9.182	8.5412
4	15	14.196	13.416	12.6589	11.9237	11.2095	10.5151	9.8397	9.182	8.5412

Pz

	1	2	3	4	5	6	7	8	9	10
1	1	1.1727	1.3623	1.5655	1.7796	2.0018	2.2294	2.4598	2.6908	2.92
2	1.0842	1.2513	1.4378	1.6402	1.8557	2.0811	2.3136	2.5506	2.7895	3.028
3	1.1735	1.3345	1.517	1.7175	1.9328	2.1598	2.3956	2.6372	2.882	3.1276
4	1.2681	1.4224	1.6	1.7975	2.0114	2.2386	2.4758	2.7203	2.9691	3.2197

Fig 3. 6 Px, Py and Pz matrices

Because the x, y and z coordinates are not stored in the same matrix, it is difficult for the RP machine to run the three different matrices at the same time. Apart from that, the sequence of the points follows the number of rows and columns from the first one to the last; this will cause the nozzle head to crash into the model during the deposition. In order to avoid this, a rearrangement of the topology point sequence is necessary.

During the rearrangement, the x, y and z coordinates of every topology point are obtained from three different matrices to three different columns in one single matrix, as shown in Fig 3. 7. Finally, when these points are arranged to form the deposition head path pattern, it is necessary that the head is moved from one track to the next in the shortest distance possible, which otherwise might lead to the sweeping transition of the tool from one end of a deposition line to the other end of the next line, crossing the entire component, completely violating the curved layered pattern and crashing into the freshly formed layers as shown in Fig. 3.8. All the data is re-listed in an N by 3 matrix, where N here is equal to the number of the data listed in each of Px, Py or Pz matrices. Then the new matrix containing X, Y and Z coordinates in different columns is saved as the text format file, and will be used as the input for the slicing program.

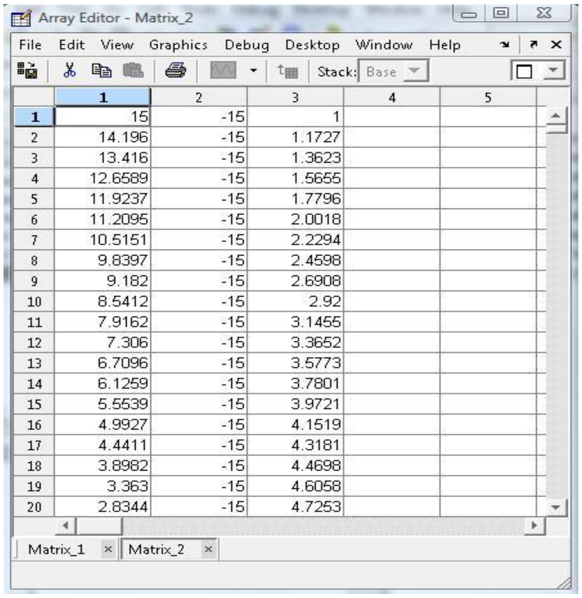

	1	2	3	4	5
1	15	-15	1		
2	14.196	-15	1.1727		
3	13.416	-15	1.3623		
4	12.6589	-15	1.5655		
5	11.9237	-15	1.7796		
6	11.2095	-15	2.0018		
7	10.5151	-15	2.2294		
8	9.8397	-15	2.4598		
9	9.182	-15	2.6908		
10	8.5412	-15	2.92		
11	7.9162	-15	3.1455		
12	7.306	-15	3.3652		
13	6.7096	-15	3.5773		
14	6.1259	-15	3.7801		
15	5.5539	-15	3.9721		
16	4.9927	-15	4.1519		
17	4.4411	-15	4.3181		
18	3.8982	-15	4.4698		
19	3.363	-15	4.6058		
20	2.8344	-15	4.7253		

Fig 3. 7 Data rearrangement in MATLAB

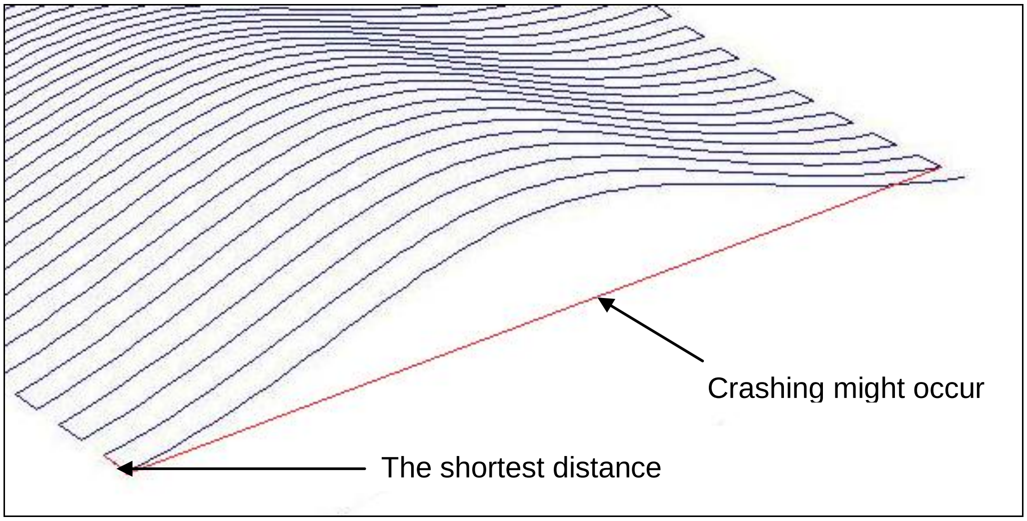

Fig 3. 8 Deposition path construction for a freeform surface

3.2.3 STL file route

The STL files are the de facto standard file format for all the RP currently and most of the models for RP are saved as STL format files. Although the STL file is made of a great deal numbers of small triangular facets, the triangle mesh is still able to represent the surfaces with reasonably high quality in terms of practical manufacturing. Therefore, gathering the surface point data from STL files is another option for the CLFDM process.

A STL file model, as shown in Fig 3. 9, can be created by any available 3D software, especially the 3D engineering software. Normally, owing to the fact that STL format files are in binary form, it is hard to gather the point data with the graphical users interface (GUI). Hence, an open source MATLAB program, written by Doron Harlev [39], is used for gathering the coordinates of vertex points of those triangles. The surface data obtained from this program is saved in data files in the form of four matrices containing X, Y, and Z coordinates and the color of each facet respectively. This data is further processed in MATLAB and the STL file model shown in Fig 3. 10 is created.

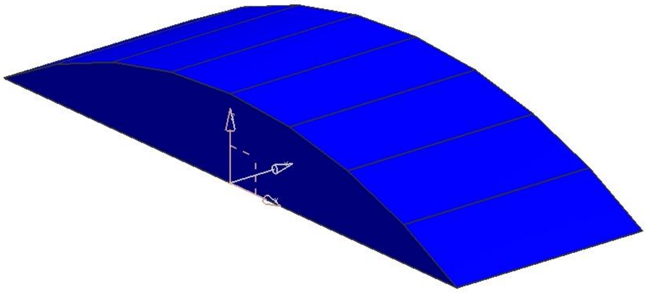

Fig 3. 9 A STL file model in CAD

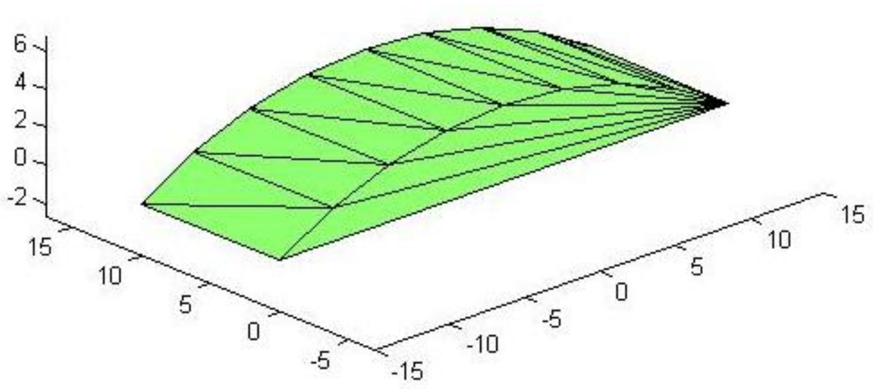

Fig 3. 10 A STL file model in MATLAB

After all coordinates of the vertices are located and saved in matrices, selected vertical planes are used to slice the STL model, which is similar to slicing with horizontal planes, as shown Fig 3. 11. Because the triangular facets share the edges, the vertical planes intersect the edges in some intersection points, and those points are the topology points of the surfaces, which is similar to gathering the data points from freeform surfaces.

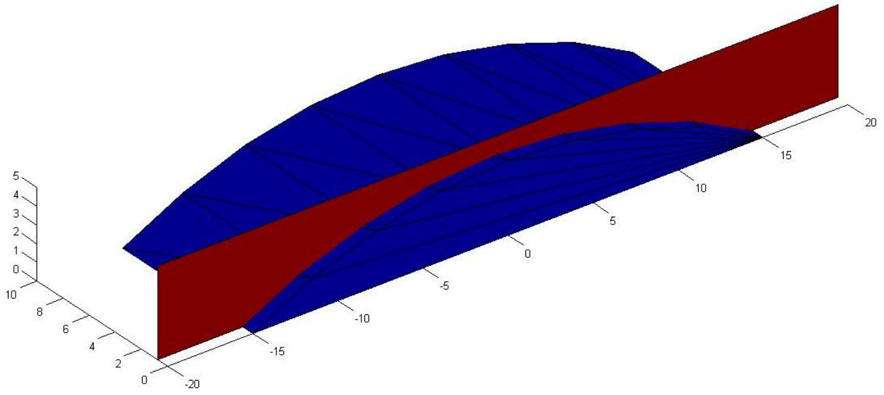

Fig 3. 11 Gathering surface point data from STL model by intersecting with a vertical plane

Then all the surface points are to be rearranged in a proper sequence and placed in a matrix with X, Y and Z coordinate columns. This matrix containing X, Y and Z coordinates is saved as a text format file and will be used as the input for the curved slicing program.

3.3 Curved slicing algorithms

Once the surface point data is generated using one of the methods discussed above, the next step is to develop parallel curved slices. The text file with the surface point data is the input to the slicing program. In this research, four different slicing algorithms have been introduced in order to slice the models with curved layers.

3.3.1 Vertical Surface Offsetting Algorithm (VSO)

VSO algorithm is the easiest and most basic slicing algorithm that works by offsetting the surface to construct the sliced layers and tool paths. This algorithm is implemented by simply lifting each point by a distance from the original place to construct a new layer until the entire surface is completed. In other words, it just increases the z-value by a layer thickness and then forms a new layer, while the x and y values are the same as on the input surface. By repeating this process on each successive new surface, a series of layers can be created.

Fig 3. 12 illustrates the VSO process. When the input text file is loaded in the slicing program, the x, y and z coordinates are stored in the matrix, which represents the shape of a surface, as shown in Fig 3. 13. $Pi_{-1,j,k}$, $P_{i,j,k}$, and $P_{i+1,j,k}$ are the points on the original surface, and $V_{i-1,j,k+1}$, $V_{i,j,k+1}$, and $V_{i+1,j,k+1}$ are the vectors in z direction. The slicing process is offsetting the z values of every data point; hence, the governing equation of VSO is as given below:

$$\overline{P_{i,j,k+1}} = \overline{P_{i,j,k}} + \overline{V_{i,j,k+1}} \qquad (3\text{-}1)$$

$P_{i-1,j,k+1}$, $P_{i,j,k+1}$, and $P_{i+1,j,k+1}$ are the new points on the offset curved layer. The vertical offsetting process is repeated continuously until all the required data points for the offset curved layer are obtained and the offset layer as well as the tool paths are constituted. Then the newly generated curved layer will be the original surface for the subsequent layers and the process is repeated as many times as required by the model.

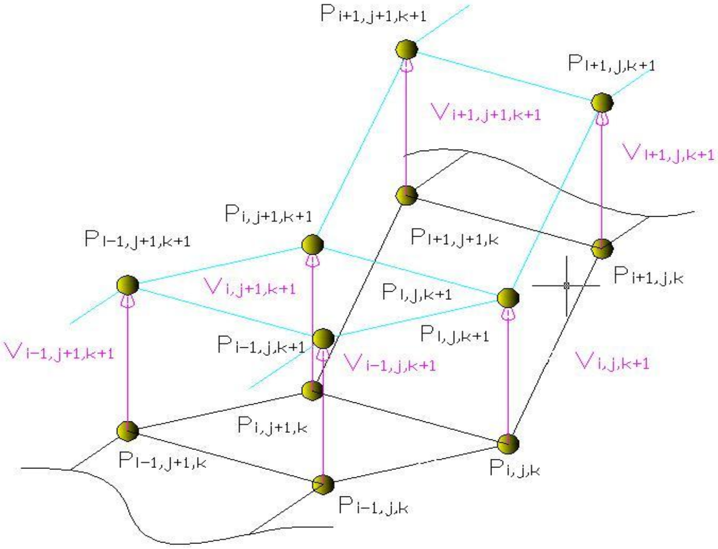

Fig 3. 12 Offsetting a curved layer with VSO algorithm

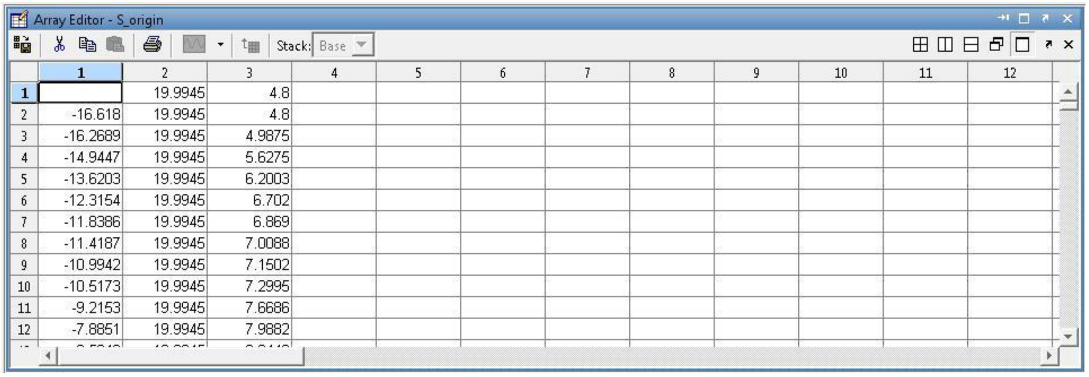

	1	2	3	4	5	6	7	8	9	10	11	12
1		19.9945	4.8									
2	-16.618	19.9945	4.8									
3	-16.2689	19.9945	4.9875									
4	-14.9447	19.9945	5.6275									
5	-13.6203	19.9945	6.2003									
6	-12.3154	19.9945	6.702									
7	-11.8386	19.9945	6.869									
8	-11.4187	19.9945	7.0088									
9	-10.9942	19.9945	7.1502									
10	-10.5173	19.9945	7.2995									
11	-9.2153	19.9945	7.6686									
12	-7.8851	19.9945	7.9882									

Fig 3. 13 Input data

Since the VSO algorithm contains the least calculations, time consumed for the calculations is less than in any other algorithm. However, there will be some problems for the parts modeled by the VSO algorithm during the deposition. When depositing fused material in the curved fashion, the thickness of the curved layer will be even from place to place, and might be a concern, especially at sharp corners. This might lead to interference in tool paths and cause the nozzle to crash on the part during the deposition. Further, the mechanical properties and shape of the model will be changed. The VSO algorithm however is fast and efficient for those thin parts without any sharp corners and curves.

3.3.2 Two Vector Cross Product Algorithm (TVCP)

TVCP is another slicing algorithm to offset curved layers. Owing to the fact that VSO algorithm is not able to make the offsetting distance evenly at every topology point, TVCP algorithm is developed, which employs the cross product of two vectors. In this slicing process, not only the *z* values of every surface point are changed but also the x and y values. The x and y coordinates of the new surface points on the offset layer are not necessarily the same as in the original layer and their locations are based on the direction of the cross product vector.

The TVCP slicing process is shown in Fig 3. 14. The data is loaded into the slicing program, which is similar to the program for VSO. Two vectors V_1 and V_2 are constructed by $P_{i,j,k}$, $P_{i-1,j,k}$ and $P_{i,j,k}$, $P_{i,j+1,k}$ respectively. The equations are as shown below:

$$\overline{V_1} = \overline{P_{i-1,j,k}} - \overline{P_{i,j,k}} \tag{3-2}$$

$$\overline{V_2} = \overline{P_{i,j+1,k}} - \overline{P_{i,j,k}} \tag{3-3}$$

Based on vectors V_1 and $V_{2,}$ the cross product vector V_{12} is constructed following the right–hand rule and the location of offsetting point will be in the direction of V_{12}. The magnitude of V_{12} should be taken equal to the thickness of the curved layer so as to keep even spacing between points on the offset curved surface and the original surface. The governing equation of V_{12} is given below:

$$\overrightarrow{V_{12}} = thickness \cdot \frac{\overrightarrow{V_2} \times \overrightarrow{V_1}}{\left|\overrightarrow{V_2} \times \overrightarrow{V_1}\right|} \tag{3-4}$$

Then, the point which V_{12} is pointing at is the point on the offset curved surface. Therefore, the governing equation of TVCP is:

$$\overline{P_{i,j,k+1}} = \overline{P_{i,j,k}} + \overline{V_{12}} \tag{3-5}$$

$P_{i,j,k+1}$ is the new point on the offset curved layer. Similarly, TVCP process is repeated continuously until all the required data points on the offset curved layer are obtained and the offset layer is formed. Then the offset curved layer will be the original surface for the new layer to be offset and the process is to be repeated until the entire model is sliced with curved layers together with the generation of the deposition path data.

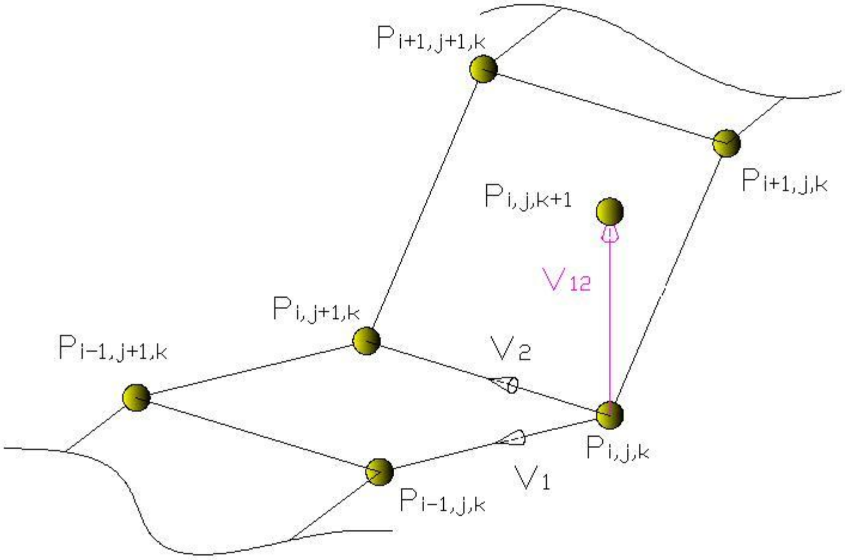

Fig 3. 14 Offsetting points with TVCP algorithm

Compared to the VSO algorithm, TVCP approach requires more number of calculations in order to make the offset layers more aligned with the original surface and the computational time is obviously high. The thickness at which the surface is offset being more even, avoids self interference and provides the models with better mechanical properties.

However, owing to the inefficient calculations during the slicing, one critical problem still exists, particularly in those places where the curvature changes drastically, as shown in Fig 3. 15. As the offsetting vector is only based on two vectors on the original curved surface, as shown in Fig 3. 14, it only demonstrates the curvature variations in the directions of the two vectors. In other words, the offsetting vector is not able to reflect the curvature variations in the entire adjacent area. It will become more obvious in places of dramatic curvature changes. Although the TVCP algorithm resolves some problems from VSO, it is again mainly suitable for those thin parts without any sudden changes in curvature.

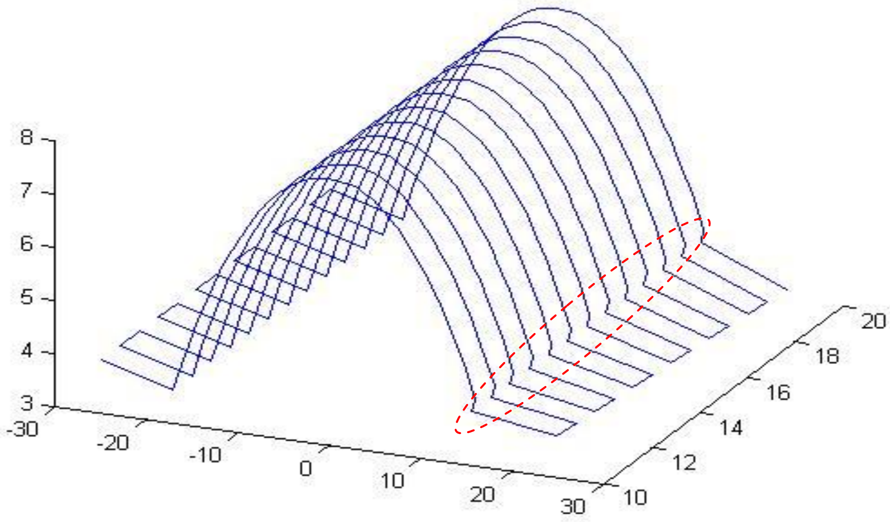

Fig 3. 15 Tool paths generated using TVCP

3.3.3 Four Vector Cross Product Algorithm (FVCP)

The FVCP algorithm is an extension to the TVCP for better slicing. Instead of using two vectors, the FVCP algorithm employs four vectors to construct the cross product vector, which reflects the curvature variations in the entire adjacent area, especially in those places of drastic curvature changes.

The FVCP slicing process is shown in Fig 3.16. As in the previous cases, the input data is loaded into the slicing program. Four Vectors V_1 , V_2 , V_3 and V_4 are constructed from any general point $P_{i,j,k}$ and the four adjacent points $P_{i-1,j,k}$, $P_{i+1,j,k}$ $P_{i,j-1,k}$, and $P_{i,j+1,k}$ respectively, which are:

$$\overline{V_1} = \overline{P_{i-1,j,k}} - \overline{P_{i,j,k}} \tag{3-6}$$

$$\overline{V_2} = \overline{P_{i+1,j,k}} - \overline{P_{i,j,k}} \tag{3-7}$$

$$\overline{V_3} = \overline{P_{i,j+1,k}} - \overline{P_{i,j,k}} \tag{3-8}$$

$$\overline{V_4} = \overline{P_{i,j-1,k}} - \overline{P_{i,j,k}} \tag{3-9}$$

In order to obtain the new offsetting point $P_{i,j,k+1}$, four cross product vectors V_{13} , V_{14}, V_{23} and V_{24} are constructed following the right–hand rule based on vectors V_1 , V_2 , V_3 and V_4. The magnitudes of all the cross product vectors are of the same and set equal to the thickness of the curved layer. The governing equations for V_{13}, V_{14}, V_{23} and V_{24} are given below:

$$\overrightarrow{V_{13}} = thickness \cdot \frac{\overrightarrow{V_3} \times \overrightarrow{V_1}}{\left|\overrightarrow{V_3} \times \overrightarrow{V_1}\right|} \tag{3-10}$$

$$\overrightarrow{V_{14}} = thickness \cdot \frac{\overrightarrow{V_1} \times \overrightarrow{V_4}}{\left|\overrightarrow{V_1} \times \overrightarrow{V_4}\right|} \tag{3-11}$$

$$\overrightarrow{V_{23}} = thickness \cdot \frac{\overrightarrow{V_3} \times \overrightarrow{V_2}}{\left|\overrightarrow{V_3} \times \overrightarrow{V_2}\right|} \tag{3-12}$$

$$\overrightarrow{V_{24}} = thickness \cdot \frac{\overrightarrow{V_2} \times \overrightarrow{V_4}}{\left|\overrightarrow{V_2} \times \overrightarrow{V_4}\right|} \tag{3-13}$$

In most of the cases those four cross product vectors are not pointing at the same end point during the calculation. Therefore, a common end point for those vectors is necessary, which will be the new point on the offset curved surface. In Fig 3. 16(a), Point Pi,j,k$_{+1}$ is the offset point on the new curved surface and V_5 is the new vector pointing from $P_{i,j,k}$ to $P_{i,j,k+1}$. The direction of V_5 can be obtained easily by adding those four cross product vectors. However, the magnitude of V_5 is hard to obtain by only adding vectors together and it is not equal to the thickness of the curved layer. For acquiring the magnitude of V_5, two more vectors $V_{13,14}$ and $V_{23,24}$ are needed.

As shown in Fig 3. 16(b), the direction of $V_{13,14}$ can be obtained by adding V_{13} and V_{14} together. The magnitude of $V_{13,14}$ equals to the distance from $P_{i,j,k}$ to the intersection point of l_1 and l_2 extensions, which are paralleled to $P_{i,j-1,k}P_{i,j,k}$ and $P_{i,j+1,k}P_{i,j,k}$ respectively. In order to calculate the magnitude of $V_{13,14}$, the angle α between V_{13} and V_{14} is need to be calculated. The equation of angle α_1 is:

$$\alpha_1 = acos\frac{\overline{V_{13}} \cdot \overline{V_{14}}}{|\overrightarrow{V_{13}}| \cdot |\overrightarrow{V_{14}}|} \tag{3-14}$$

Because l_1 is paralleled to $P_{i,j-1,k}P_{i,j,k}$, so V_{14} is perpendicular to l_1, $V_{13,14}$ is equal to:

$$\overrightarrow{V_{13,14}} = \frac{thickness}{cos\frac{\alpha_1}{2}} \cdot \frac{\overrightarrow{V_{13}} + \overrightarrow{V_{14}}}{|\overrightarrow{V_{13}} + \overrightarrow{V_{14}}|} \tag{3-15}$$

Then repeating the same calculations on $V_{23,\,24}$:

,

$$\alpha_2 = acos\frac{\overline{V_{23}} \cdot \overline{V_{24}}}{|\overrightarrow{V_{23}}| \cdot |\overrightarrow{V_{24}}|} \tag{3-16}$$

$$\overrightarrow{V_{23,24}} = \frac{thickness}{\cos\frac{\alpha_2}{2}} \cdot \frac{\overrightarrow{V_{23}} + \overrightarrow{V_{24}}}{\left|\overrightarrow{V_{23}} + \overrightarrow{V_{24}}\right|} \qquad (3\text{-}17)$$

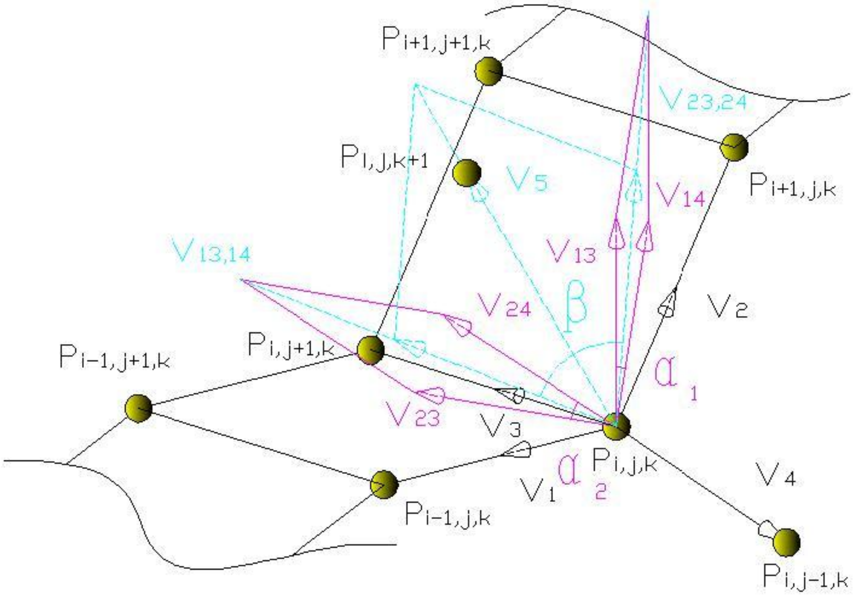

(a) Overall schematic

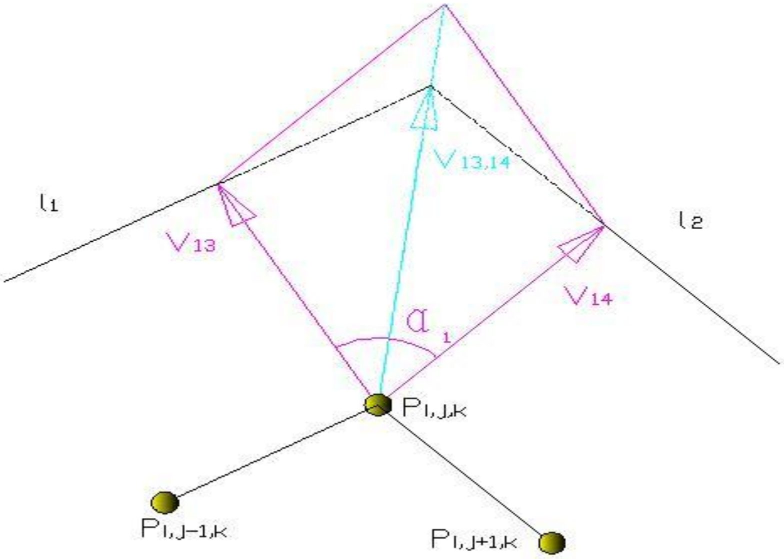

(b) Schematic of $V_{13,14}$

Fig 3. 16 Offsetting a point using FVCP algorithm

Because V_5 is based on $V_{13,14}$ and $V_{23,24}$, a similar calculation will be repeated again so as to get V_5.

$$\beta = acos\frac{\overrightarrow{V_{13,14}} \cdot \overrightarrow{V_{23,24}}}{\left|\overrightarrow{V_{13,14}}\right| \cdot \left|\overrightarrow{V_{23,24}}\right|} \tag{3-18}$$

Meanwhile, the magnitude of V_5 is needed to be re-calculated. Hence, the govern equation of V_5 is:

$$\overrightarrow{V_5} = \frac{thickness}{cos\frac{\alpha_1}{2}cos\frac{\beta}{2}} \cdot \frac{\overrightarrow{V_{13,14}} + \overrightarrow{V_{23,24}}}{\left|\overrightarrow{V_{13,14}} + \overrightarrow{V_{23,24}}\right|} \tag{3-19}$$

Then, the point which V_5 is pointing at is the point of the offsetting curved surface. Therefore, the final expression for FVCP is:

$$\overrightarrow{P_{i,j,k+1}} = \overrightarrow{P_{i,j,k}} + \overrightarrow{V_5} \tag{3-20}$$

$P_{i,j,k+1}$ is the new point on the offset curved layer. Similarly, FVCP process is repeated continuously until the required data points for the entire offset curved layer are obtained and the offset layer is formed. Again a further repetition of the whole process with the newly generated layer would allow construction of data points and deposition head path ways for as many curved layers as needed to complete the CAD model.

Compared to VSO and TVCP, FVCP algorithm needs many more calculations and obviously more computational time. However, it goes beyond TVCP, and the resulting curved layers evenly match the shape of the original surface, even at places of drastic curvature changes.

But the FVCP algorithm has its own limitation, in that it is too sensitive and dependent. In the FVCP slicing method, the input data needs to be sufficient and complete. If one of the data points is missing in the input data, the whole slicing process would be getting into a dull loop. Therefore, it is just fit for those thin parts with sufficient data, although it resolves some problems from VSO and TVCP.

3.3.4 Modified Four Vectors Cross Product Algorithm (MFVCP)

The MFVCP algorithm is a modified version of the FVCP. Instead of using four vectors, the MFVCP algorithm employs two vectors on the surface and one auxiliary vector to construct the cross product vector. Those three vectors can represent the curvature variations in the entire adjacent area. Unlike FVCP, the MFVCP algorithm is less sensitive and more independent by assuming all the data point lying on the same vertical plane.

The MFVCP slicing process is shown in Fig 3. 17. After loading the input data into the slicing program, two vectors V_1 and V_2 are constructed by $P_{i,j,k}$, $P_{i-1,j,k}$ and $P_{i,j,k}$, $P_{i+1,j,k}$ respectively:

$$\overline{V_1} = \overline{P_{i-1,j,k}} - \overline{P_{i,j,k}} \qquad (3\text{-}21)$$

$$\overline{V_2} = \overline{P_{i+1,j,k}} - \overline{P_{i,j,k}} \qquad (3\text{-}22)$$

Whilst the auxiliary vector V_3 is perpendicular to the vertical plane J from $P_{i,j,k}$.

Two cross product vectors V_{13} and V_{23} are constructed following the right–hand rule based on vectors V_1, V_2, V_3. The magnitudes of all the cross product vectors are equal to the thickness of the curved layer. The governing equations of V_{13}, and V_{23} are:

$$\overrightarrow{V_{13}} = thickness \cdot \frac{\overrightarrow{V_1} \times \overrightarrow{V_3}}{\left|\overrightarrow{V_1} \times \overrightarrow{V_3}\right|} \qquad (3\text{-}23)$$

$$\overrightarrow{V_{23}} = thickness \cdot \frac{\overrightarrow{V_3} \times \overrightarrow{V_2}}{\left|\overrightarrow{V_3} \times \overrightarrow{V_2}\right|} \qquad (3\text{-}24)$$

Similar to FVCP, V_5 is based on V_{13} and V_{23}, The equation of angle α is:

$$\alpha = acos \frac{\overline{V_{13}} \cdot \overline{V_{23}}}{\left|\overrightarrow{V_{13}}\right| \cdot \left|\overrightarrow{V_{23}}\right|} \qquad (3\text{-}25)$$

And the governing equation of V_5 is:

$$\overrightarrow{V_5} = \frac{thickness}{cos\frac{\alpha}{2}} \cdot \frac{\overrightarrow{V_{13}} + \overrightarrow{V_{23}}}{\left|\overrightarrow{V_{13}} + \overrightarrow{V_{23}}\right|} \qquad (3\text{-}26)$$

Then, the point which V_5 is pointing at is the point of the offset curved surface. Therefore, the governing equation of FVCP is:

$$\overrightarrow{P_{i,j,k+1}} = \overrightarrow{P_{i,j,k}} + \overrightarrow{V_5} \qquad (3\text{-}27)$$

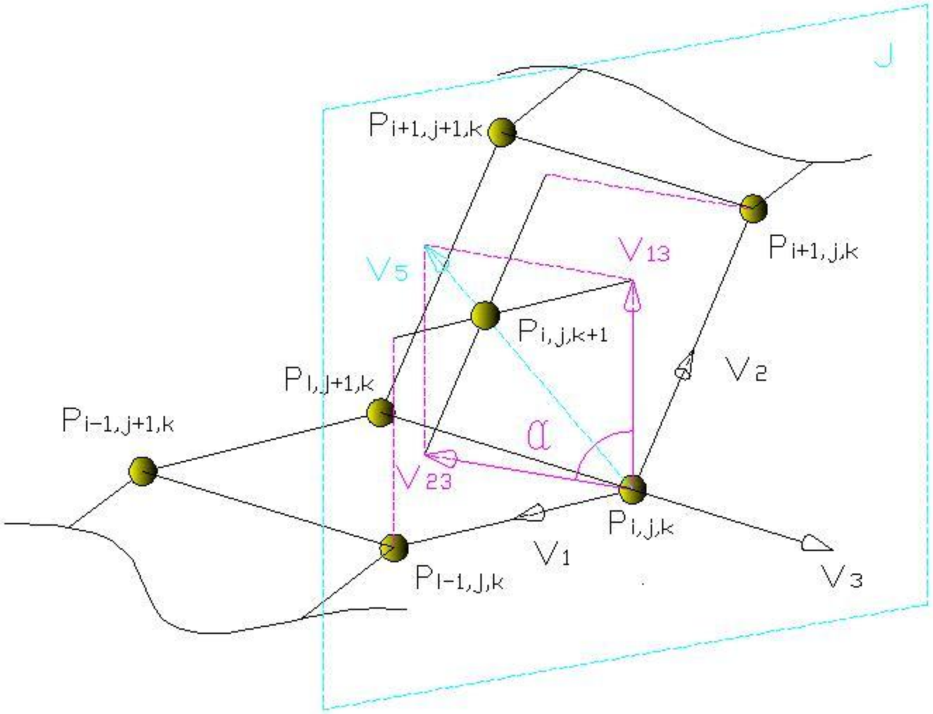

Fig 3. 17 Offsetting a point using the MFVCP algorithm

P $_{i,j,k+1}$ is the new point on the offsetting curved layer. Similarly, MFVCP process is repeated continuously until the required data points for the offset curved layer are generated and the offsetting layer is formed. The process is then repeated for the entire model.

Compared to FVCP, the calculations and the time for slicing are reduced. It has all advantages of TVCP and FVCP and is less sensitive and more independent. Even if some of the data points are missing, the algorithm can still continue with the slicing process. Hence, MFVCP algorithm is the best solution for the construction of the curved layered slices.

3.4 Curved slicing complexities

Although the most appropriate slicing algorithm has been chosen and run in the RP machine, there still are some complexities need to be overcome properly during the slicing process. These are self intersections and duplicated interferences.

3.4.1 Self Intersection (SI) and Self intersection elimination algorithm (SIEA)

Self Intersection (SI)

After the curved surface is offset, inward points and outward points, as shown in Fig 3. 18, may occur in the slicing tool paths owing to the drastic slope changes of curves.

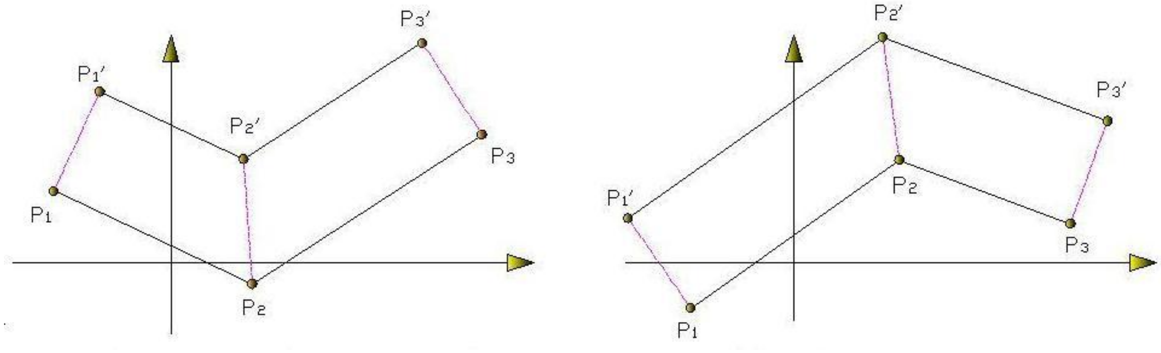

(a) *(b)*

Fig 3. 18 (a) Inward offset and (b) Outward offset points

In a random vertical plane, for instance, plane J in Fig 3.17, line $P_1P_2P_3$ is the tool path on the original surface, whereas line $P_1'P_2'P_3'$ is the tool path on the next layer, which is offset from $P_1P_2P_3$. If those points are close to each other, self intersections might occur. For those outward points, the offset lines have a trend to expand, as shown in Fig 3. 19. Even if the adjacent points are very close, there is still enough space for them and self intersection will never happen in outward points. At the endpoints of two offset lines, the MFVCP slicing program will extend those two offset lines and combine them in a new common endpoint.

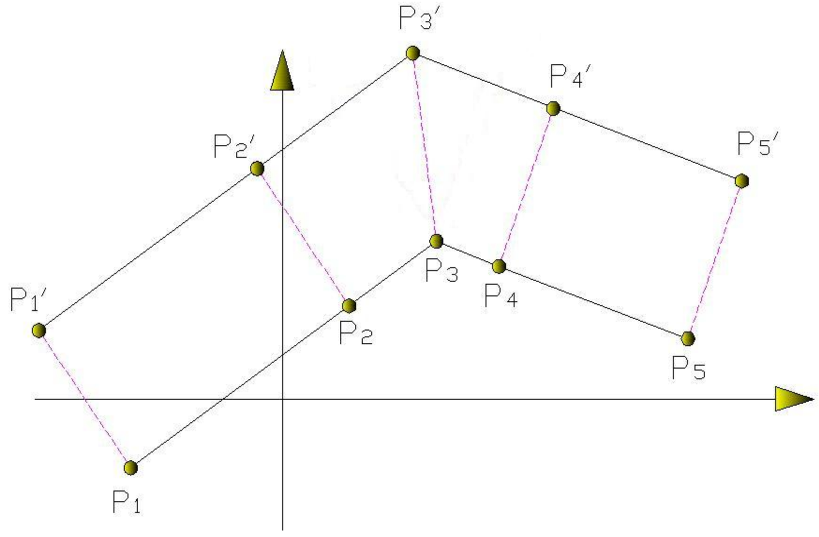

Fig 3. 19 Offsetting a convex surface

In the Line $P_1P_2P_3P_4P_5$, the direction of the tool motion follows the sequence of the points from P_1 to P_5. After offsetting, the direction of the tool motion will not be changed; it is still following the sequence of the offset points. However, instead of passing through the offsetting new end points P'_{3a} and P'_{3b} , it will pass through the new common endpoint P'_3 of the two offset lines.

Self intersection mostly occurs in concave shapes owing to the deep thickness in the trough. One of the self intersection cases is shown in Fig 3. 20. The offset points are P'_1,P'_2 ,P'_3,P'_4 and P'_5. Ideally, it is better if the new offset line is $P'_1P'_3P'_5$ and the nozzle head passes through P'_1 ,P'_3 and P'_5 , skipping P'_2 and P'_4 . However, in the actual case, P'_2 and P'_4 still exist, and the tool still follows the full sequence of points, including P'_2 and P'_4. It means the nozzle head would work from P'_1 to P'_5 and goes throughP'_2 , P'_3 andP'_4 . Therefore, the SI situations would occur and it would make the nozzle head crash on the parts during the deposition.

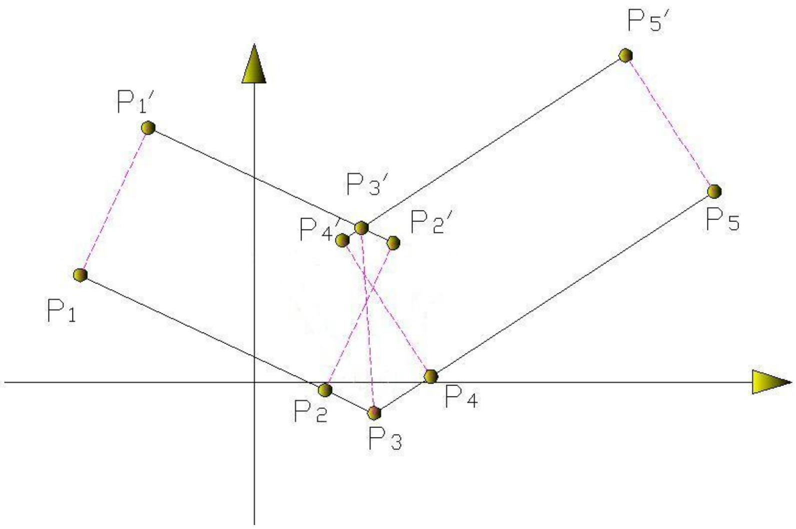

Fig 3. 20 Offsetting a concave surface

If self intersecting points resulted in the first offset layer, the errors would continue and multiply during the subsequent offsetting process, resulting in the curved layers not matching with the shapes they are supposed to take. The deposition head path curves become erroneous and the errors get accumulated and magnified from one layer to the next. The cutter paths of one of the solid models distorted due to self intersected points is shown in Fig 3. 21(a) below. Compared to the original part in Fig 3. 21(b), the deposition path data and the final shape of the part are lost. Hence, Self Intersection is a serious problem and needs an Elimination Algorithm (SIEA).

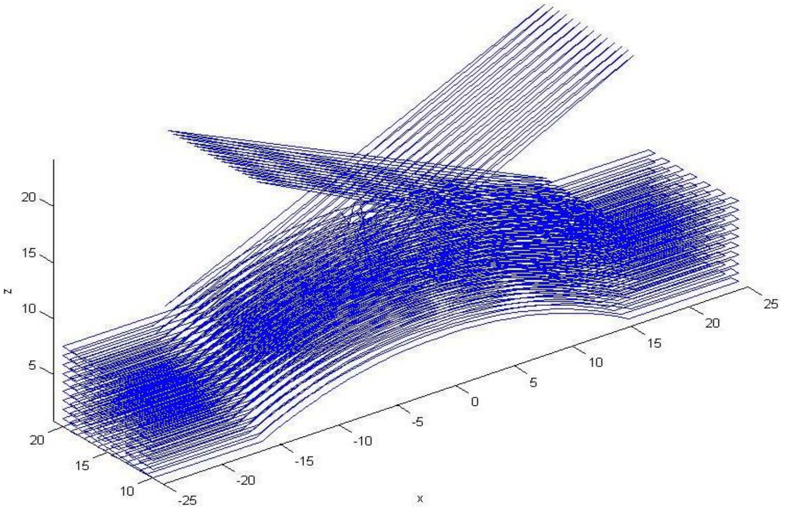

(a) Distorted deposition head path data

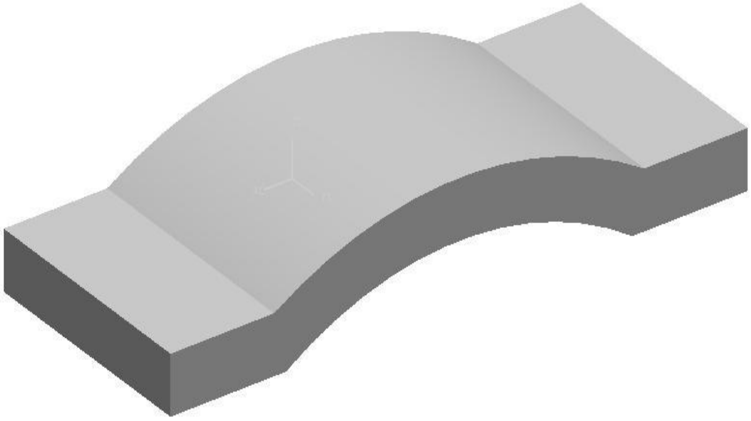

(b) Original part

Fig 3. 21 Self Intersection problems

Self Intersection elimination algorithm (SIEA)

In order to eliminate the self intersecting points, the algorithm developed needs some additional data to be supplied with each surface point. For this, three extra columns are added in the input data files after the columns containing X, Y and Z coordinates. The fourth, fifth and sixth columns, which are named as Extra Information (EI) columns, have been introduced in the input matrix, and contain data representing the serial number of the point, tool direction and the constitutive vertical plane respectively. As shown in Fig 3. 22 Extra Information (EI) columns in the input Matrix, the data in the fifth column represents the direction of tool motion: “1” indicates that the motion of the nozzle head is forwards, and “0” indicates backward motion. Further, when these values of three successive points are considered together, a number of possible motions result as shown in Table 3. 1.

Table 3. 1 Motions of deposition nozzle

Motion	Previous	Now	Next
Back	0	0	0

Back-Left	0	0	1
Back (Pulse)	0	1	0
Left-Forward	0	1	1
Left-Back	1	0	0
Forward(Pulse)	1	0	1
Forward-Left	1	1	0
Forward	1	1	1

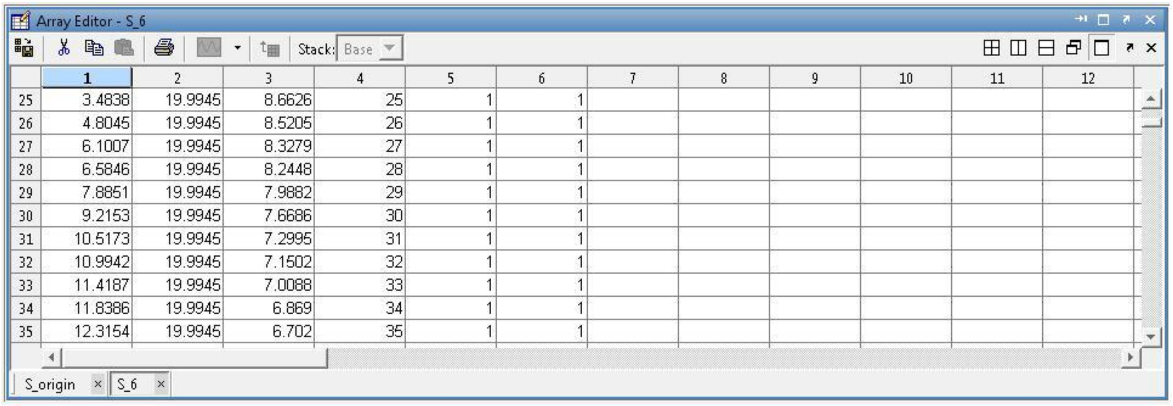

	1	2	3	4	5	6	7	8	9	10	11	12
25	3.4838	19.9945	8.6626	25	1	1						
26	4.8045	19.9945	8.5205	26	1	1						
27	6.1007	19.9945	8.3279	27	1	1						
28	6.5846	19.9945	8.2448	28	1	1						
29	7.8851	19.9945	7.9882	29	1	1						
30	9.2153	19.9945	7.6686	30	1	1						
31	10.5173	19.9945	7.2995	31	1	1						
32	10.9942	19.9945	7.1502	32	1	1						
33	11.4187	19.9945	7.0088	33	1	1						
34	11.8386	19.9945	6.869	34	1	1						
35	12.3154	19.9945	6.702	35	1	1						

Fig 3. 22 Extra Information (EI) columns in the input Matrix

There are eight combinations of 1s and zeros identified in Table 3. 1, which identify eight different possible motions of the deposition head. For example, the sequence 0 0 0 indicates backward motion from the first node to the last. Similarly, 1 1 1 indicates forward motion from the first to the last node. However, 1 1 0 represents a forward motion from node 1 to node 2 and then a reversal from node 3, which signifies that the cutter will take a leftward step from node2 to 3 and starts moving backward from node 3. These are the typical cases where the tool reaches the end of a deposition line and takes a side-step and starts moving backward in the subsequent line. The other combinations explain similar such situations. The meanings of some of these combinations are illustrated in Fig 3. 23.

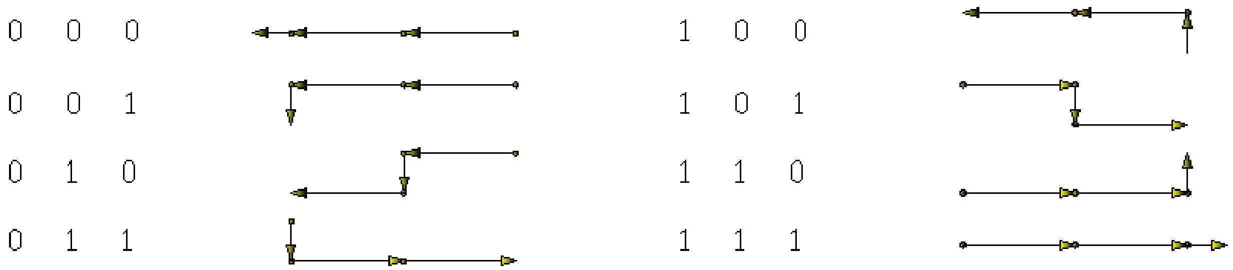

Fig 3. 23 Combinations of head motions

In Fig 3. 20, P_2' and P_4' are the extra points resulting in self intersection. Those extra points have to be eliminated; otherwise the tool would crash on the parts during the deposition. In order to eliminate the extra points, the information in the EI columns will be used. The whole operation of eliminating these extra points involves decisions to be made based on several aspects of the data related to the points that happens in different stages as described below:

Stage I

First, the base points on the surface are sorted based on the vertical plane number input in column 6. All points lying on the same vertical plane are grouped together. The next stage is to establish whether at each of these points, the surface profile is convex or concave. This is done as explained in the next stage.

Stage II: Identifying the concavity

As explained earlier, the self intersection is a problem in concave troughs only. Hence, it is important to find out whether the surface in question is convex or concave. Every two adjacent points on a vertical plane J can be used to construct a line segment with a slope K. When the tool moves forward along three nodes, when the value of the fifth column (direction column) is "1", two adjacent line segments would be formed for any three consecutive points as shown in Fig 3. 24.

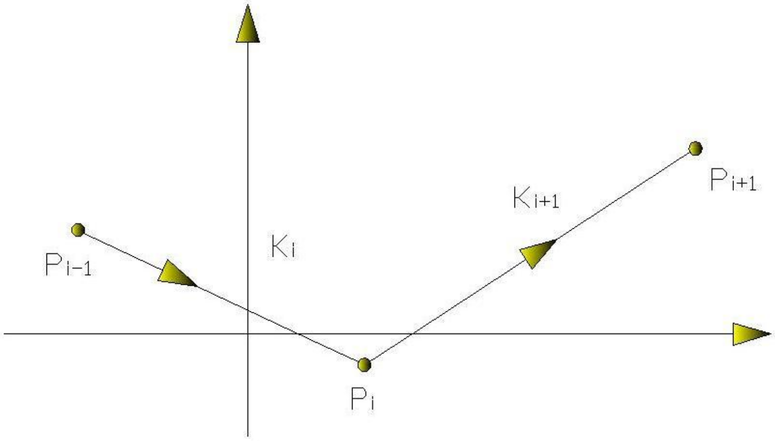

Fig 3. 24 Forward motion

The equations of the two line segments can be obtained from the coordinates of P_1, P_2 and P_3. The slopes of the two line segments K_i and K_{i+1} can be calculated by deriving these two equations. A comparison of the two slopes allows estimation of the nature of the trough. If K_i < K_{i+1} the sequence of points forms a concave trough and the rest of the stages of self intersection elimination algorithm will be carried out on these points. Otherwise, the program leaves the algorithm and proceeds with the next point. This procedure is repeated for each and every surface point. For the points at the start and the end of a line, extra points are created outside the line by incrementing the X values, just for the evaluation of the slopes of two successive line segments. Sample calculations for a set of three points are shown below:

One concave point case is shown in Table 3. 2

Table 3. 2 Concave point data

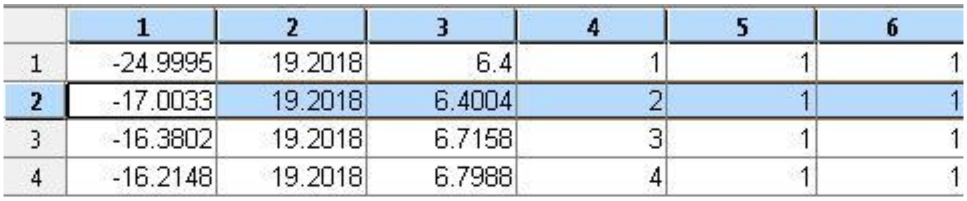

	1	2	3	4	5	6
1	-24.9995	19.2018	6.4	1	1	1
2	-17.0033	19.2018	6.4004	2	1	1
3	-16.3802	19.2018	6.7158	3	1	1
4	-16.2148	19.2018	6.7988	4	1	1

The values of fifth and sixth column are “1”, which means the deposition head motion there is forward and all the points are in the same vertical plane. Assume the first point, second point and the third point areP_1 , P_2 and P_3 respectively. So,

$$P_1 = (-24.9995 \quad 6.4000)$$
$$P_2 = (-17.0033 \quad 6.4004)$$
$$P_3 = (-16.2148 \quad 6.7158)$$

Thus, the slope K_{12} and K_{23} are:

$$K_{12} = \frac{6.4000 - 6.4004}{(-24.9995) - (-17.0033)} = 0$$
$$K_{23} = \frac{6.7158 - 6.4004}{(-16.2148) - (-17.0033)} = 0.5062$$

By comparison, K_{23} is greater than K_{12}, which means, P_2 is the concave point. The serial number of the point where the surface profile is identified as concave is used to identify points in the offset layers where subsequent correction methods need to be applied.

Stage III

The self intersection case of Fig 3. 20 is repeated in Fig 3. 25 for explaining the lgorithm used to eliminate self intersection. Once the points that were offset from a concave surface are identified like P3’ shown in Fig 3.25, as all these points are lying on the same vertical plane, self intersection can be identified and eliminated by comparing the X coordinates of successive (increasing serial number) points. Points P_1' to P_5' are all on the same vertical plane and have increasing serial number. There are two checks made now. If the X coordinate of a point with a lower serial number (such as P_2') is greater than that of a point with a higher serial number (P_3'), the point with the lower serial number will be eliminated, which is P_2' in the above case. Similarly, if a point with a higher serial number (Such as P_4') has a lower X coordinate than that of a point with a lower serial number (such as P_3'), eliminate the point with the higher serial number, which is P_4' in this case.

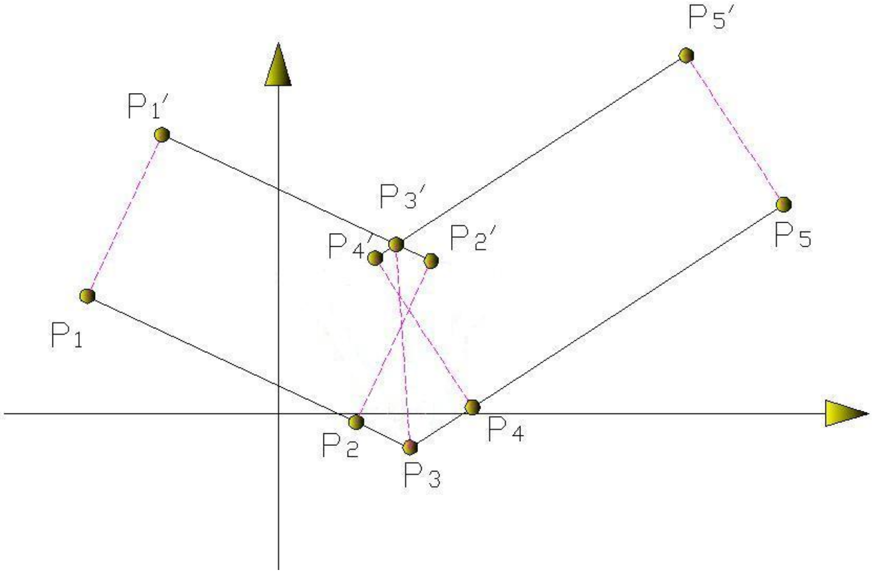

Fig 3. 25 Self Intersecting Points

When tool moves backwards in which case, the value of the fifth column (direction column) would be “0”; the two adjacent lines would be formed as shown in Fig 3. 26. Similar to the previous case, K_i is always smaller than K_{i+1} at points where a concave trough forms. Hence the elimination process proceeds in the same fashion as in the previous case, but with a variation in the X values compared. As shown in Fig. 3.26 if the X coordinate of a point with a lower serial number (such as P_2') is greater than that of a point with a higher serial number (P_3'), the point with the lower serial number will be eliminated, which is P_2' in the above case. Similarly, if a point with a higher serial number (Such as P_4') has a lower X coordinate than that of a point with a lower serial number (such as P_3'), eliminate the point with the higher serial number, which is P_4' in this case.

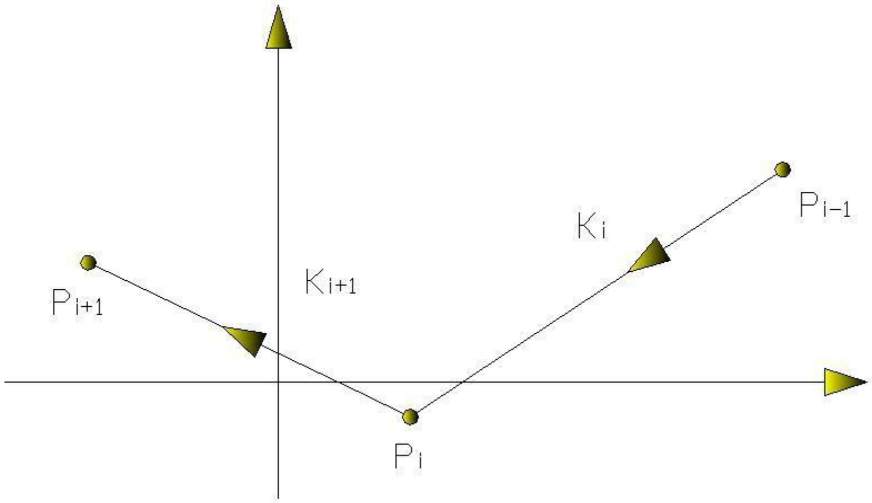

Fig 3. 26 Backward motion

The self intersection elimination algorithm is used to check all the points on each of the deposition path curves targeting elimination of all self intersection points. Once self intersection points are removed, the curved layers attain shapes matching the actual surfaces of the part.

3.4.2 Multi-point Interference (MI) and Elimination Algorithm (MIEA)

Multi-point Interference (MI)

Similar to self intersections, the Multi-point interferences occur in concave troughs as shown in Fig 3. 27, where two or more points on the deposition path become concurrent. The resulting duplicated points in the matrix are shown in Fig 3. 28.

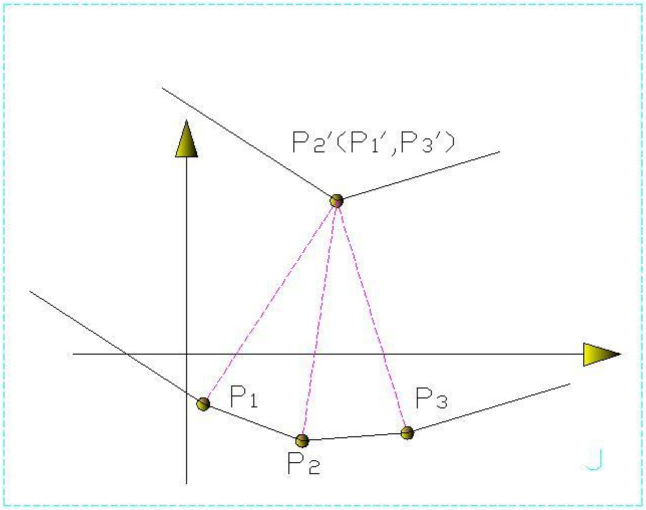

Fig 3. 27 Multi-point Interference

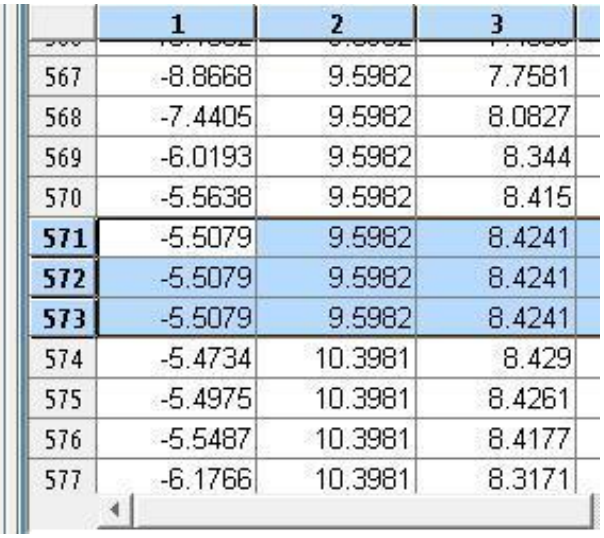

	1	2	3
567	-8.8668	9.5982	7.7581
568	-7.4405	9.5982	8.0827
569	-6.0193	9.5982	8.344
570	-5.5638	9.5982	8.415
571	-5.5079	9.5982	8.4241
572	-5.5079	9.5982	8.4241
573	-5.5079	9.5982	8.4241
574	-5.4734	10.3981	8.429
575	-5.4975	10.3981	8.4261
576	-5.5487	10.3981	8.4177
577	-6.1766	10.3981	8.3171

Fig 3. 28 Duplicated points

In plane J, $P_1P_2P_3$ is the line on the original surface, whereas $P_1'P_2'P_3'$ is the offset line. Due to the concurrency of the three points, the offset line is reduced to a single point and results in redundancy. However, inside the program, they are still treated as three different points.

Unlike self intersecting points on the same layer, these multi-points points are no big harm to the layer, if they exist on the final layer as the machine would work on those three points as one point. There may be a little more of material deposition due to a slightly higher dwell period. However, if that layer happens to be one of the base layers from which other curved layers are offset, singularities may arise. As vectors are constructed with two points that are geometrically the same, the vector operations will result in singularities. The ill calculated coordinates result in a dull loop on the machine. Fig 3. 29 shows the effect of duplicate points on the final deposition path pattern. These missing connections affect the continuity of the filament and the RP machine ceases working after encountering an ill formed point. Therefore, Multi-point Interference Elimination Algorithm (MIEA) is necessary.

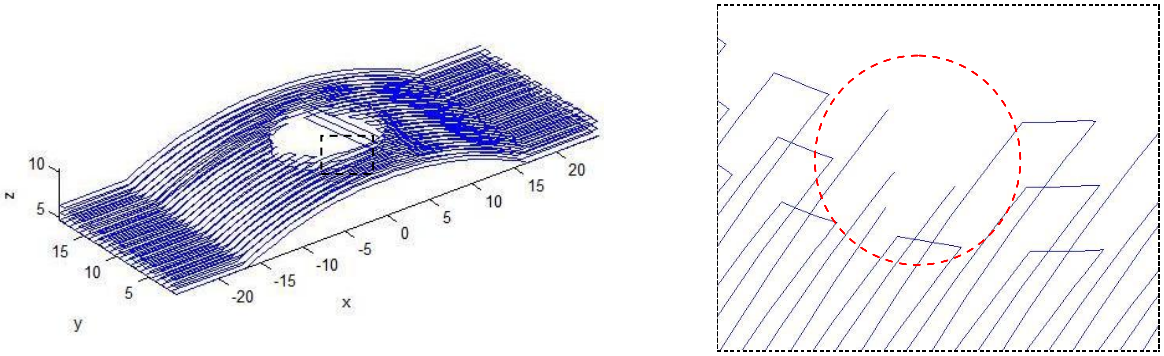

Fig 3. 29 Effect of duplicate points: missing links in deposition path patterns

Multipoint Interference elimination (MIE)

As shown in Fig 3.30, some duplicated points might exist in the matrix. In order to eliminate the duplication, a further check is input into the program, which works essentially based on a verification of the coordinates of successive points. This module scans all points along the deposition path lines in each layer comparing the coordinates of each pair of successive points. Each point on a given layer would have a unique geometric location and if the coordinates of two successive points come out to be the same, the second point will be dropped from the matrix. For instance points P_2' and P_3' of Fig 3. 27, will be eliminated, from the data point matrix as shown in Fig 3. 30.

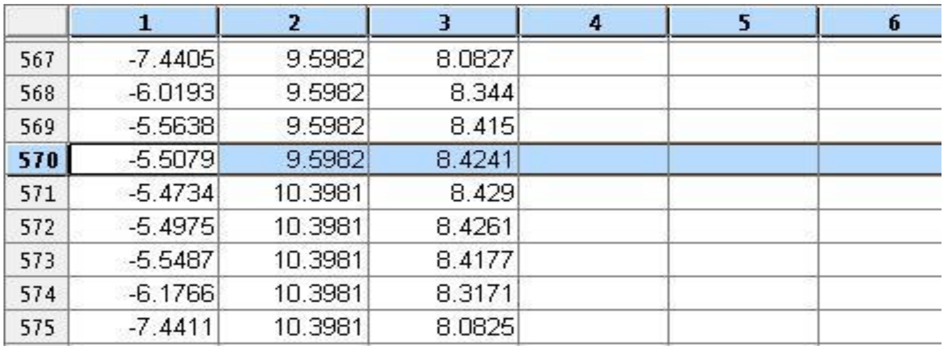

	1	2	3	4	5	6
567	-7.4405	9.5982	8.0827			
568	-6.0193	9.5982	8.344			
569	-5.5638	9.5982	8.415			
570	-5.5079	9.5982	8.4241			
571	-5.4734	10.3981	8.429			
572	-5.4975	10.3981	8.4261			
573	-5.5487	10.3981	8.4177			
574	-6.1766	10.3981	8.3171			
575	-7.4411	10.3981	8.0825			

Fig 3. 30 Duplication is eliminated in the data point matrix

3.5 Support material structure

After running the Self Intersection Elimination SIEA program, a series of curved layers, including the bottom surface will be created. The bottom surface should be used as the top surface of the support structure, which forms the substrate for the fused deposition of the model using curved layers. For instance, the bottom surface of Fig 3. 1 is as shown in Fig 3. 31.

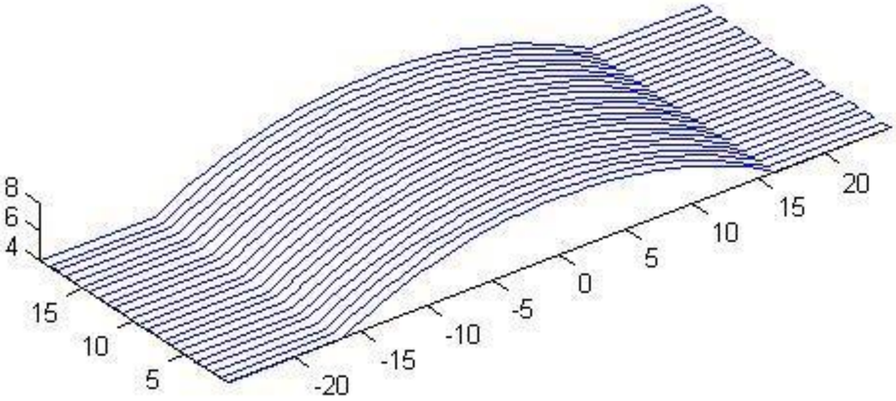

Fig 3. 31 The bottom surface

In order to build the part shown in Fig 3. 1, a simple half cylinder-like support structure, as shown in Fig 3. 32, is required as the material deposited in curved layered fashion cannot float in the air without the support structure during the deposition. The support structure would be built in flat layers because it is easy to build and the quality requirement of the top surface is not very high.

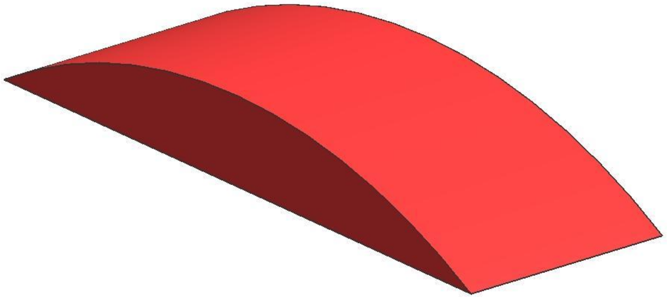

Fig 3. 32 Support structure

Although the support structure shown in Fig 3. 32 is a solid block, however, in actual case, only data points based on the bottom surface of the part are known. As a result, the flat layered support structure would have to be generated based on the bottom surface of the curved layered model.

There are two possible solutions to the problem of generating the flat layer support structure: directly building the support structures from STL files using CAD software, or slicing the bottom surface of the part with flat layers. The former method is similar to the processing in traditional RP. In this research, the latter method is used, as shown in Fig 3. 33. As the layer thickness is preset, the total number of the flat layers can be evaluated by dividing the total height with the layer thickness.

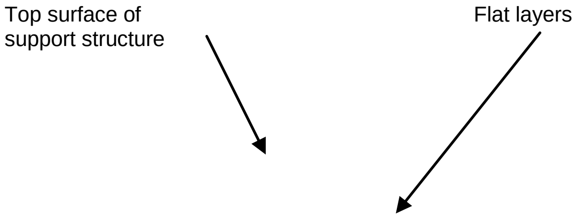

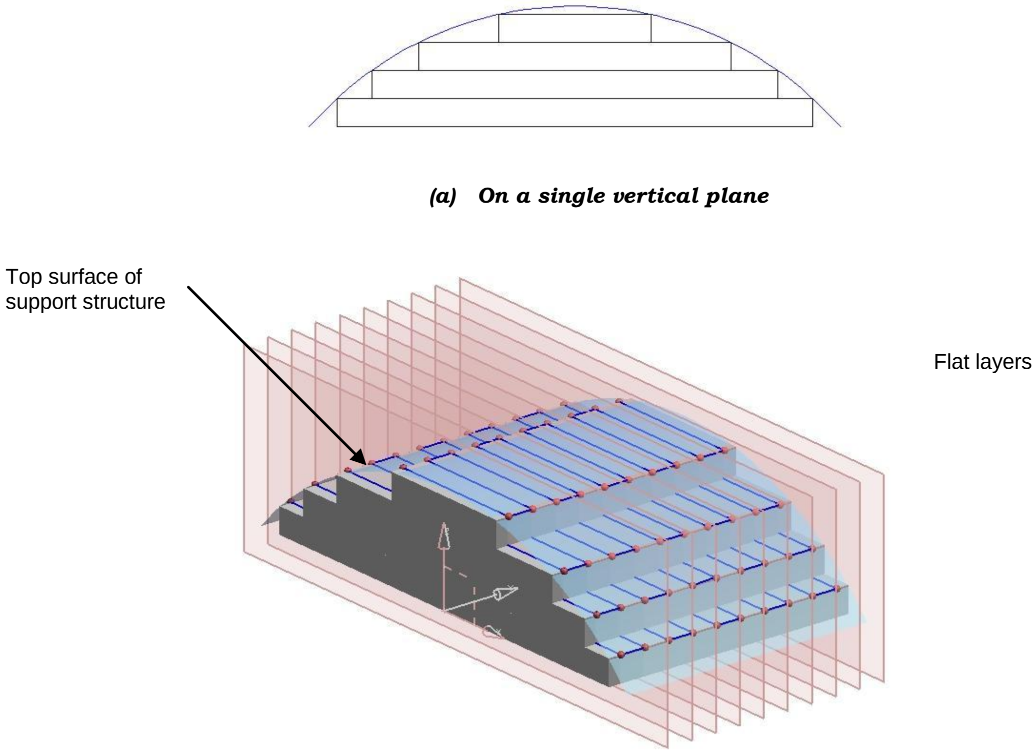

(a) On a single vertical plane

(b) When repeated on a series of vertical plane

Fig 3. 33 Evaluation of flat layered support structure

Algorithm for flat layer support structure

On any of the vertical plane, the deposition paths are constructed by a series of straight line segments. Three types of relationships are likely to occur between a randomly placed line segment and the top surface of the support structure layer. The top layer of the support structure is below the lowest point of the straight line, or above the highest point, or intersects with the straight line, as shown in Fig 3. 34.

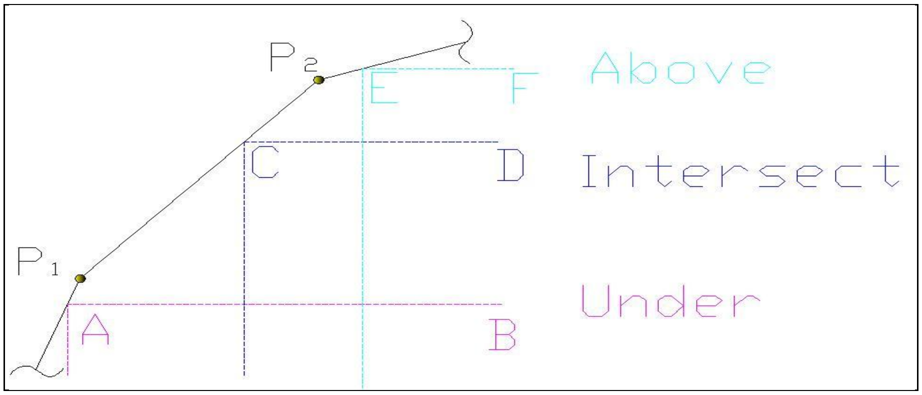

Fig 3. 34 Relationship between top surface of support structure and flat layers

The flat layer slicing algorithm for the support structure uses the bottom layer of the curved part as the base and proceeds evaluating different layers comparing their relative positions with respect to the line segments defining the bottom surface. In Fig 3. 34, P_1P_2 is a random line segment on the bottom surface of the model, which is ideally the top surface of the support structure and P_1 is the lowest point of the straight line and P_2 is the highest. AB, CD and EF are three possible top surfaces of the flat layers of the support structure with different thicknesses.

The top surface, say EF of the flat layer is above P_2 means total height of the flat layer exceeds the highest point of the line segment P1P2. When this happens, this flat layer will be discarded if P_2 is the highest point on this curve in a vertical plane and the flat layer slicing process will end. Otherwise, this layer will be processed considering the next straight line segment and the slicing process continues.

If the top surface CD of the flat layer intersects with P_1P_2, the flat layer becomes a valid and acceptable flat layer of the support structure. Those coordinates of intersection points would be calculated and used to evaluate the shape of that flat layer. This case might happen more than once in the same line segment, depending on the thickness of the flat layers and the total height of the stacked layers.

If the top surface EF of the flat layer is belowP1, it means that the flat layer has not yet reached the domain of P1P2 in the elevation. However, this case will never arise, as the current algorithm works from bottom upwards checking whether the flat layer is within the line segment or above it.

When the top surface of the flat layer intersects with the straight line in the same vertical plane J, as shown in Fig 3. 35, there is a unique intersection point between the straight line and the layer. The linear equation of the straight line segment is obtained from the coordinates of the two coplanar end points. Then, the coordinate of the intersecting point can be calculated because the z value is equal to the total height of the support structure. The unknown X coordinate of the intersection point can be calculated. This process is repeated until all the points of the flat layer are calculated. Once all the points of a flat layer are evaluated, the tool path pattern for the deposition nozzle can be generated. For instance, the tool path of support structure of the part of Fig 3. 1 is shown in Fig 3. 36.

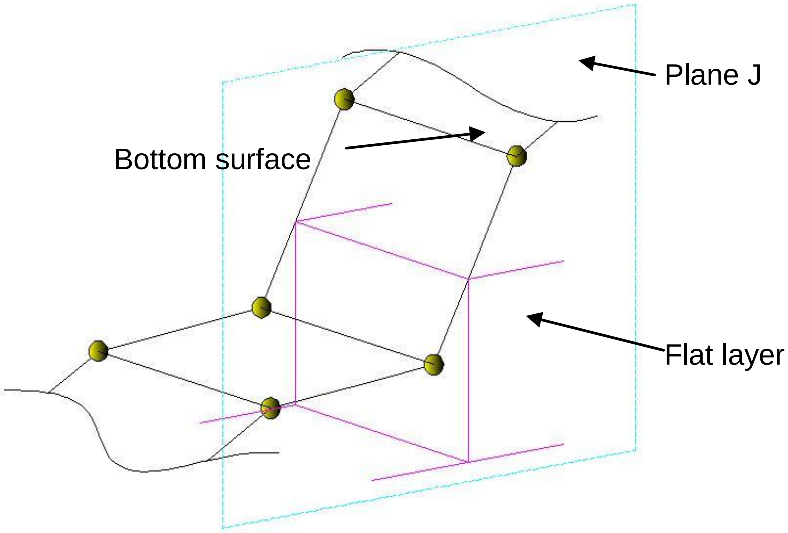

Fig 3. 35 Top surface of support structure and flat layers

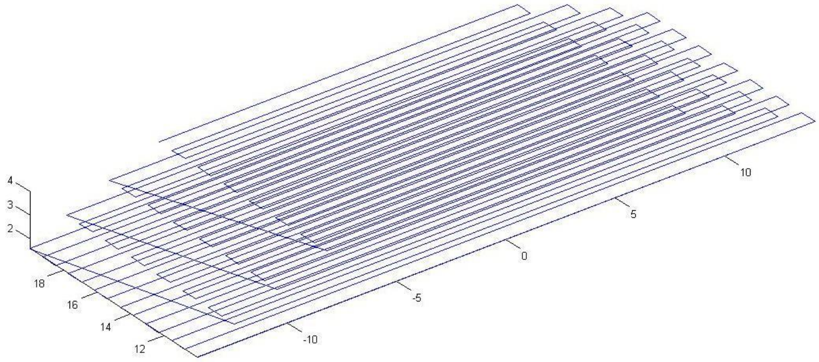

Fig 3. 36 The deposition path lines of the support structure

There might be some complications arising if the curvature of the surface is not symmetric. For examples, the curved surface shown in Fig 3. 37(a) is symmetric about a central vertical axis and for every line segment considered on the left side, there is a matching line segment on the other side, both of which will be used in the evaluation of a particular flat layer. If the curved part is unsymmetrical placed as shown in Fig 3. 37(b), the bottom most line segment on the right side is the starting point for the evaluation of the flat layer, and the algorithm finds a blank space towards the left, as there is no line segment on which the flat layer can be terminated. This is sorted out by providing a means of finding the boundary limit of the part, like for example the extreme left portion of the part and extended flat layers as shown in Fig 3. 37(c) are formed, which is any way necessary, as these layers provide support for the part to be built above them.

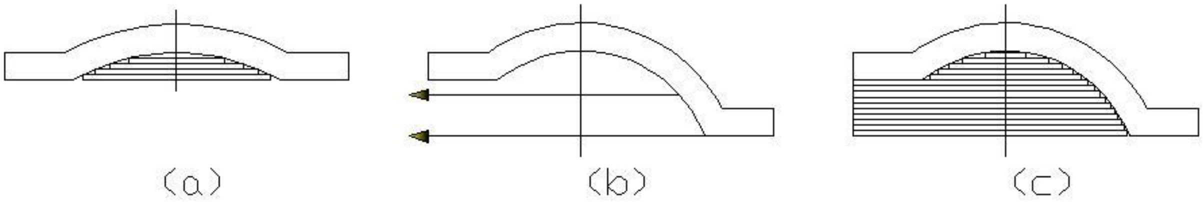

Fig 3. 37 Complications of curved surface

3.6 Case studies

As mentioned before, there are three different data generation schemes: using G&M code and surface modeling methods or following the STL file route. In this research, the G&M code and surface modeling methods are used for curved slicing of a few typical cases. As all the models are symmetric along the Z direction, there is no difference whether the top or bottom surface is considered for generating the base surface features. Also, it will not any difference if the layers are constructed from the bottom upwards or from the top downwards.

3.6.1 Case I: Simple curved object

A solid CAD model with a combination of simple curved and flat features, which is created by UGNX, is shown in Fig 3. 38

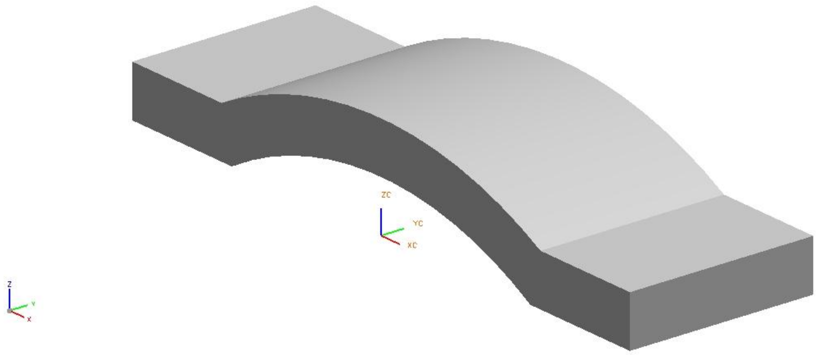

Fig 3. 38 Case I: A simple CAD solid model

The model is combined with simple curved features in the middle and flat features at both ends. Following the features of the model, a machining tool path for the top surface of the model was generated based on G and M codes developed using the CAM software, as shown in Fig 3. 39 below. The yellow line is the starting point of the tool path whereas the white line is the end point. The tool path finally reflects the outer shape, including all features on the model. In this case, a flat cutter is used and its diameter is set equal to the diameter of the nozzle head.

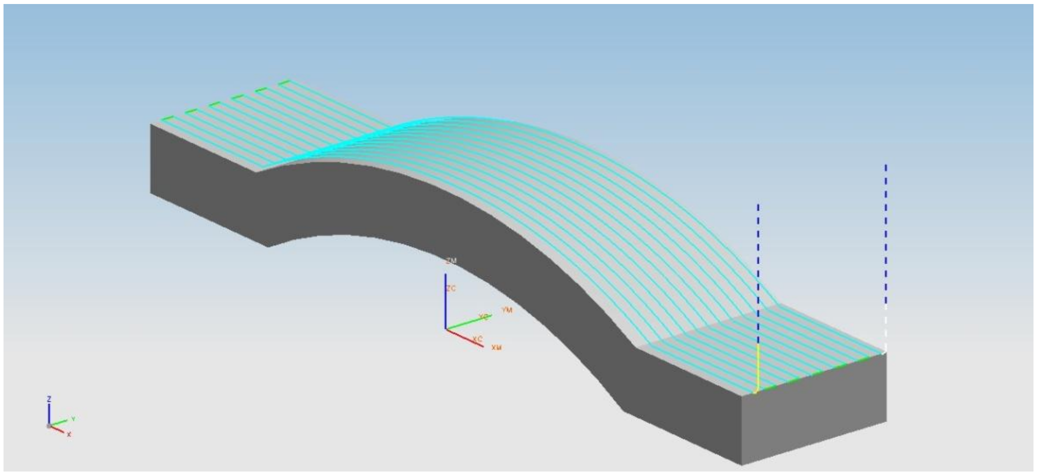

Fig 3. 39 Tool path generation of Case I based on G and M code

The coordinates of all points on the top surface are generated while the tool path is created. They are recorded by the software and output as a post process file in the form of cutter location source file (CLSF),which iss saved as a text file as shown in Fig 3. 40.

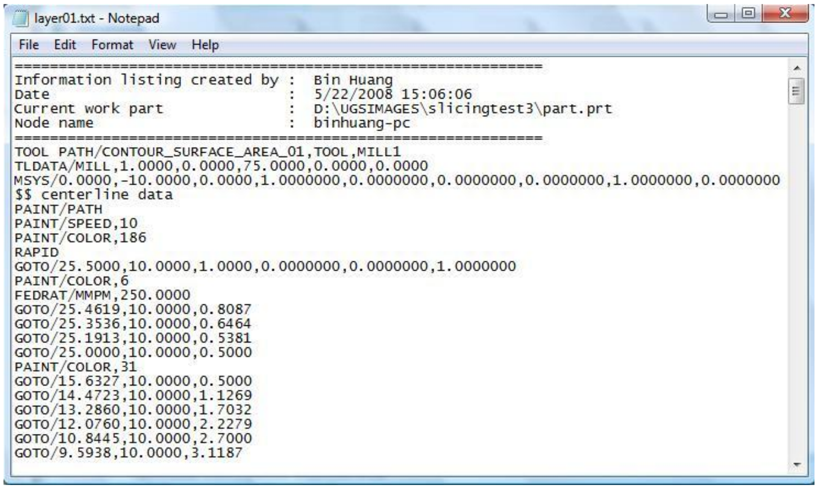

```
============================================================
Information listing created by :  Bin Huang
Date                           :  5/22/2008 15:06:06
Current work part              :  D:\UGSIMAGES\slicingtest3\part.prt
Node name                      :  binhuang-pc
============================================================
TOOL PATH/CONTOUR_SURFACE_AREA_01,TOOL,MILL1
TLDATA/MILL,1.0000,0.0000,75.0000,0.0000,0.0000
MSYS/0.0000,-10.0000,0.0000,1.0000000,0.0000000,0.0000000,0.0000000,1.0000000,0.0000000
$$ centerline data
PAINT/PATH
PAINT/SPEED,10
PAINT/COLOR,186
RAPID
GOTO/25.5000,10.0000,1.0000,0.0000000,0.0000000,1.0000000
PAINT/COLOR,6
FEDRAT/MMPM,250.0000
GOTO/25.4619,10.0000,0.8087
GOTO/25.3536,10.0000,0.6464
GOTO/25.1913,10.0000,0.5381
GOTO/25.0000,10.0000,0.5000
PAINT/COLOR,31
GOTO/15.6327,10.0000,0.5000
GOTO/14.4723,10.0000,1.1269
GOTO/13.2860,10.0000,1.7032
GOTO/12.0760,10.0000,2.2279
GOTO/10.8445,10.0000,2.7000
GOTO/9.5938,10.0000,3.1187
```

Fig 3. 40 Cutter location Source File (CLSF) for Case I

The next step is to remove unwanted portions of information such as tool settings, spinning speed etc, from the CLSF as for example, the shaded portions in Fig 3. 41.

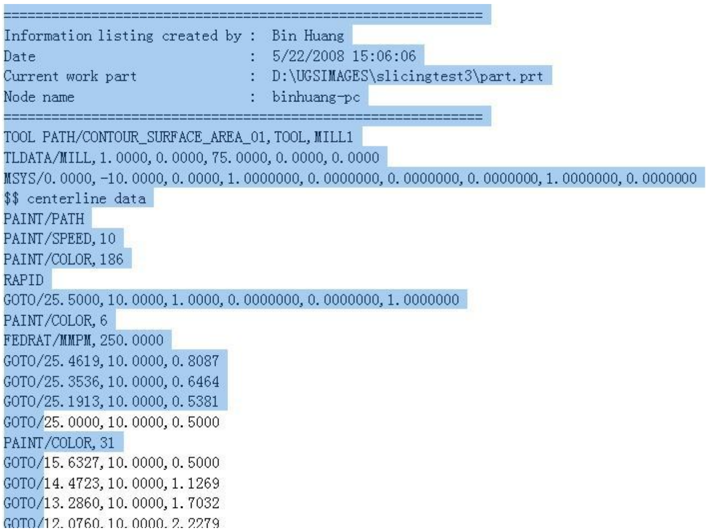

```
=============================================================
Information listing created by :  Bin Huang
Date                           :  5/22/2008 15:06:06
Current work part              :  D:\UGSIMAGES\slicingtest3\part.prt
Node name                      :  binhuang-pc
=============================================================
TOOL PATH/CONTOUR_SURFACE_AREA_01,TOOL,MILL1
TLDATA/MILL,1.0000,0.0000,75.0000,0.0000,0.0000
MSYS/0.0000,-10.0000,0.0000,1.0000000,0.0000000,0.0000000,0.0000000,1.0000000,0.0000000
$$ centerline data
PAINT/PATH
PAINT/SPEED,10
PAINT/COLOR,186
RAPID
GOTO/25.5000,10.0000,1.0000,0.0000000,0.0000000,1.0000000
PAINT/COLOR,6
FEDRAT/MMPM,250.0000
GOTO/25.4619,10.0000,0.8087
GOTO/25.3536,10.0000,0.6464
GOTO/25.1913,10.0000,0.5381
GOTO/25.0000,10.0000,0.5000
PAINT/COLOR,31
GOTO/15.6327,10.0000,0.5000
GOTO/14.4723,10.0000,1.1269
GOTO/13.2860,10.0000,1.7032
GOTO/12.0760,10.0000,2.2279
```

Fig 3. 41 Extra information in the CLSF file of Case I

The text file is manually modified and finally contains only the X, Y and Z coordinate data as shown in Fig 3. 42, and this iss used as the input data file for the curved layered slicing program.

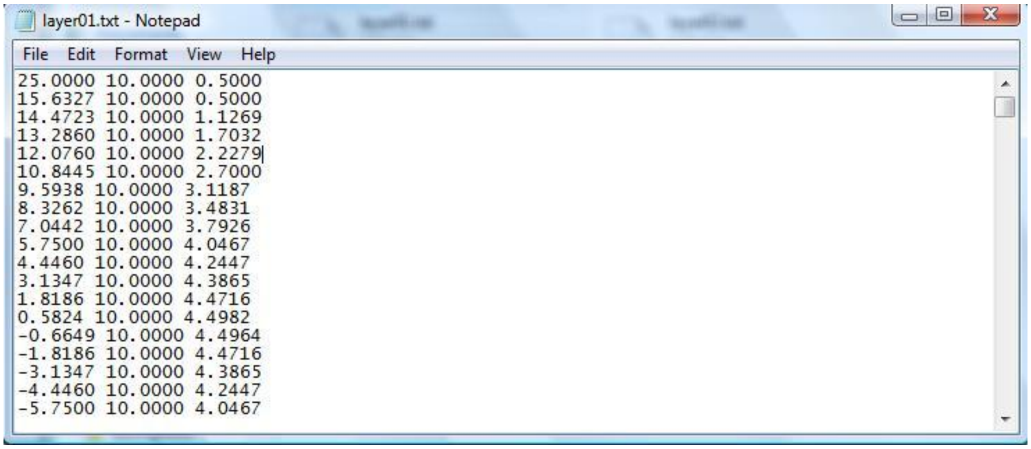

```
25.0000 10.0000 0.5000
15.6327 10.0000 0.5000
14.4723 10.0000 1.1269
13.2860 10.0000 1.7032
12.0760 10.0000 2.2279
10.8445 10.0000 2.7000
9.5938 10.0000 3.1187
8.3262 10.0000 3.4831
7.0442 10.0000 3.7926
5.7500 10.0000 4.0467
4.4460 10.0000 4.2447
3.1347 10.0000 4.3865
1.8186 10.0000 4.4716
0.5824 10.0000 4.4982
-0.6649 10.0000 4.4964
-1.8186 10.0000 4.4716
-3.1347 10.0000 4.3865
-4.4460 10.0000 4.2447
-5.7500 10.0000 4.0467
```

Fig 3. 42 Surface point data file of Case I

The text file containing X, Y and Z coordinates of the data points on the top surface of the CAD model is transferred as input data to the MFVCP slicing program, written in MATLAB. Fig 3. 43 shows the shape of the tool path of the original curved layer.

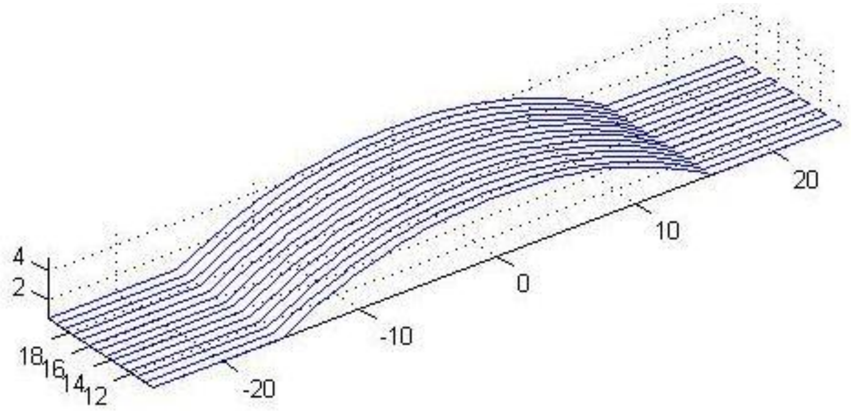

Fig 3. 43 Original curved layer of the model of Case I

After running the MFVCP program in MATLAB, the data points of subsequent curved layers are calculated, and the tool paths of each curved surface are evaluated, as shown in Fig 3. 44. The coordinates of data points on all curved layers are recorded and saved as an output file in the text format, which is a proper format for ready use on the RP platform.

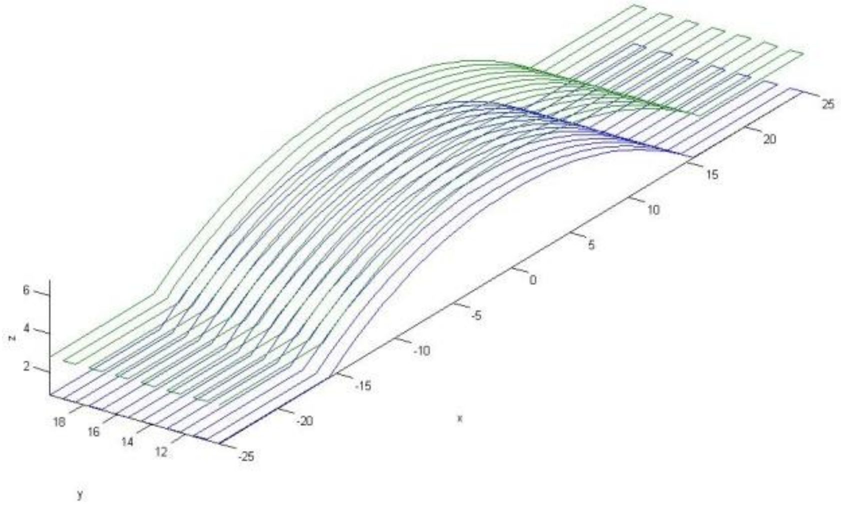

Fig 3. 44 Tool path curves in different layers of Case I

3.6.2 Case II Tapered curved object

A solid CAD model with simple curved and flat features, almost similar to the previous one, but with a certain amount of tapering along the length is considered next as shown in Fig 3. 45 for testing the CLFDM models developed.

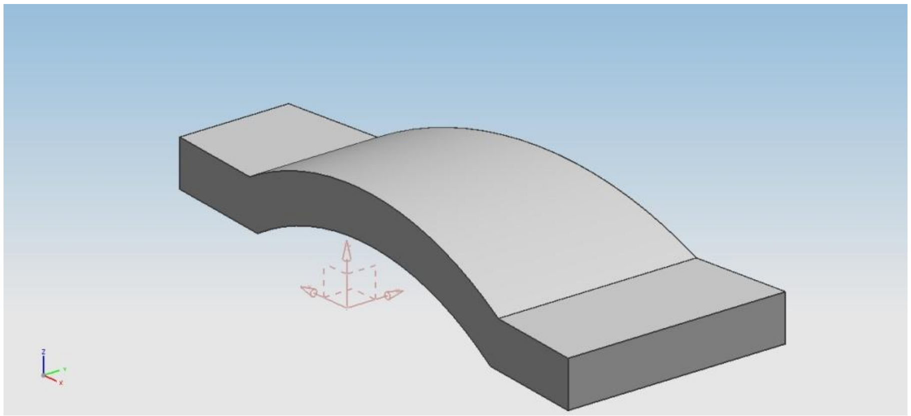

Fig 3. 45 A simple CAD solid model with tapered feature

Following those features on the model, the cutter path data for the top surface of the model is generated based on G and M codes using the CAM software, as shown in Fig 3.41 below. While the dashed line marked as 1 signifies the starting point of the tool path, the dashed line marked 2 is the end point. The tool path data corresponds to a flat cutter of diameter equal to the nozzle diameter.

Unlike the part in the previous case, the tool path in this case is not continuous along the length on either side of the width of the specimen as seen from the top vied of the specimen in Fig 3. 46.

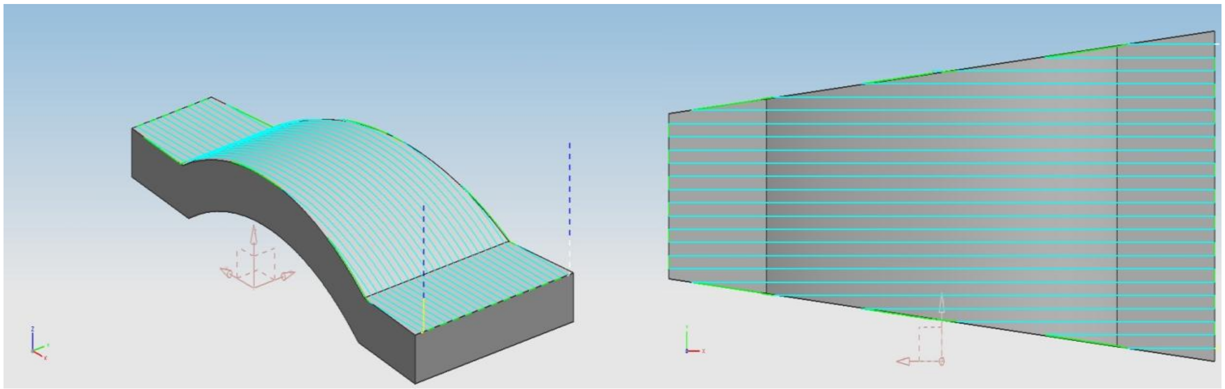

Fig 3. 46 Cutter paths on the top surface of a tapered specimen

A similar modification of the CSLF data as detailed earlier and subsequent evaluation of the deposition path resulted in the pattern shown in Fig 3. 47 for the first curved layer.

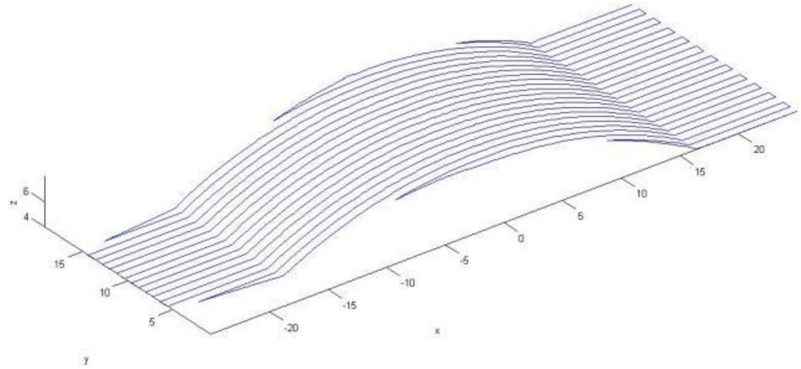

Fig 3. 47 Original curved layer of the model of Case II

After running the MFVCP program in MATLAB, the data points of the next curved layer are calculated, and they formed the deposition path pattern for the next curved layer, as shown in Fig 3. 48. The coordinates of data points on the curved layers are stored in the text file in the sequence of the deposition formats of each layer, starting from the first one and stacking the others one over the other, in the same sequence as they are evaluated.

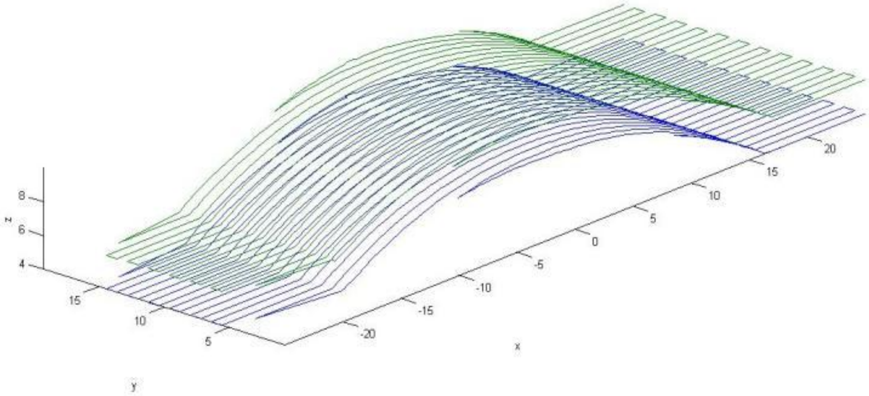

Fig 3. 48 Tool path of the offsetting surfaces of Case II

3.6.3 Case III Simple curved object with a hole

The shape of this model is similar to the one in Case I but with an additional hole at the top, as shown in Fig 3. 49.

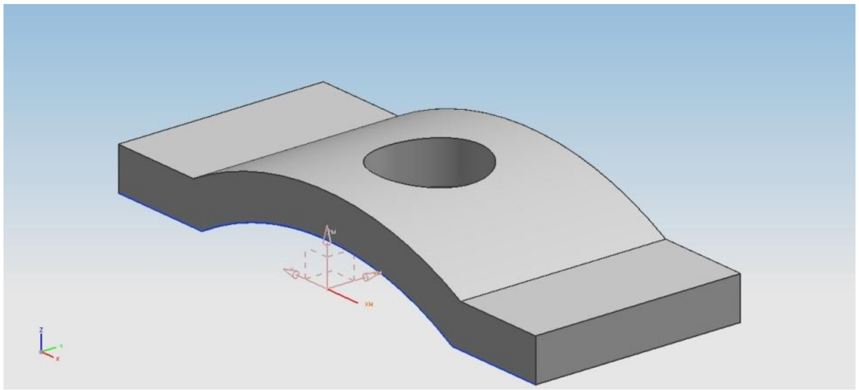

Fig 3. 49 A simple CAD solid model of Case III

The cutter path profile of the top surface of the model is generated based on G and M code automatically via the CAM software, as shown in Fig 3. 50. The start and end points are marked as 1 and 2 on the respective dashed lines. The total tool path matches with the typical features of the model. In this case, a flat cutter is used and its diameter is set equal to the diameter of the nozzle head. Unlike the part without a hole, as in Case I, the tool path in this case keeps jumping from one side of the hole to the other.

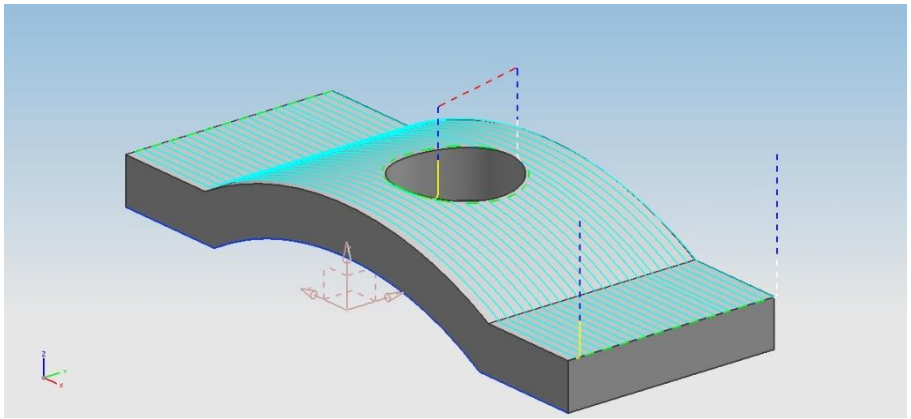

Fig 3. 50 Tool path generated in Case III

The coordinates of all points on the top surface are generated while the tool path is created The CLSF data is modified and the first layer deposition path pattern is generated as shown in Fig 3. 51. When used for fused deposition, this pattern arises a complication.

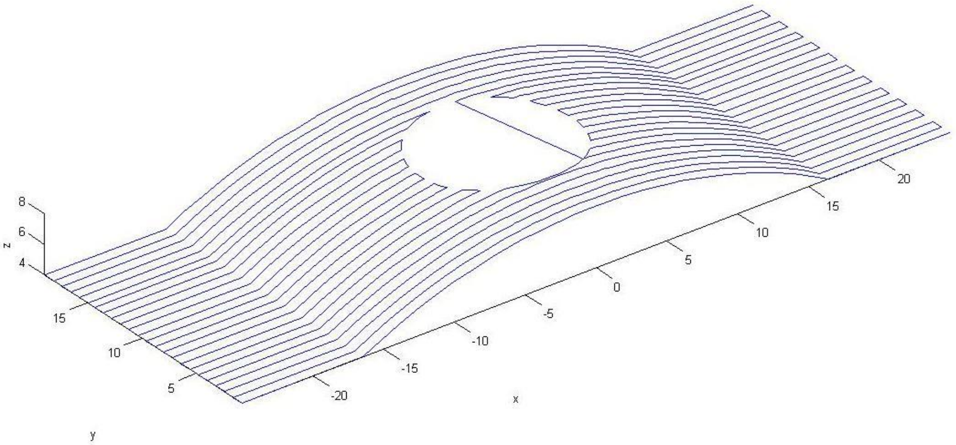

Fig 3. 51 Original curved layer of the model of Case III

Unlike the two previous cases, the tool path in this case jumps across the hole, and causes errors when used as a deposition path way. Therefore, the coordinates from those points have to be removed. The data from the top surface is as shown in Fig 3. 51. The straight line tool path crossing the middle of the hole should be avoided while depositing. This still remains as a concern, but one of the solutions is to manually remove such connections. Alternatively, the deposition process can also be halted programmatically while traversing along such lines.

After running the MFVCP program in MATLAB, the data points on the subsequent curved layers are calculated, and they formed the tool path pattern of the next offset surface, as shown in Fig 3. 52. The coordinates of data points on all curved layers created are recorded and saved in the output file in text format, which is a proper format for ready use on the RP machine.

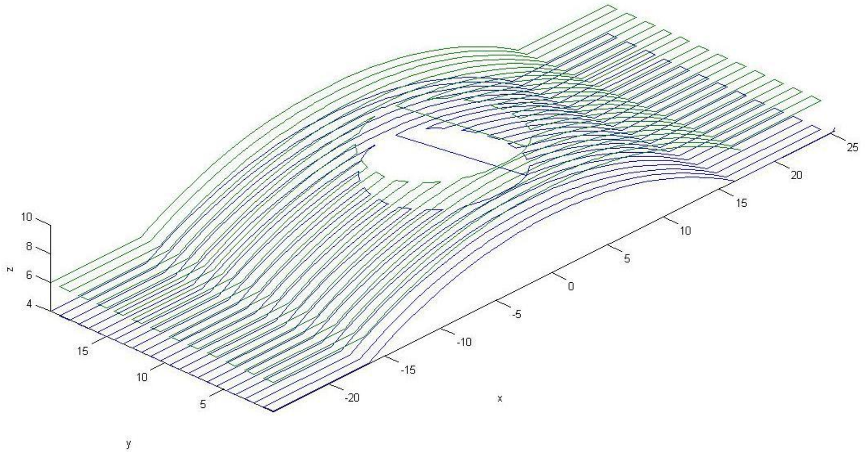

Fig 3. 52 Tool path of the offset surfaces of Case III

3.6.4 Case IV Free form surface

A Bezier surface is created as shown in Fig 3. 53 for a set of key point data input into the MATLB program developed for modeling Bezier surfaces. The number of surface points and the distance between adjacent points can be set depending on the required quality. The task is then to use the model of the free-form surface created and develop curved slices, assuming a sold shape below the surface.

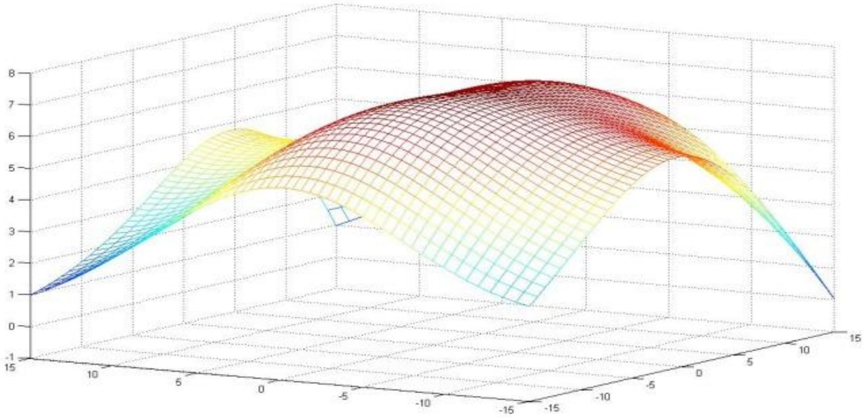

Fig 3. 53 Free form surface model

The X, Y and Z coordinates of all the points of a grid considered on the surface are calculated by considering a series of equi-spaced isoparametric lines in both directions and using the Bezier model. The X, Y and Z coordinate data is directly written in a text file and the deposition path pattern developed for the top surface is as shown in Fig 3. 54.

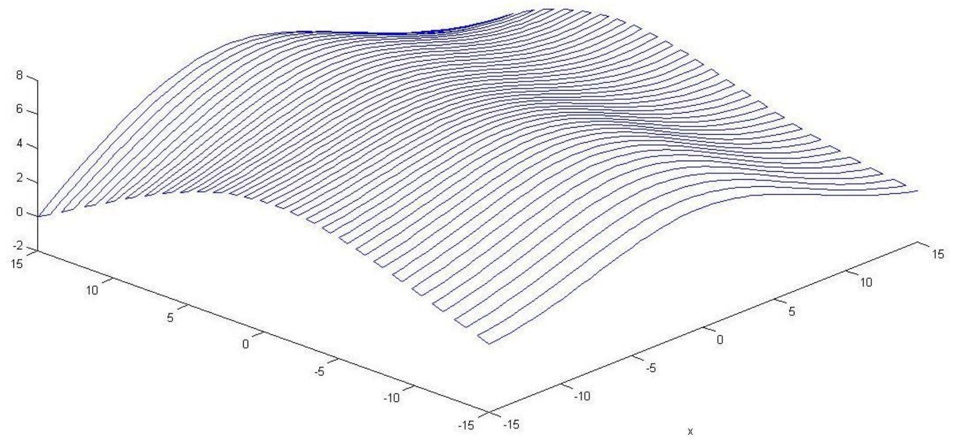

Fig 3. 54 Deposition path pattern for the free form surface of the model of Case IV

After running the MFVCP program in MATLAB, the data points of the subsequent curved layers are calculated, and they formed the tool path pattern of the next curved layer, as shown in Fig 3. 55. The process is repeated as many times as needed to complete the model and the coordinates of data points on all curved layers are recorded and saved as an output file in text format. The text file can then be used directly on the RP machine to print the 3D part using Curved Layered Fused Deposition Modeling.

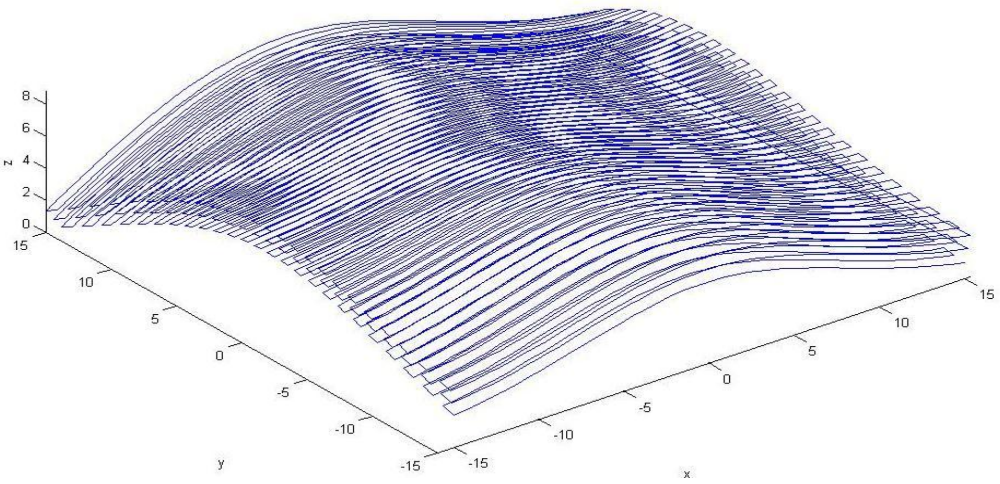

Fig 3. 55 Deposition path pattern of a couple of curved layers conforming to the shape of the free form surfaces of Case III

Chapter 4

Hardware Platform for CLFDM

4.1 General requirements for CLFDM

RP machines for traditional FLFDM require a three-axis computer numerical controlled (CNC) system driven by servo or stepper motors, for motions along x, y and z directions. They also need an extrusion head or other curing or binding devices mounted on the platform for the materials deposition or solidification. Apart from the basic requirements mentioned above, some other auxiliary devices are also used during the deposition processing.

Similar to the basic requirements of FLFDM or other RP machines, a three-axis CNC machine is the priority requirement currently for this research, or a five-axis CNC machine for the future, in order to ensure perpendicularity of the deposition head while depositing on surfaces of varying curvature. Similarly, an extrusion head is also required for the material deposition.

For the traditional FLFDM machine as mentioned in Chapter 2, the extrusion head only works on the x and y directions for the flat layer deposition processing and then lifts up a certain distance equal to the thickness of the layer in the z direction and continues depositing the next layer. So the precision requirement for the motion in the z direction is relatively lower than in x and y directions. Compared to a traditional FLFDM machine, the CLFDM machine requires the extrusion head operating in x, y and z directions simultaneously, which means that all three motors need to be controlled at the same time by both software and hardware. The motor employed for the motion along the Z axis must be as sensitive as the ones used for x and y motions.

Additionally, the length of the tip on the extrusion head is relatively short and close to the heating chamber, and might cause collision during the curved layer deposition. In order to avoid this, a long-nose tip is required.

In essence, a three-axis CNC system, with equal and high precision motion along all three axes, and an extrusion head with sufficiently long-nose tip are the basic requirements of the test setup for the CLFDM proposed in this research.

4.2 Hardware options

There are many options involving modification of either FDM or CNC machines available for practical implementation of CLFDM. Apart from using the available machines, a DIY three-axis CNC machine also can be one of the possible alternatives. Considering all possibilities, five different options emerged as potential candidates for being practical CLFDM systems. They are:

- DIY three-axis CLFDM machine,
- Modified three-axis CNC machine,
- Modified commercial FDM machine,
- Modified commercial inkjet printer
- Modified open source FDM machine.

4.2.1 DIY three-axis CLFDM machine

As the minimum requirement for the CLFDM is a three-axis CNC system, with the accuracies of all three motors equal and high, and an extrusion head with a long-nose tip, building a three-axis CNC system is a viable option. Many open sources and tutorials are available on the internet [40] for DIY CNC machines with structural materials varying from wood to metal, along with bills of materials. The components required for building the CNC systems are available in the local supplier shops and DIY electronic outlets. These DIY CNCs can read the G and M code during machining and the price of a typical system can be around $2000, including both hardware and software.

According to reports by people who constructed and tested these machines, DIY CNC machines could machine reasonably well, and the accuracy and quality of final finishing of models are reasonably. Fig 4. 1 shows a DIY CNC machines constructed by prospective CNC hobbyists [40].

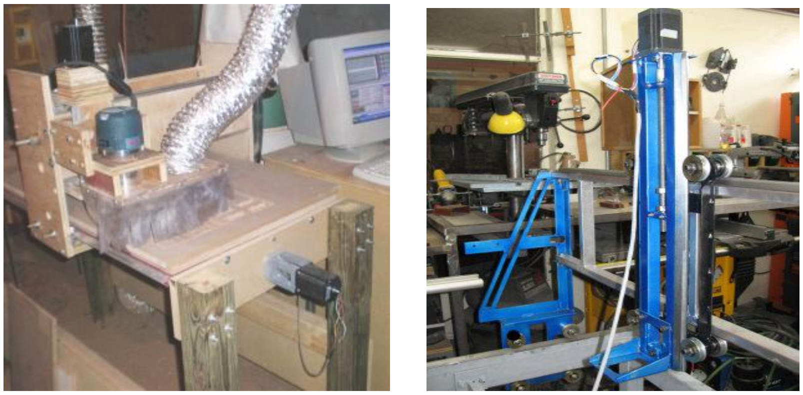

Fig 4. 1 DIY CNC machines

Although the DIY CNCs have a lot of advantages, the main shortcoming is the need to build a deposition head and integrate it with the rest of the system. An extrusion head together with a software control system needs to be designed and built. Considering the time of construction,   a DIY three-axis CNC system is not a perfect option for this research though it remains a potential candidate for future research on CLFDM.

4.2.2 Modifying a three-axis CNC machine

Alternatively, an existing CNC machine can be retrofitted with an extrusion head or a cheaper used system can be procured. There are quite a few good quality second hand commercial CNC machines available from the online resources. A desktop-like second hand CNC machine would be ideal for this research and a system named High-Z S-720 CNC-Router [41], made in

Germany, shown in Fig 4. 2 has come out as one of the possible options for building the CLFDM system.

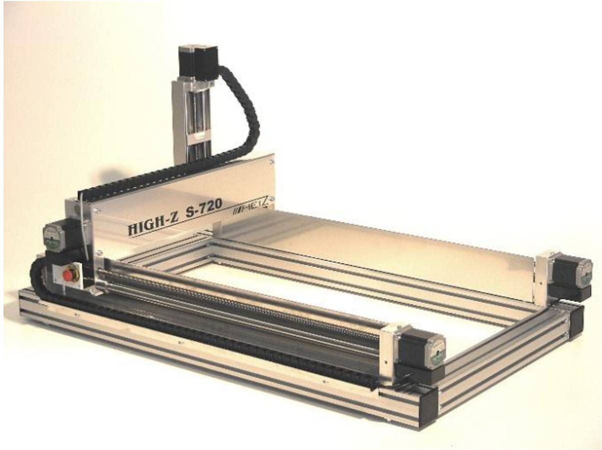

Fig 4. 2 High-Z S-720 CNC-Router

The good side of working on these commercial CNC machines is the time saved in building an entire machine, as well as testing. Additionally, the working precision of the commercial CNC machines would be much higher than the DIY machines. The software for the commercial machines is also easy to use. Nevertheless, they suffer from the same shortcoming as in the above case that an extrusion head needs to be designed, built and integrated with the mainframe, which is time consuming and an unnecessary detour from the main focus of this research, which is developing a CLFDM system. Considering the time required and the complexities of building the extrusion head, modifying a three-axis CNC machine is not the best option for this research although it overcomes some disadvantage of a DIY three-axis CLFDM machine.

4.2.3 Modifying a commercial FDM machine

Using a commercial FDM machine, such as Stratasys FDM 3000 [42], shown in Fig 4. 3 is a perfect solution to the problem of developing a working CLFDM system capable of producing parts of sufficient quality. Used FDM machines at relatively cheaper prices could be located with online vendors. The FDM machine meets the minimum requirements for the CLFDM and eliminates altogether the need for designing and constructing a deposition head and at the most, needs replacement of the flat nozzle with a long-nose nozzle. However, the main challenge is that the software is in the form of a black box and without access to the source code, it will be an involving task to try and modify the control system to achieve curved layered deposition as against the customary flat layered processing.

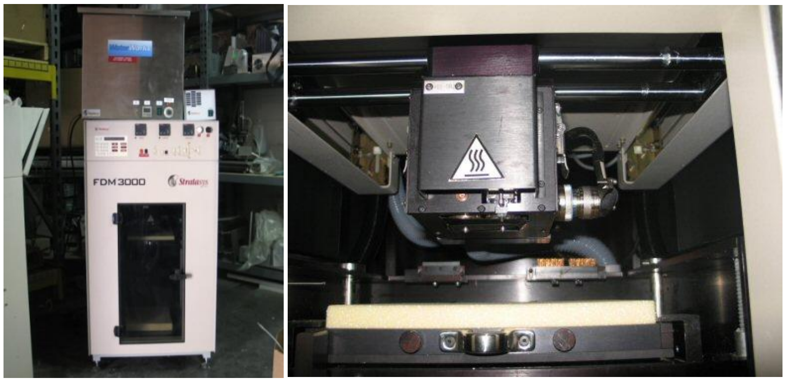

Fig 4. 3 Stratasys FDM 3000 Rapid Prototyping Machine

4.2.4 Modifying a commercial inkjet printer

In order to find a less expensive and less time consuming solution for the CLFDM system, a further alternative is to modify a commercial inkjet printer. The inkjet printers, as shown in Fig 4. 4, are easy to purchase from shops and websites, and the prices are more reasonable, and the accuracy of the inkjet printer is up to pixels, which is far higher than the expectations of the current project. The software for the inkjet printer is available and easy to use compared with other options.

Fig 4. 4 Inkjet printer

The ink cartridge holder needs to e replaced by an extrusion head. The main problem with the inkjet printers is that they only work on x and y axis. To make it suitable for this research, an additional stepper motor controlled Z axis is required and the software for the inkjet printer needs to be modified to control the motions on three different axes. Additionally, some more electronic components and an extra step motor are required in the medication. In other words, the cost and the time required are increased and considering all this, the inkjet printer option is dropped from the methodology.

4.2.5 Modifying an open source FDM machine

Compared to those options mentioned above, modifying an open source FDM machine appears to be a more promising option. The open source FDM machines, which are similar to the DIY CNC machines, are constructed by users with components available in the market. These open sources FDM machines are three-axis CNC machines with an extrusion nozzle or a similar such device, which totally meets the minimum requirements of this research.

The open source FDM machines have a CNC machine base, and can work on three axes independently. In other words, they work similar to the CNC machine, but instead of using the milling tool, they have an extrusion head and can implement the deposition during the RP processing. The hardware or electronic components for constructing these FDM machines are easily available and relatively cheap. The software, which can be downloaded from the website, has a user-friendly interface and works on the personal computer. Though the assembly is relatively simple, considerable amount of time is required to modify the system to suit to CLFDM and the accuracy of these machines is relatively lower than that of commercial FDM machines.

Considering the time required and other complexities, and the total cost, an open source FDM machine is considered as the most ideal option, in spite of some inherent limitations. Currently, there are two kinds of open source FDM machines available for procuring online, one is the RepRap machine and the other is a Fab@home machine.

RepRap Machine

RepRap [43], which is the short form of Replicating Rapid-prototyper is made by Adrian Bowyer from Bath University, and is one of the open source FDM machines. It is a practical self-copying 3D printer, as shown in Fig 4. 5. The RepRap machine is a scaffold like machine, which uses aluminum sticks as its casing. Two stepper motors are mounted on the top of the casing, which are used to control the motions of the tool carriage in x and y directions. A work table controlled by the z direction stepper motor can move up and down. A thermoplastic extrusion head is mounted on the tool carriage and it can melt a variety of plastics and extrude them out in a thin stream to form a filament for the deposition processing.

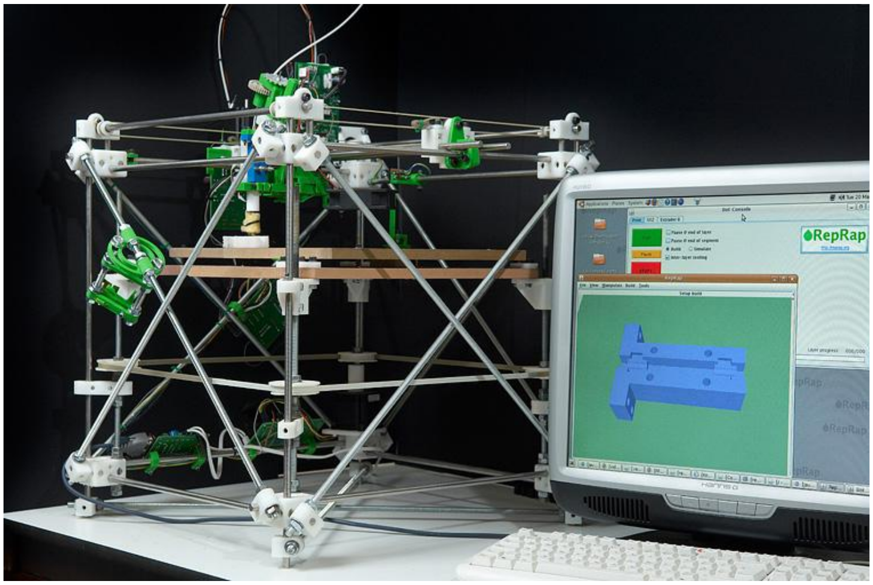

Fig 4. 5 RepRap machine

From the RepRap website, the bill of materials (BOM) and the instruction manual are available. The BOM specifies all the components and the hardware parts to construct the RepRap machine. According to the BOM, all those components of the RepRap machine, including the electronic and mechanical hardware, can be obtained from the suppliers all around the world. The firmware, which is written in C language, is for the RepRap microcontroller to control all the deposition motions of the machine during the fabrication. The software, which is written in Java, is for the personal computer application, as well as, the user interface. The software allows users to load and position the STL files for the object fabrication, then set up objects for printing and control the machine interactively. The user interface offers a graphic-based communications environment between users and the RepRap machine.

However, the hardware components require to be gathered from different suppliers all over the world and it might take quite some time and effort to put everything together. Further, the RepRap software can read and print the STL file and G code file objects, but cannot read text data file output, from the MATLAB slicing program and as a result this option is dropped from considertaation for this research..

Fab@home Model 1 machine

Similarly, the Fab@home machine Model 1 [44], also named Model 1, is another open source FDM machine made by Evan Malone from Cornell University, and is shown in Fig 4. 6. Similar to RepRap machine, the Model 1 also has an outside casing. Instead of using the scaffold-structure like casing, the Model 1 uses the laser-cut acrylic sheets as its chassis. Inside the chassis, the motion system consists of an x-y axis gantry type system and the z worktable that is controlled by three stepper motors. Unlike RepRap machine, the Fab@home Model 1 has a standard syringe deposition tool, which consists of a disposable syringe barrel, tips and piston. The position of syringe piston is controlled by a linear stepper motor and accordingly the material flows.

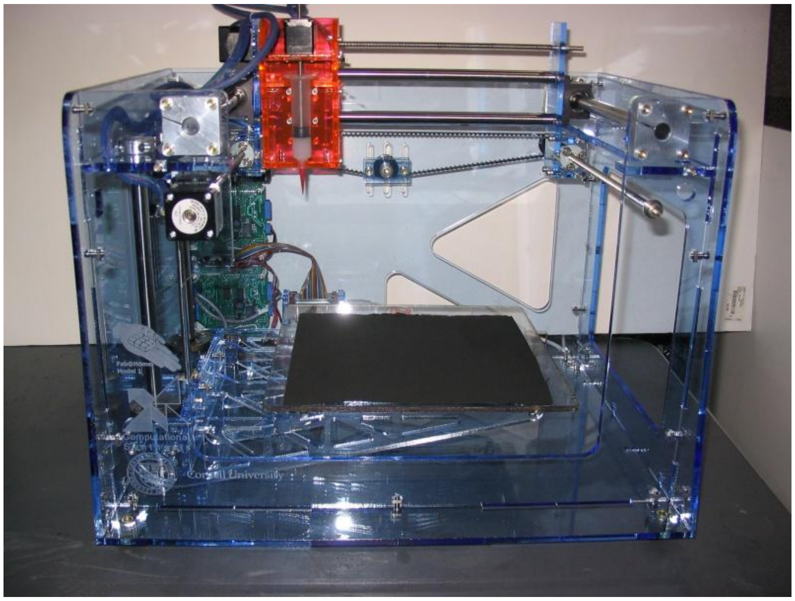

Fig 4. 6 Fab@home Model 1 machine

Similarly, the bill of materials (BOM) and the instruction manual are available on the Fab@home website. According to the BOM, all those components of the Fab@home machine, including the electronic and mechanical hardware, can be obtained from the suppliers all around the world individually or even completely assembled units or kit requiring for assembly can be ordered. The instruction manual indicates all the assembly steps in detail. Following the instruction manual, the construction of Model 1 can be completed and then the machine will be ready for RP fabrication.

The firmware and the software of Model 1 are also available on the fab@home website. The firmware, which is developed in C and C++, is for the microcontroller of Model 1 to run all the operations of the machine. The software is for the user interface in the personal computer, which enables the user to control the machine, import, position, assign material and generate and execute manufacturing plans for geometry data which is imported in the form of STL files and text files. Similar to the user interface in RepRap machine, the user interface here has the same functions. Additionally, it can monitor the motions of the Model 1 with the real-time position information sent back by the micro controller during the fabrication.

Compared to the RepRap machine, the Fab@home Model 1 is a more basic machine and for beginners. It cannot able to print the objects with thermoplastics as there are no heating elements working on the deposition tool. It cannot generate the G-codes with its own software. However, it can read text files generated from the MATLAB slicing program. Besides, because it is a basic machine, it easily allows for development for further research. Considering the time required for procuring the hardware components the machine construction, the software compatibility, and the cost, it is concluded that this is the best option for this research.

4.3 Constructing the hardware platform

Construction of the Fab@home Model 1 machine is relatively easy to achieve with proper preparation and planning. Once all the parts of Model 1 and the required tools are procured the construction of Model 1 can be completed with in less than a week. As all the procedures and the assembly steps are documented on the Fab@home website, only the critical components and major procedures used to construct the Model 1 will be discussed in this section.

4.3.1 The Chassis

The model 1 Chassis, as shown in Fig 4. 7, consists of a Base Assembly, Z-carriage Assembly and XY-carriage Assembly, which are well documented in the instruction manual and not mentioned again here. With the major positioning system components constructed individually, this step involved combining them into the Model 1 Chassis. The XY-carriage was mounted on the top of the Base Assembly while Z-carriage was mounted above the bottom of the Assembly by using the threaded brass inserts that were melted into the base already. And then the x, y and z stepper motors were also fastened onto the base and connected to XY carriage and Z carriage with lead screws.

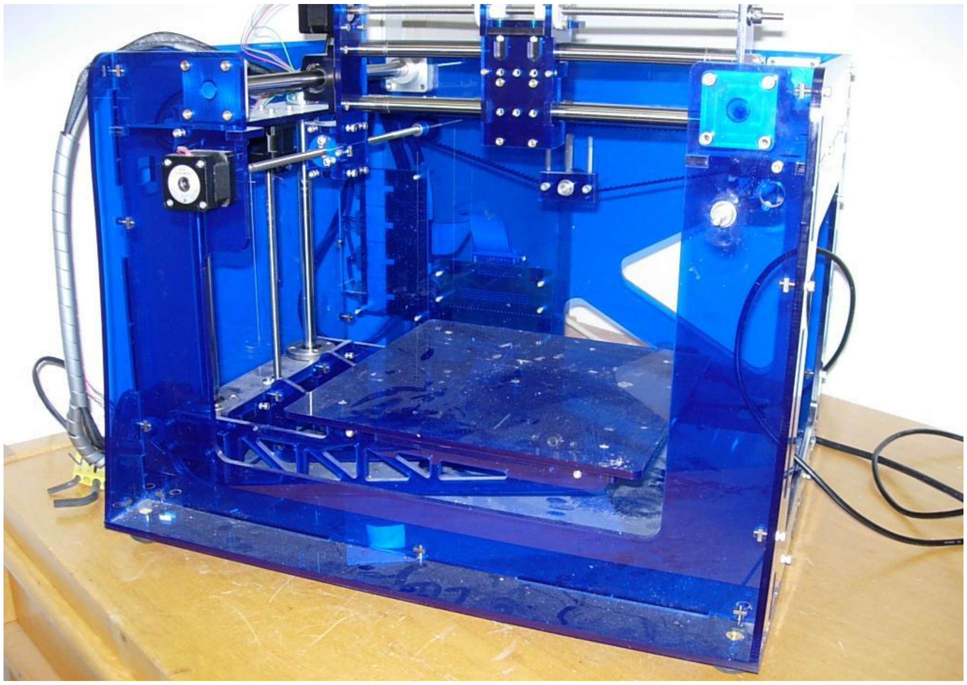

Fig 4. 7 Model 1 Chassis

4.3.2 The Syringe Tool

The Model 1 Syringe Tool, as shown in Fig 4. 8, is the standard deposition head for the Fab@home Model 1 and it consists of a disposable syringe barrel, tips and pistons to hold the materials. The syringe stepper motor is mounted on the acrylic sheet, which is the top of the syringe casing. And then all the acrylic sheets are put together and fastened with screws and nuts to the Syringe Tool casing. The disposable syringe barrel with the tip is fit into the middle of the casing. A lead screw with shaft collar and shoulder screw is put through the stepper motor. After that, the Syringe Tool is mounted on the Z-carriage.

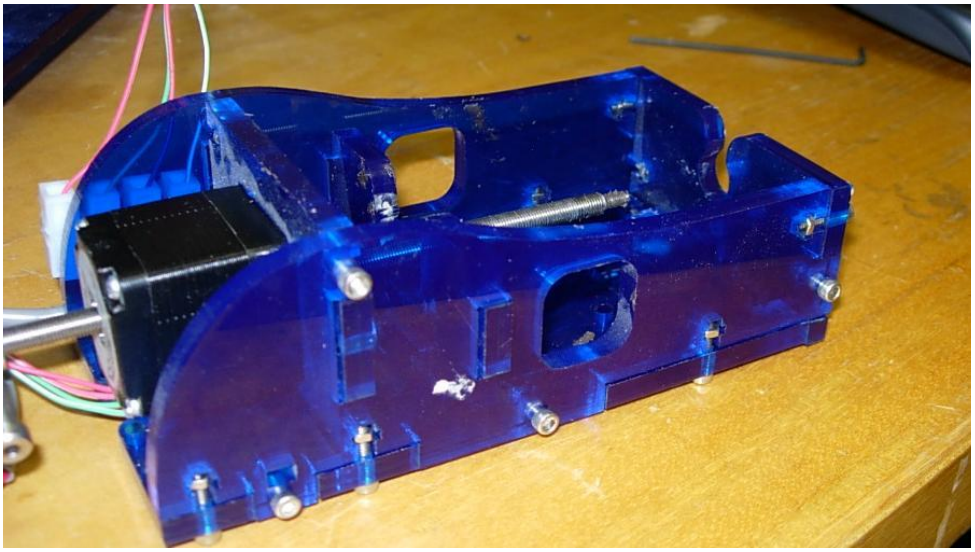

Fig 4. 8 Model 1 1-Syringe Tool

4.3.3 Electronics

The Model 1 Electronics consists of Elpac Power Supply, AC Power Cord, Olimex LPC-H2148 Microcontroller Board, Xylotex XS-3525/8S-4 Stepper Motor Driver Board, Winford Engineering DB-25 Breakout Board, Limit switches and some Cables. Among those components mentioned above, the most important electronic components are LPC-H2148 Microcontroller, Stepper Motor Amplifier Board and DB-25 Breakout Board.

LPC-H2148 Microcontroller Board

The LPC-H2148 Microcontroller Board as shown in Fig 4. 9, contains the LPC-H2148 Microcontroller, and is used to communicate instructions between the Model 1 software and hardware. The microcontroller has a large RAM space, 512kB flash memory and 40kB of RAM allows motion commands to be buffered. The USB connector allows the LPC-H2148 Microcontroller to be directly connected to a computer with a USB cable, for the data transfer from the PC. The standard JTAG connector on the board allows the microcontroller to be programmed.

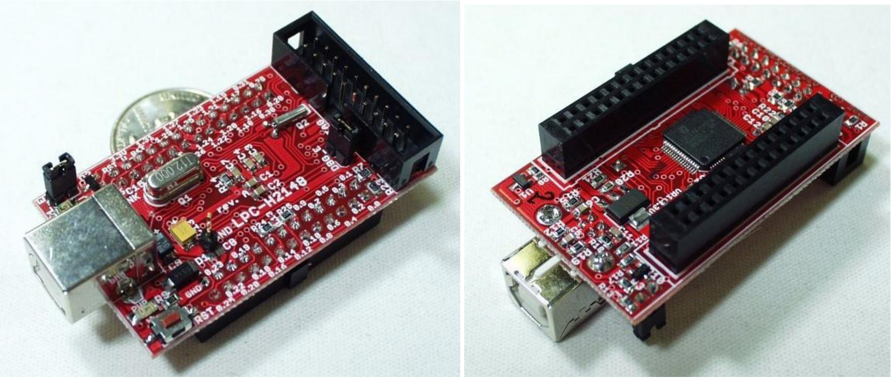

Fig 4. 9 LPC-H2148 Microcontroller Board

Xylotex XS-3525/8S-4 Stepper Motor Driver Board

The Xylotex XS-3525/8S-4 Stepper Driver Board as shown in Fig 4. 10 is to provide the power and control signals to the stepper motors of the positioning system and deposition tool in Model 1. The Xylotex XS-3525/8S-4 Stepper Motor driver is a 4 axis pulse-width-modulated (PWM) current controlled bipolar micro-stepping controller. Each axis driver has a ± 2.5 Amp/phase at 35 Volt maximum continuous Output Rating. Each axis accepts Step and direction signals, along with two jumper inputs to define micro steps per full step. Instructions are transferred to this device from the microcontroller and computer.

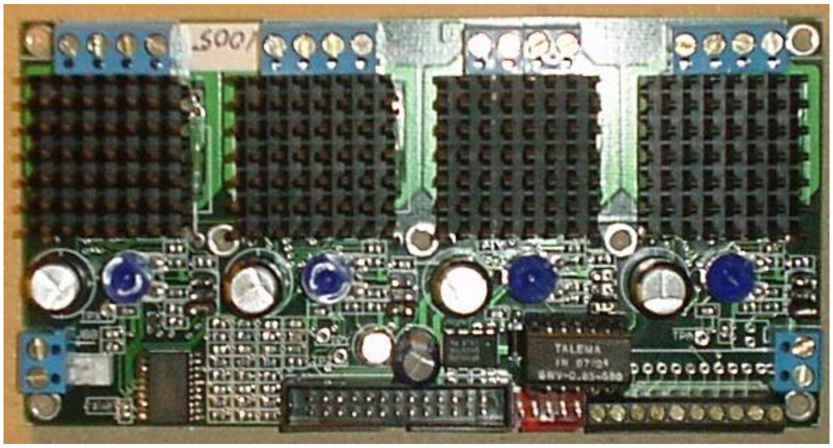

Fig 4. 10 Xylotex XS-3525/8S-4 Stepper Motor Driver Board

Winford Engineering DB-25 Breakout Board

The Winford Engineering DB-25 Breakout Board as shown in Fig 4. 11, is to simplify the connections between the stepper motor driver board and the microcontroller. The Winford Engineering DB-25 Breakout Board allows 200 Volt maximum between any two signals and 2.25A maximum on any signal. The DB-25 Breakout Board connects the stepper motor driver board with a DB-25 to IDC 26 Ribbon Cable and connects the microcontroller board with other two Ribbon Cables prepared in earlier stage.

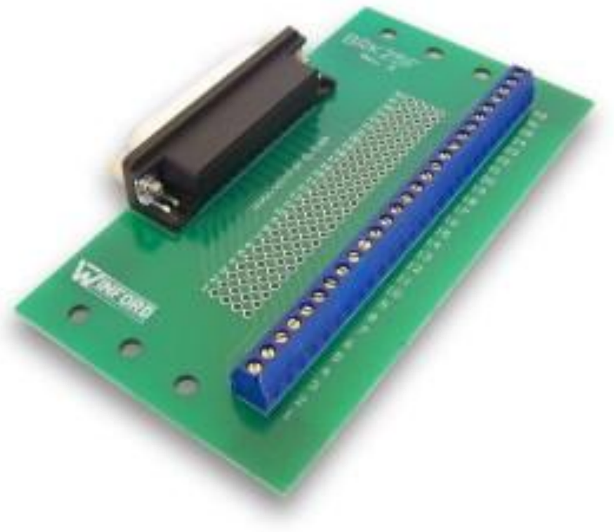

Fig 4. 11 Winford Engineering DB-25 Breakout Board

Mounting the Electronics

Elpac Power Supply, AC Power Cord, Olimex LPC-H2148 Microcontroller Board, Xylotex XS-3525/8S-4 Stepper Motor Driver Board, Winford Engineering DB-25 Breakout Board, Limit switches are all interconnected with the cables together following the wiring diagrams supplied by Fab@home website, as shown in Fig 4. 12. All the electronics components are mounted on the back of the Model 1 Chassis, as shown in Fig 4. 13.

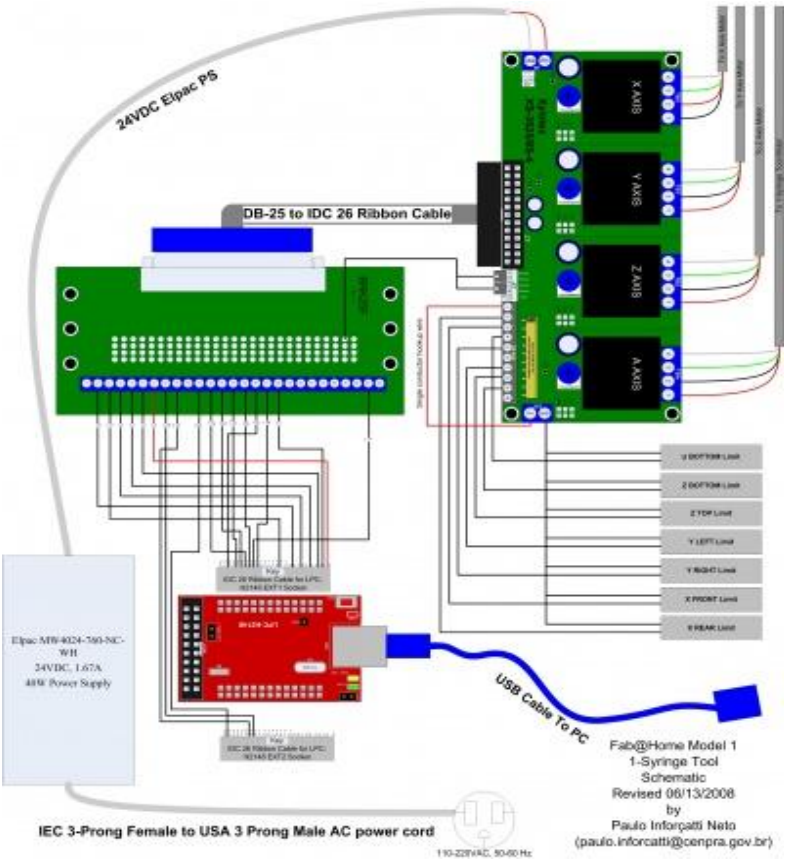

Fig 4. 12 Schematic of the electronics layout

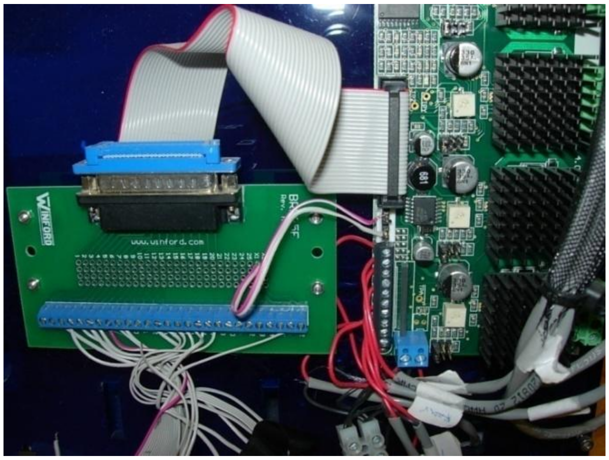

Fig 4. 13 Mounting the Electronics

4.3.4 The Firmware

The firmware, which is written in C using Rowley CrossWorks for ARM, is the software that runs on the LPC2148 microcontroller. When the microcontroller is received, a simple demonstration firmware is pre-loaded onto it from the manufacturer. It needs to be replaced with the Fab@home firmware. The firmware is to communicate the computer and Model 1, and receives the signals from the software and then tells Model 1 what positions and motions to achieve.

JTAG Adapter Cable

In order to program the LPC-H2148 microcontroller, a JTAG adapter is required with the firmware development environment. However, the JTAG adapter is not included in the required assembly of Model 1. Currently, there are two JTAG adapters known to be compatible with Rowley CrossWorks. First one is Parallel Port to ARM JTAG adapter from SparkFun. Another one is USB to ARM JTAG adapter from Rowley. Considering the prices and the time required for the shipment, both options are not good and making a new compatible JTAG adapter is the only option.

In order to make a new JTAG adapter, the JTAG pin layout and the connection between the ARM's standard 2 × 10 pin JTAG connector and DB25 Parallel Port is necessary. The layout of JTAG connector is easily obtained from the SparkFun official website, as shown in Fig 4. 14. The connection between JTAG and DB25 parallel port is found in the SparkFun forum. Following the information mentioned above, a new compatible JTAG adapter is made as shown in Fig 4. 15.

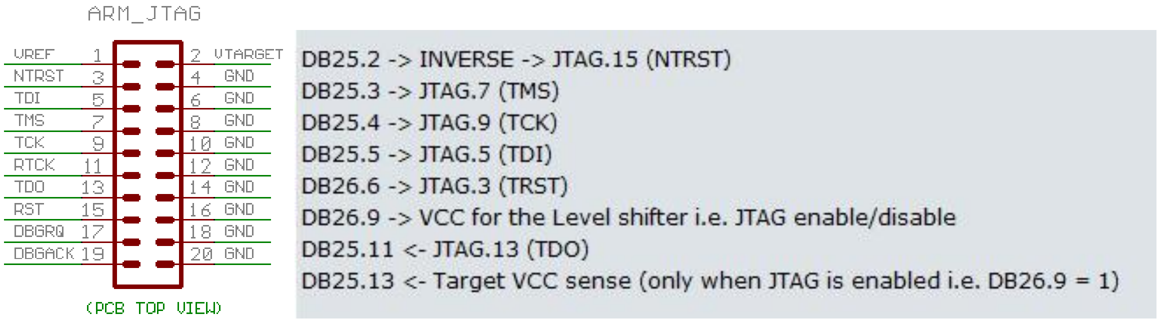

DB25.2 -> INVERSE -> JTAG.15 (NTRST)
DB25.3 -> JTAG.7 (TMS)
DB25.4 -> JTAG.9 (TCK)
DB25.5 -> JTAG.5 (TDI)
DB26.6 -> JTAG.3 (TRST)
DB26.9 -> VCC for the Level shifter i.e. JTAG enable/disable
DB25.11 <- JTAG.13 (TDO)
DB25.13 <- Target VCC sense (only when JTAG is enabled i.e. DB26.9 = 1)

Fig 4. 14 JTAG layout and its relationship with DB25

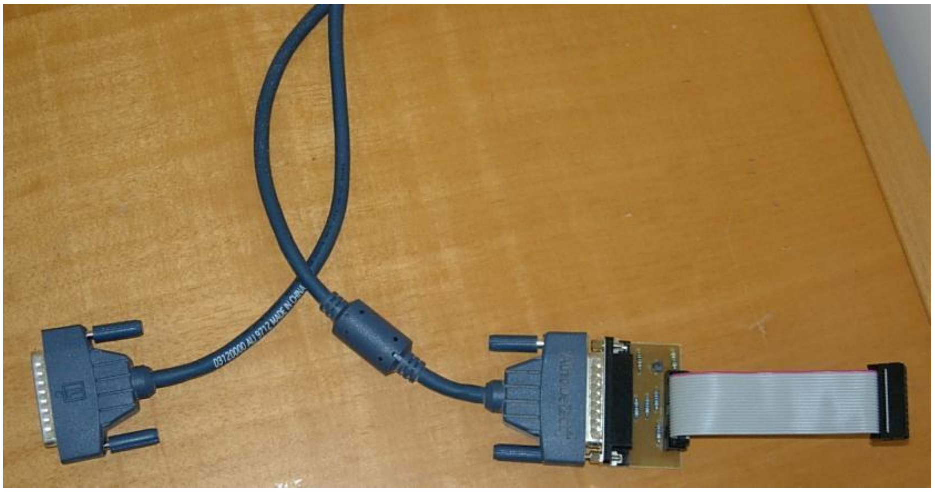

Fig 4. 15 A DIY JTAG adapter

Programming the microcontroller with firmware

In order to program the microcontroller, the Fab@Home firmware and other support software packages were downloaded, including the Rowley CrossWork for ARM and Chip Support Package for the LPC2000 Family. Programming the microcontroller with CrossWork involves connecting it to the computer via JTAG adapter, which has already been made in the earlier stages and the USB cable, included in the purchased Model 1 kit, simultaneously, as shown in Fig 4. 16. Then the CrossWorks is run on the computer and the Workaround Dummy Project and the Fab@Home firmware are opened up and run in CrossWorks. The Fab@Home firmware is finally downloaded onto the microcontroller. Then the microcontroller is ready for working and the JTAG adapter is removed.

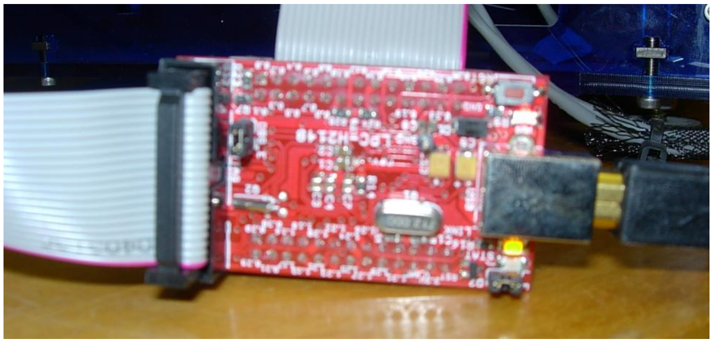

Fig 4. 16 Connection of JTAG adapter and USB

4.3.5 Software

The software, which is written in C++ with Microsoft Visual Studio using Open GL graphics rendering, is a Model 1 application providing users a graphical user interface (GUI) as shown in Fig 4. 17, providing simulated as well as synchronized motion of the graphics with the physical motion of the Model 1. It also provides an easy importing and manipulation of STL model files and text data files, and communicates to the Model 1 via a USB cable. Further manipulation of the CAD model files such as alterations in position on the working space or the scale of the output model are possible in the software environment. Material properties are assigned to the selected fabrication model form previously determined material property files. However, this software only runs under Microsoft Windows currently.

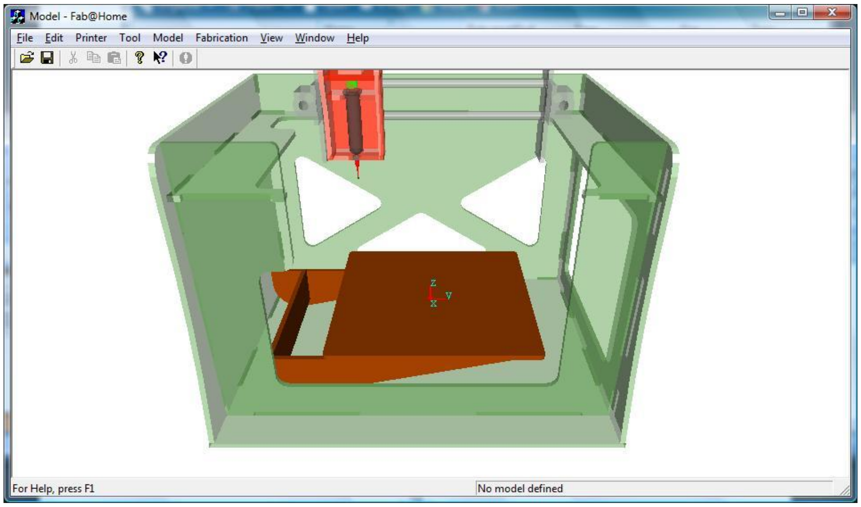

For Help, press F1

No model defined

Fig 4. 17 Model 1 Software

Model 1 Driver and Software Installation

In order to run the Model 1 by a computer, Model 1 Driver and Software installation is required. The driver and the software for Model 1 are downloaded from the Fab@Home website. After connecting the Model 1 and computer with USB cable, the Model 1 driver needs to be selected from the computer manually for the first time and would be connected to the computer automatically after that.

4.3.6 Commission the Model 1

The final commissioning of Model 1 includes several steps, which are mounting the belt, truing the XY carriage, adjusting motor current and leveling the Z-table. Mounting the belt ensures that two sides of the X axis are driven at the same speed so that the X and Y axes remain perpendicular to each other at all times. Truing the XY Carriage ensures the X-rails are parallel to each other, Y-rails are parallel to each other and the X-rails are perpendicular to the Y-rails. Adjusting motor current is to regulate the currents through the stepper motors, preventing them from overheated. From the manufacturer's website the relationship between the voltage at the test points is as shown in Fig 4. 18, and the motor current follows Eq. 4.1, as shown below:

$$Motor\ Current = \frac{Voltage}{1.44} \tag{4-1}$$

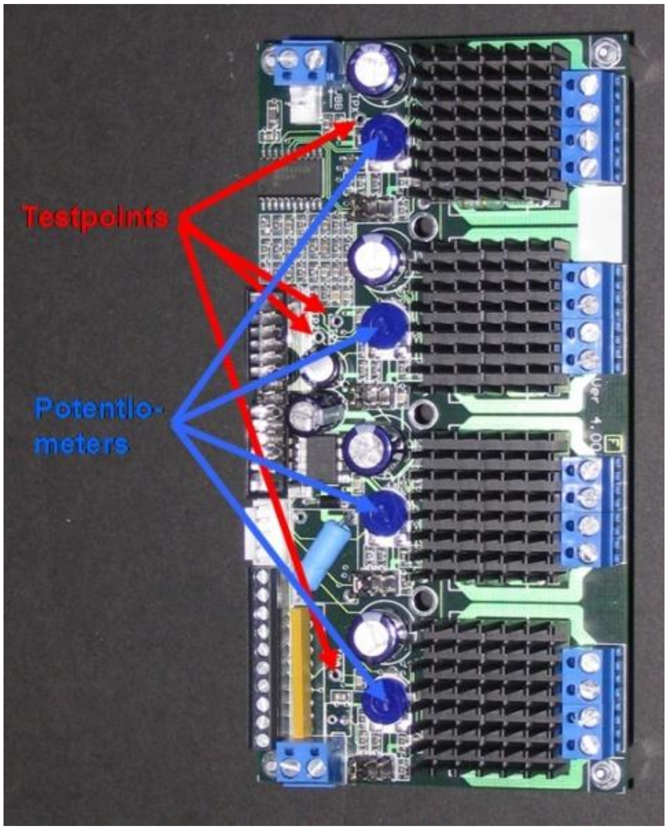

Fig 4. 18 Testing points on Xylotex XS-3525/8S-4 Stepper Motor Driver Board

Leveling the Z-table allows the table to be leveled relative to the plane of the XY-carriage. It is important to have the Z-table parallel to the XY plane so that the deposition tool maintains a constant distance from the table during the deposition processing.

4.4 Testing hardware for FDM

4.4.1 Material Testing

SILAFLEX RTV silicone

SILAFLEX RTV silicone [45], as shown in Fig 4. 19, is a 1-part, room-temperature vulcanizing (RTV) silicone household sealant/caulk/adhesive. It is available in several colours, including transparent, white, black, bronze, and beige. It is easily dispensed from a variety of taper tip diameters, tolerates high temperatures (~392F/200C), and is very chemically inert. It is tack free in 1-2 hours per mm of thickness, and fully cured in 24 hours. When cured, it forms a semi-soft rubber material. It can also be used to make molds for other materials, including epoxies.

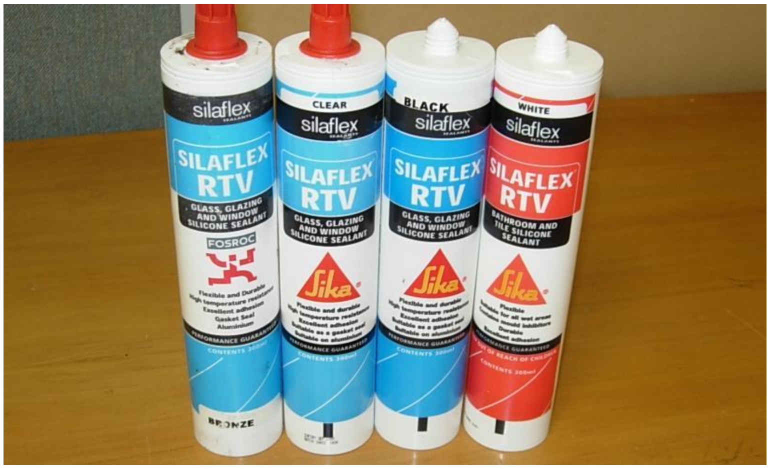

Fig 4. 19 SILAFLEX RTV silicone

FabEpoxy

FabEpoxy [46], as shown in Fig 4. 20, is a special 2 part epoxy formulated for Fab@Home by Kraftmark Company of Spring City, PA, USA. Is has been designed to be thixotropic (meaning that it will flow when it is extruded, but does not flow after extrusion, so layers stack up), and to have a relatively long "pot life" (meaning time between when it is mixed and when it starts to harden) of 2-3 hours in typical conditions. It has sufficient time to be used in a syringe full of the material, without having it hardened inside the syringe. At room temperature, the material takes 24 hours or so to become rigid; it can be accelerated by slightly raising the temperature during curing.

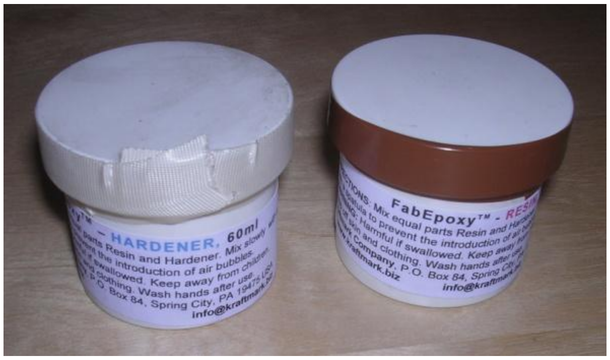

Fig 4. 20 FabEpoxy

As mentioned above, both SILAFLEX RTV silicone and Fabepoxy are the best material options for this research although they are not the best for the production of actual engineered parts. Considering the price and the model properties, the RTV silicone is the best for both support structures and the actual object, whereas, Fabepoxy can only be the object material.

4.4.2 Printing and Testing

The functioning of Model 1 needs to be tested before using it for CLFDM, in order to optimize all the aspects like the positioning system and the material deposition head during the deposition process. This printing test ensures whether the material is deposited on the work surface in accordance with the pre-programmed tool paths. This is crucial for fabricating the objects precisely as per the detailed instructions from the software. The information from the deposition software such as the current position and rate of deposition from the material deposition head need to be monitored during the printing test.

The Model 1 is connected to the computer via a USB cable before the printing. In the GUI of the Model 1 software, machine home position, safe position and origin position of Model 1 are needed to be set in the Jog Tool before the actual deposition process begins. And then the STL files are imported into the GUI, other parameters, including the parameters of deposition head, the geometry position of the STL files and the material, also are to be set. After all the preparations are done, the printing test is executed.

Some simple objects of different shapes, sizes and structures are printed to determine the capabilities of the fabricated FDM system with a 0.8mm diameter tip. Both SILAFLEX RTV silicone and FabEpoxy are used as test materials. The test objects contained straight edges, curved edges and gradients.

The first attempt is a square block in FabEpoxy, and its CAD model and dimensions are as shown in Fig 4. 21. The square block is printed to ensure the proper working parameters of the FabEpoxy for its future curved layer printing. Although the accuracy is not very critical in this research, it would be a potential requirement in the future improvements. The straight edges of the square block also ensure the capability of Model 1 in printing the straight lines and right corners.

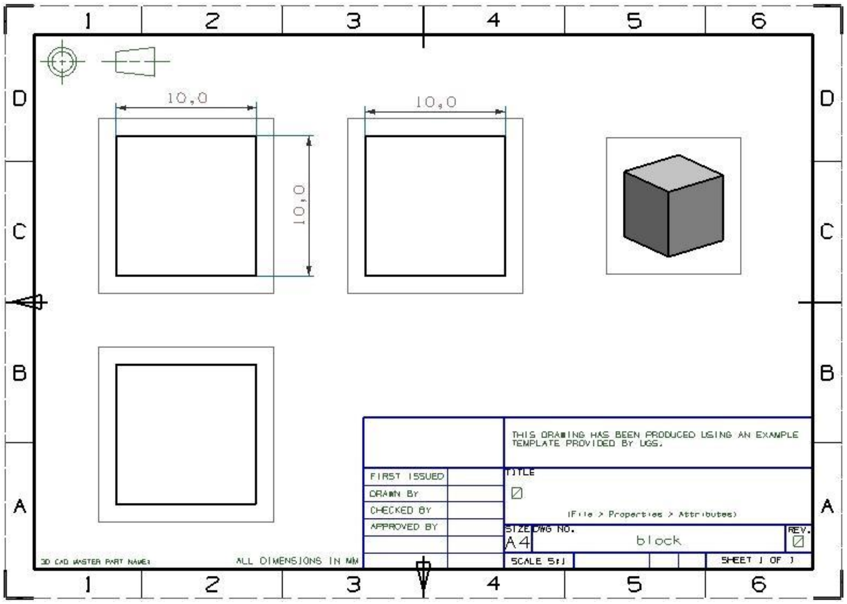

Fig 4. 21 Dimensions square block model

The sample model of square block produced is shown in Fig 4. 22. It is 10 mm both in length and width, and 12 mm in height, which approximately matched with the dimensions of the CAD model.

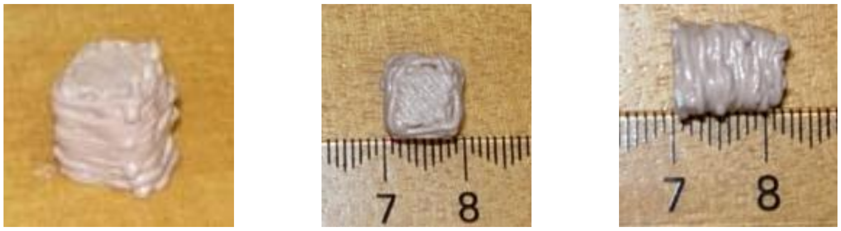

Fig 4. 22 The sample model of square block

The second attempt is a half cylinder in bronze and clear SILAFLEX RTV silicone respectively, and its CAD model dimensions are as shown in Fig 4. 23. The curved edges of the half cylinder ensure the capability of Model 1 in printing such shapes and the resulting stair-stepping effects can be studied.

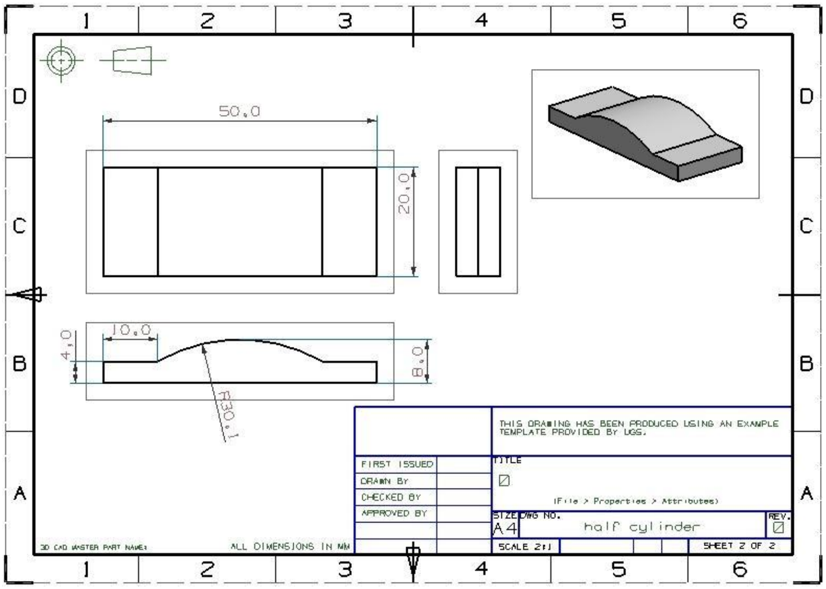

Fig 4. 23 Dimensions half cylinder model

The printed sample model of half cylinder is shown in Fig 4. 24. It is 25 mm in length, 10 mm in width, and 5 mm in height, which approximately matched with the dimensions of the CAD model.

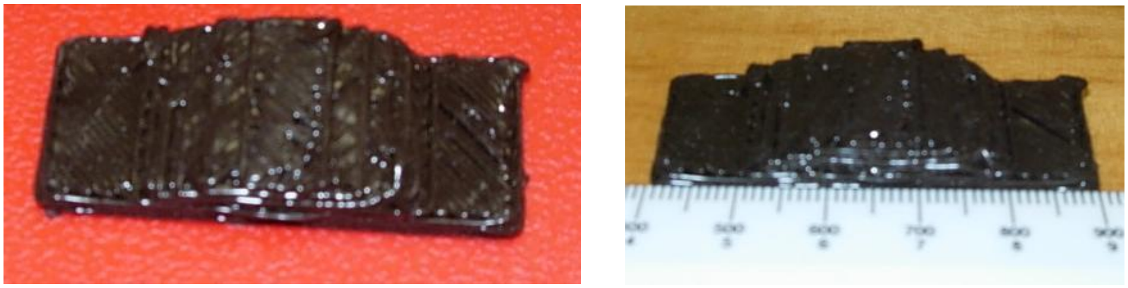

Fig 4. 24 The sample model of half cylinder

The third attempt is printing a simple boat model in bronze and clear SILAFLEX RTV silicone together, as per the dimensions of the CAD model shown in Fig 4. 25. The curved edges of the half cylinder should ensure the capability of Model 1 in printing curved lines and multiple layers.

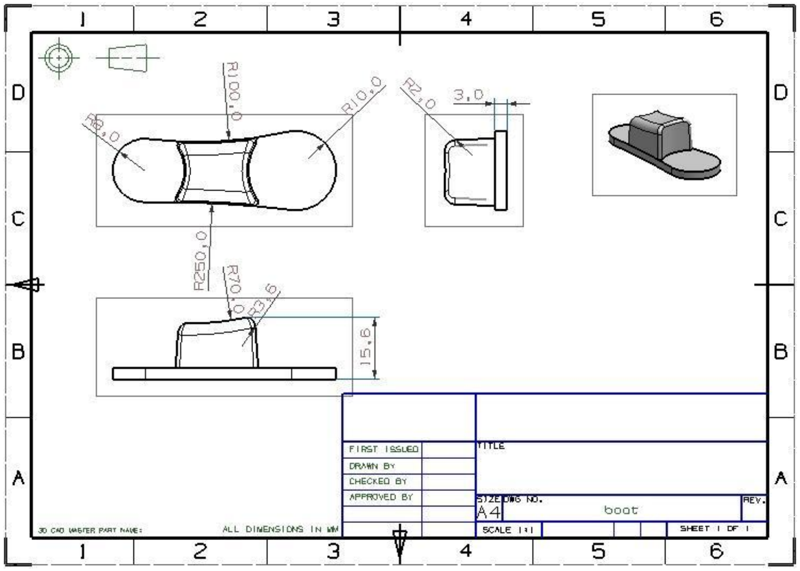

Fig 4. 25 Dimensions boat model

The sample model boat printed is as shown in Fig 4. 26. It is 55 mm in length, 19 mm in width, and 15 mm in height, which relatively matched with the dimensions of the CAD model.

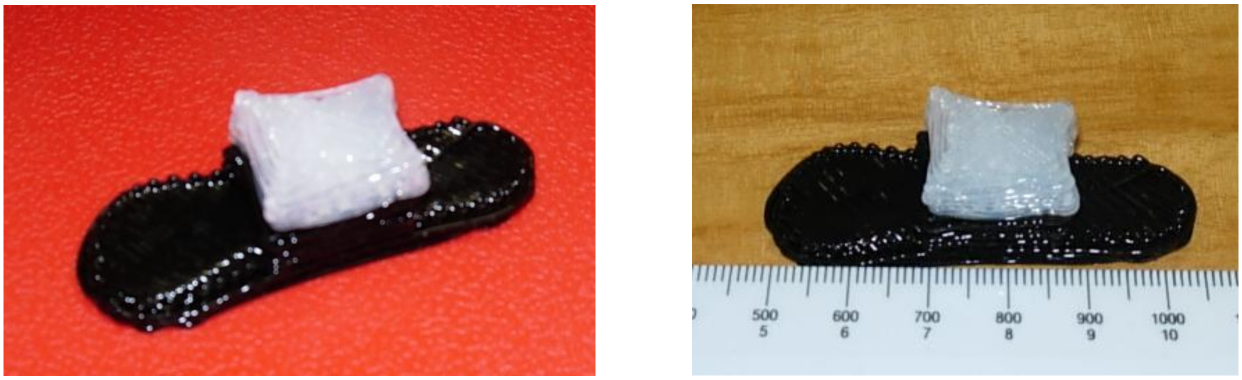

Fig 4. 26 The sample model of boat

From the results of these simple tests, it is clear that the FDM system assembled works and the accuracy of printing is sufficient for the purpose of testing the CLFDM algorithms developed in this research. All the issues of the hardware are resolved and the system is ready for use in CLFDM. The next chapter details how the FDM system is used to physically implement the CLFDM algorithms discussed earlier.

Chapter 5

Integration of hardware and software solutions for CLFDM

5.1 Creating CLFDM Objects

In the printing test of Model 1, some objects were printed in the traditional flat layer FDM. It was also proved the Model 1 has the capability of printing the objects with CLFDM method. In the Chapter 3, some objects, which have the curved features, were initially created for the actual CLFDM test with Model 1. Different shapes and structures of different sizes were created in different ways to prove the flexibility of CLFDM concept and the better quality of finish surfaces.

5.1.1 Case I Simple curved object

The simple curved object mentioned in Chapter 3 was first put into Model 1 for the actual fabrication. It has simple curved feature in middle and flat features at both ends and it dimensions are as shown Fig 5. 1, which is very useful shape ensuring the Model 1 capability of using CLFDM method in the actual case. This simple curved object test could prove the capability of Model 1 to accept other file formats other than STL file format. Also, this object helps to calibrate the pre-set working parameters of the syringe tool fitting the CLFDM method or not.

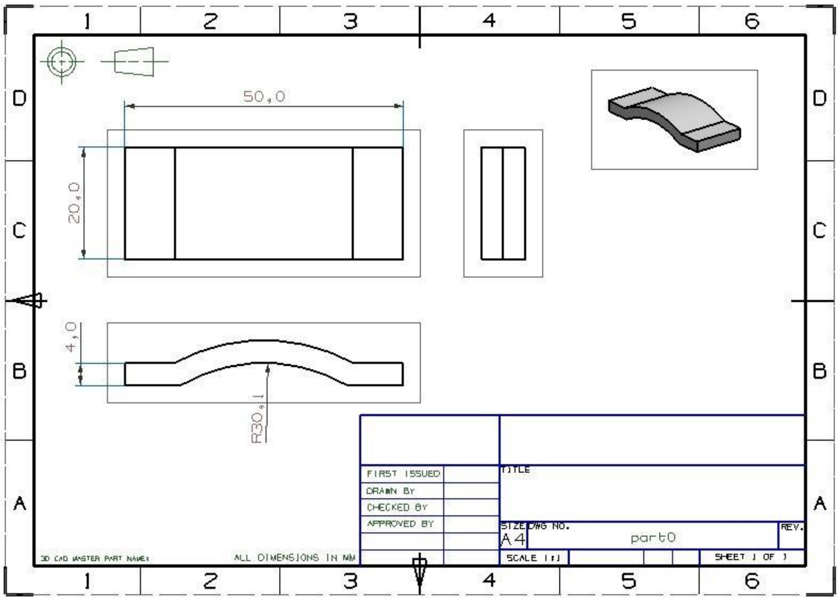

Fig 5. 1 Simple curved object

Owing to this object has an overhang arc feature, the support structure needed to be created before it is put into the fabrication. The support structure would be created with the flat layers because the quality of the finish surface is not necessary to be as high as the object, in other word the bigger stair-stepping effect would be acceptable in this research. The flat layers also could reduce the time spending on the slicing processing. The tool path of support structure was created by support structure program in MATLAB, which was initially written and then it was outputted in form of text file, as shown in Fig 5. 2.

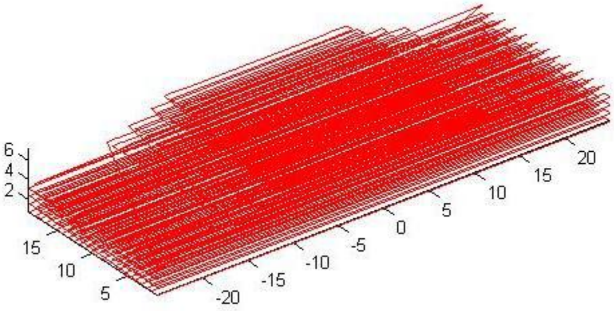

Fig 5. 2 Case I support structure

The surface data was gathered via the G and M code generation module in the CAD software and saved in the form of text file; the text file was transferred into the slicing program in MALTAB. Running the slicing program, this object was sliced into five layers. The pattern of the tool path was created simultaneously, as shown in Fig 5. 3, and then the output text file was generated. Once the output text file was loaded into the software of Model 1, the pattern of the tool path was displayed on the GUI.

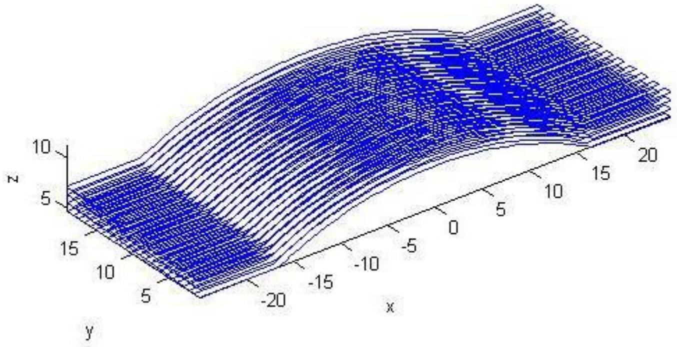

Fig 5. 3 Case I object part

Owing to the output text files were just containing the data of the tool paths but not the entire object part and the support structure, only the tool path pattern could be displayed in the GUI of Model 1, as shown in Fig 5. 4. When the data was transferred into Model 1, the deposition head followed the coordinates from the data and printed the object and the support structure. The simulation run were tried before the material put in the syringe barrel to check whether crashes happen on the deposition processing.

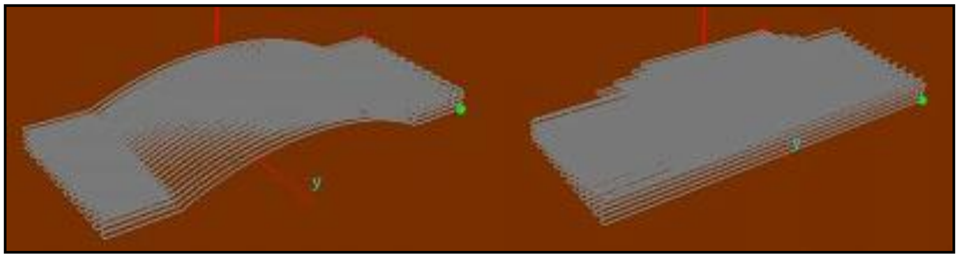

Fig 5. 4 Tool path of Case I object part and its support structure

A simulation was run on the Model 1 for checking the potential crashes might happen on the deposition processing. Then the object material was loaded into the syringe barrel and the actual deposition processing was run. A simple result model of simple curved object with the support structure was created after the deposition processing, as shown in Fig 5. 5. The surface of the result model totally matched the shape of the CAD model. It proved the CLFDM is an achievable processing with the three axis FDM machine.

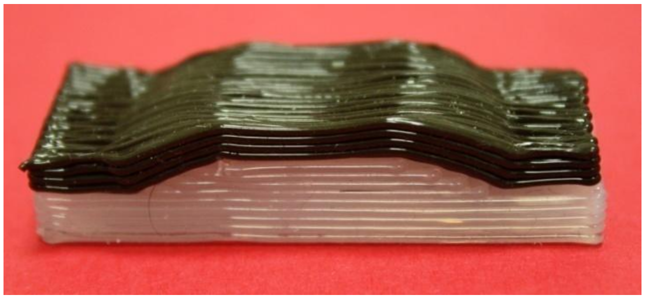

Fig 5. 5 Simple curved object and its support structure

5.1.2 Case II Tapered curved object

The tapered curved object mentioned in Chapter 3 was the second model put into Model 1 for the actual fabrication. As mentioned in Chapter 3, this model has simple curved feature in middle and flat features at both ends with tapering at both side along the length and its dimensions are as shown in Fig 5. 6, which is another useful shape ensuring the Model 1 capability of using CLFDM method in the actual case. This tapered curved object test could prove the capability of Model 1 to build the filament in a special curve pattern.

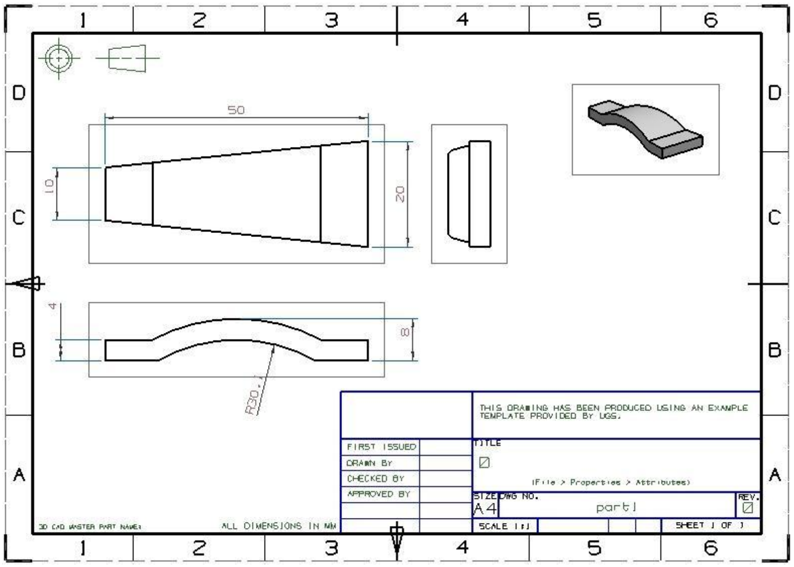

Fig 5. 6 Tapered curved object with the support structure

Similarly, the tapered curved object also has an overhang arc feature, hence, the support structure needed to be created before it is put into the fabrication. The tool path of support structure was created by support structure program in MATLAB and then it was outputted in form of text file, as shown in Fig 5. 7.

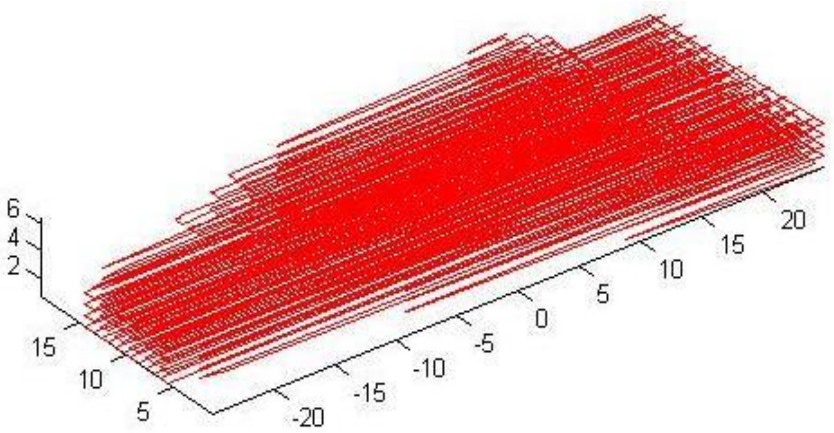

Fig 5. 7 Case II support structure

The surface data was gathered via the G and M code generation module in the CAD software and saved in the form of text file; the text file was transferred into the slicing program in MALTAB. Running the slicing program, this object was sliced into five layers. The pattern of the tool path was created simultaneously, as shown in Fig 5. 8, and then the output text file was generated.

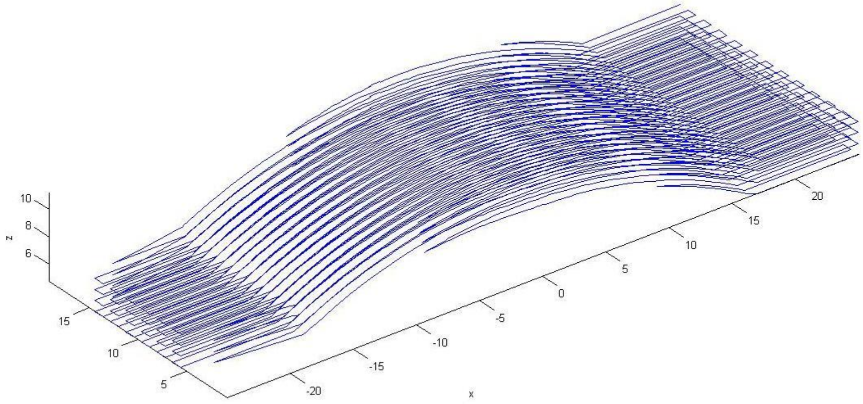

Fig 5. 8 Case II object part

Once the output text file was loaded into the software of Model 1, the pattern of the tool path was displayed on the GUI, as shown in Fig 5. 9.

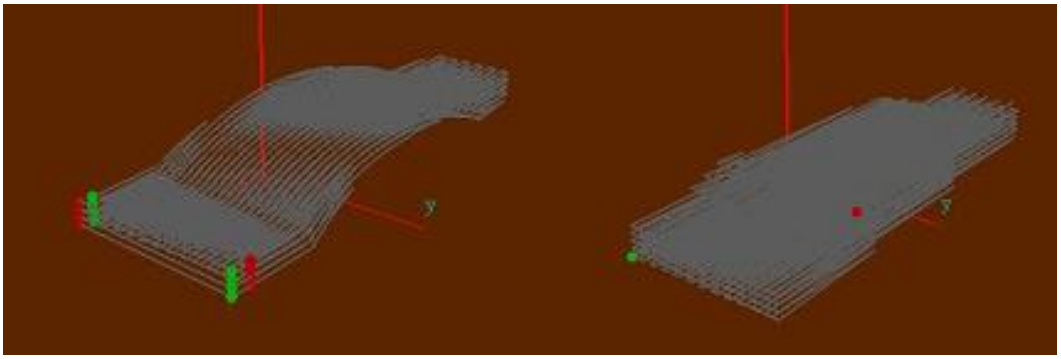

Fig 5. 9 Tool path of Case II object part and its support structure

A simulation was run on the Model 1 for checking the potential crashes might happen on the deposition processing. Then the object material was loaded into the syringe barrel and the actual deposition processing was run. A simple result model of tapered curved object with the support structure was created after the deposition processing, as shown in Fig 5. 10. It proved Model 1 can build the filament in a special curve pattern.

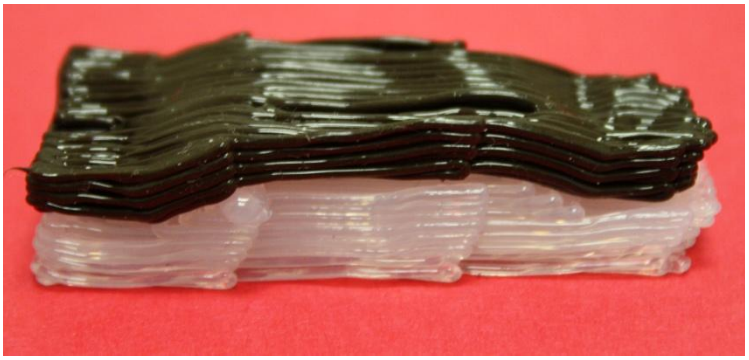

Fig 5. 10 Tapered curved object and its support structure

5.1.3 Case III Simple curved object with a hole

The Simple curved object with a hole mentioned in Chapter 3 was the third model put into Model 1 for the actual fabrication. As mentioned in Chapter 3, this model has simple curved feature in middle and flat features at both ends with an additional hole at the top. Its dimensions are as shown in Fig 5. 11, which is another useful shape ensuring the Model 1 capability of using CLFDM method in the actual case. This tapered curved object test could prove the capability of Model 1 to build the model with the internal edge loops.

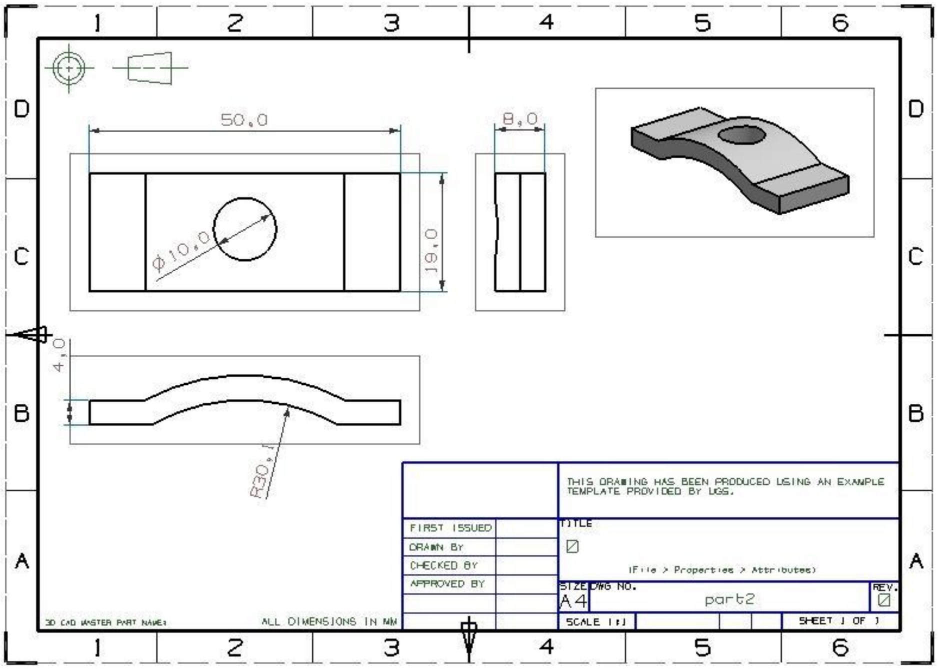

Fig 5. 11 Simple curved object with a hole

Similarly, this curved object also has an overhang arc feature, hence, the support structure needed to be created before it is put into the fabrication. The tool path of support structure was created by support structure program in MATLAB and then it was outputted in form of text file, as shown in Fig 5. 12.

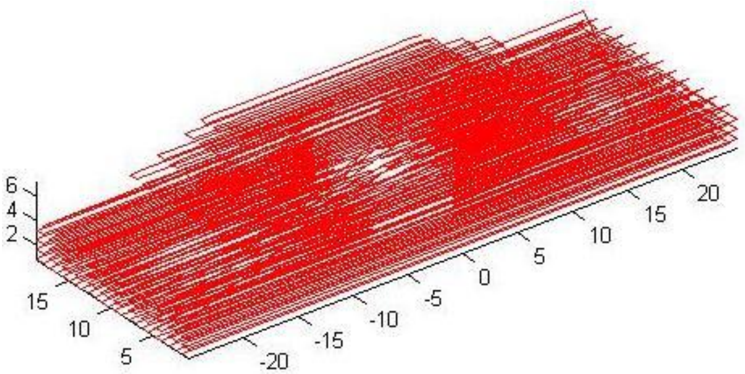

Fig 5. 12 Case III support structure

The surface data was gathered via the G and M code generation module in the CAD software and saved in the form of text file; the text file was transferred into the slicing program in MALTAB. Running the slicing program, this object was sliced into five layers. The pattern of the tool path was created simultaneously, as shown in Fig 5. 13, and then the output text file was generated.

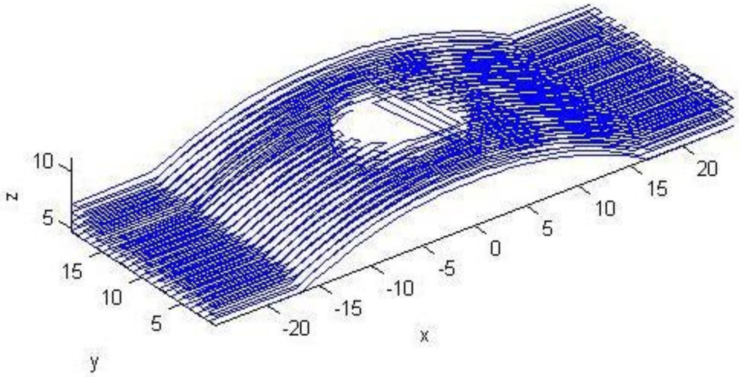

Fig 5. 13 Case III object part

Once the output text file was loaded into the software of Model 1, the pattern of the tool path was displayed on the GUI, as shown in Fig 5. 14.

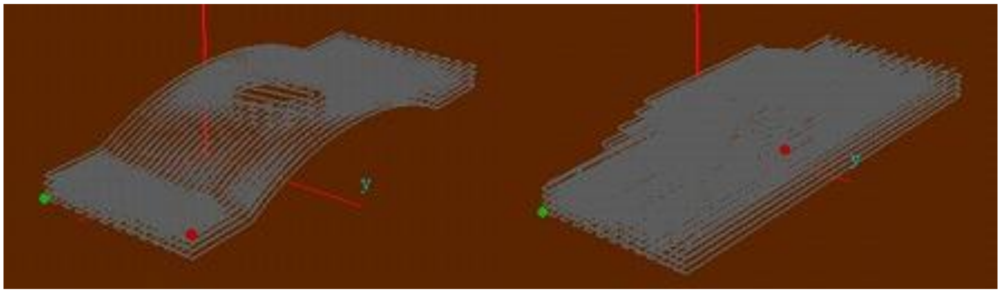

Fig 5. 14 Tool path of Case III object part and its support structure

A simulation was run on the Model 1 for checking the potential crashes might happen on the deposition processing. Then the object material was loaded into the syringe barrel and the actual deposition processing was run. A simple result model of tapered curved object with the support structure was created after the deposition processing, as shown in Fig 5. 15. It proved Model 1 can build the model with the internal edge loops.

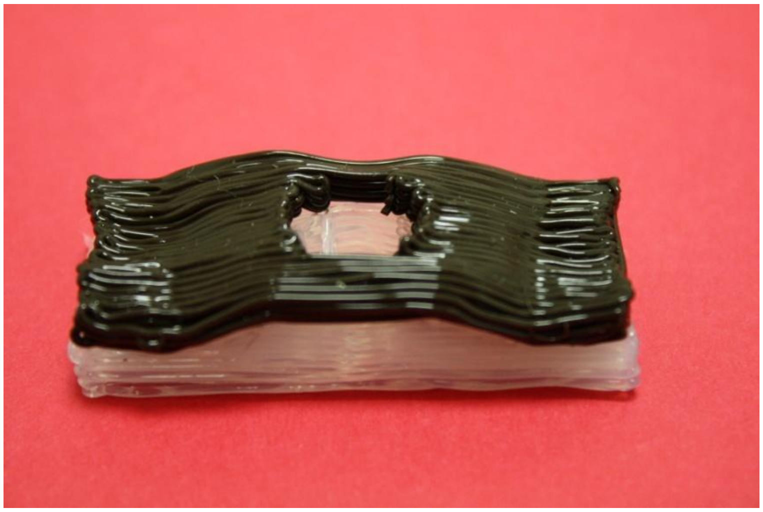

Fig 5. 15 Simple curved object with a hole and its the support structure

5.1.4 Case IV Free form surface

The Free form surface mentioned in Chapter 3 was the fourth model put into Model 1 for the actual fabrication. As mentioned in Chapter 3, this model is based on a free form surface, which created from a set of key point data, as shown in Fig 5. 16. The x, y and z coordinates of control points are as shown in three matrixes below:

$$B_x = \begin{bmatrix} -15 & -15 & -15 & -15 & -15 \\ -5 & -5 & -5 & -5 & -5 \\ 0 & 0 & 0 & 0 & 0 \\ 5 & 5 & 5 & 5 & 5 \\ 15 & 15 & 15 & 15 & 15 \end{bmatrix}$$

$$B_y = \begin{bmatrix} 15 & 5 & 0 & -5 & -15 \\ 15 & 5 & 0 & -5 & -15 \\ 15 & 5 & 0 & -5 & -15 \\ 15 & 5 & 0 & -5 & -15 \\ 15 & 5 & 0 & -5 & -15 \end{bmatrix}$$

$$B_y = \begin{bmatrix} 1 & 3 & 9 & 3 & 2 \\ 2 & 3 & 15 & 9 & 5 \\ 4 & 3 & 5 & 6 & 8 \\ 8 & 3 & 15 & 5 & 5 \\ 1 & 3 & 8 & 7 & 0 \end{bmatrix}$$

Its dimensions depend on the key point data set. This free form surface object test could prove the capability of Model 1 to build the general models with different dimensions.

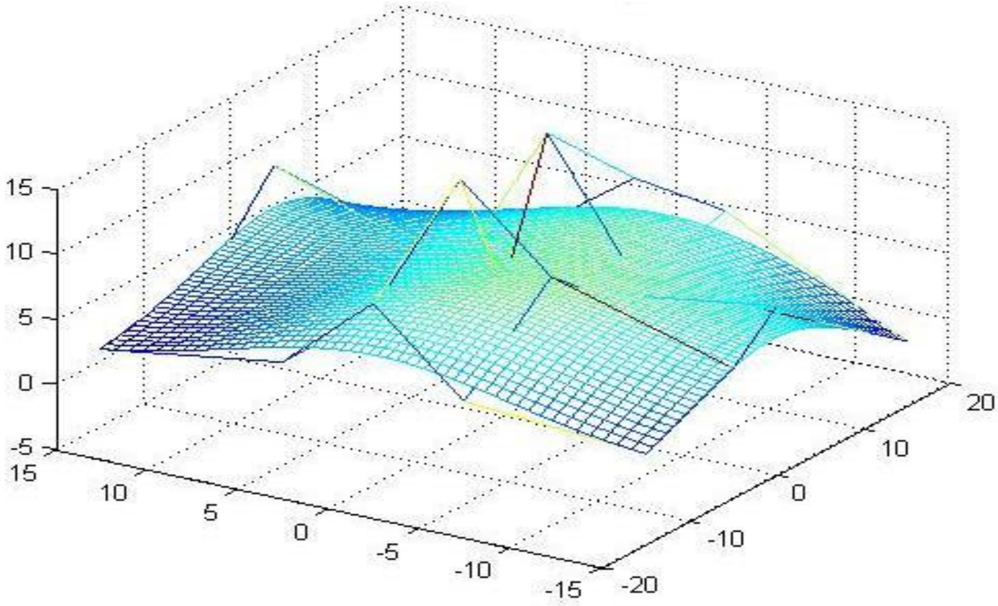

Fig 5. 16 Free form surface model

Support structure needed to be created before it is put into the fabrication owing to the overhanging. The tool path of support structure was created by support structure program in MATLAB and then it was outputted in form of text file, as shown in Fig 5. 17.

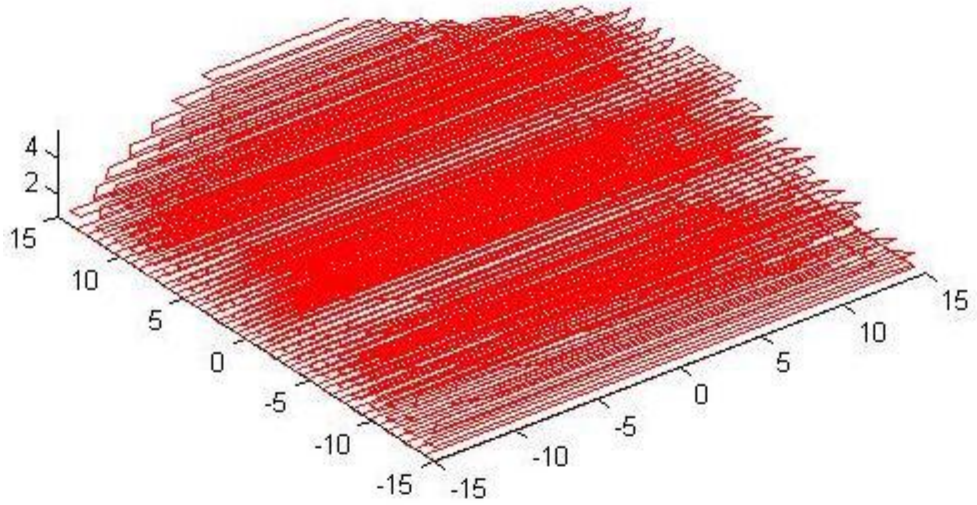

Fig 5. 17 Case IV support structure

The surface data was gathered via data gathering program in MATLAB and saved in the form of text file; the text file was transferred into the slicing program in MALTAB. Running the slicing program, this object was sliced into five layers. The pattern of the tool path was created simultaneously, as shown in Fig 5. 18, and then the output text file was generated.

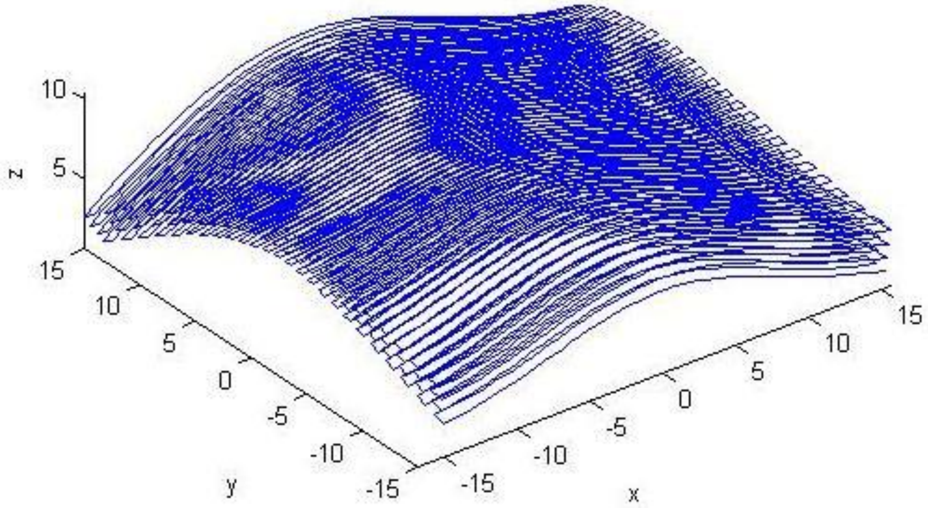

Fig 5. 18 Case IV object part

Once the output text file was loaded into the software of Model 1, the pattern of the tool path was displayed on the GUI, as shown in Fig 5. 19.

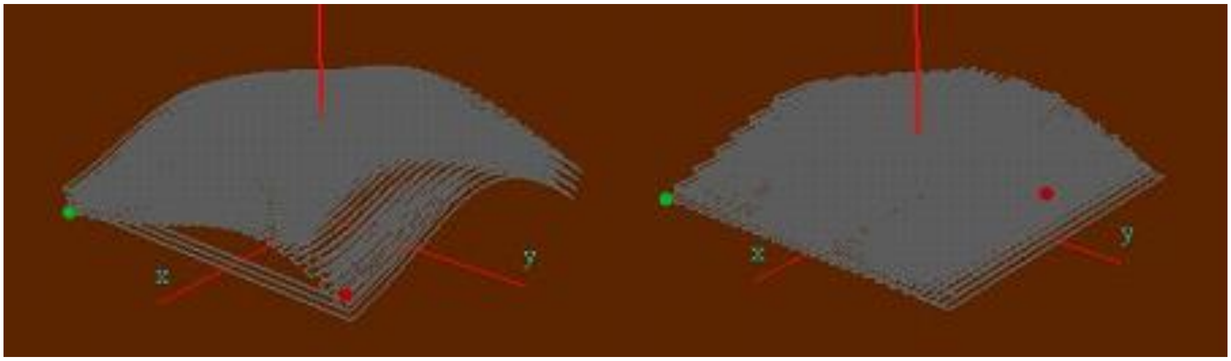

Fig 5. 19 Tool path of Case IV object part and its support structure

A simulation was run on the Model 1 for checking the potential crashes might happen on the deposition processing. Then the object material was loaded into the syringe barrel and the actual deposition processing was run. A simple result model of tapered curved object with the support structure was created after the deposition processing, as shown in Fig 5. 20. It proved Model 1 can build the general models with different dimensions.

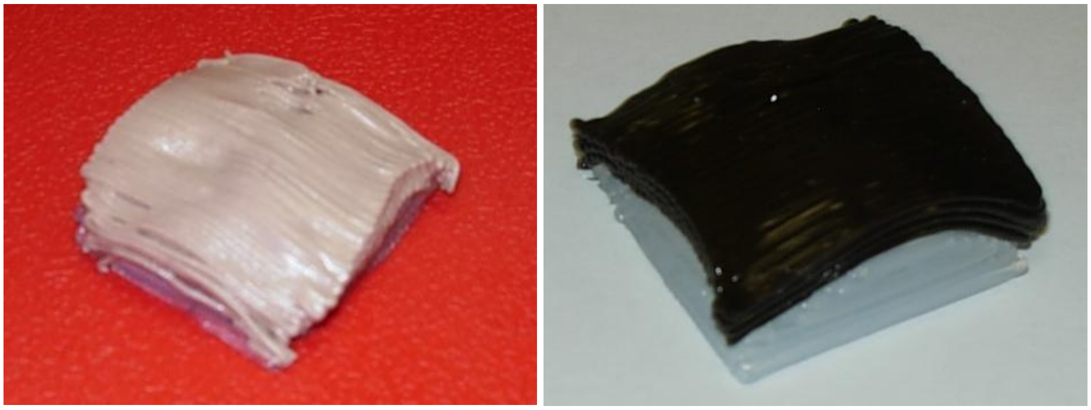

Fig 5. 20 Free form surface model and its the support structure

Chapter 6

Conclusion

The main objectives of the project, including the development of curved layered slicing algorithms, building a suitable FDM platform and practical implementation of CLFDM have been successfully achieved. Several case studies involving geometrical complications of increasing complexities have been successfully modelled and physically produced. The mathematical algorithms were effective in resolving most practical difficulties. The software and hardware integration was also quite effective. Overall, the project objectives are met and a robust CLFDM system is developed, and the concept of CLFDM is proved to be practical and useful for processing thin shell type parts using FDM. The following are the main conclusions that could be drawn form the mathematical and experimental evaluations conducted as part of this research:

- The Fab@home Model 1 is assessed as the best solution for constructing the FDM platform for experimental investigations in CLFDM
- Mathematical models are constructed for CLFDM using surface data generated through either G and M code data generated by a solid modelling package or by mathematically modelling freeform surfaces
- Vertical Surface Offsetting (VSO) method is simple, but leads to degeneration and consequent distortion in the shape of the model.
- Two Vector Cross Product (TVCP) results in uniform thickness and better mechanical properties, but it involves more number of calculations and cannot solve the sudden changes in curvature.
- Four Vector Cross Product (FVCP) method allows curved layers to be built closely confined to the shape of the original surface, but it involves

more computational time, and is too sensitive and dependent on the orientation of neighbouring surface points.

- Modified Four Vectors Cross Product (MFVCP) method, while retaining the ability to reflect the surface variations, reduces the sensitivity and computational time. This is found to be the best solution for the curved layered slicing and is employed as the key model for CLFDM in this research.
- the hardware and software solutions are perfectly integrated into a successful CLFDM system
- The MFVCP algorithm is successfully tested considering curved layered slicing of objects of varying geometrical complexities
- Physical parts of sliced objects are successfully constructed using CLFDM

References

[1] K. G. Cooper, "What Is Rapid Prototyping," in *Rapid prototyping technology selection and application* New York: Marcel Dekker, 2001, p. 1.

[2] C. W. Hull, "Apparatus For Production of Three Dimensional Objects by Stereolithography," 1986.

[3] D. T. Pham and S. S. Dimov, in *Rapid Manufacturing: The Technologies and Applications of Rapid Prototyping and Rapid Tooling*, 2001, p. 6.

[4] K. G. Cooper, "Selective Laser Sintering," in *Rapid prototyping technology selection and application* New York: Marcel Dekker, 2001.

[5] K. G. Cooper, "Stereolithography," in *Rapid prototyping technology selection and application* New York: Marcel Dekker, 2001, pp. 110-116.

[6] K. G. Cooper, "Fused Deposition Modeling," in *Rapid prototyping technology selection and application* New York: Marcel Dekker, 2001, pp. 68-87.

[7] K. G. Cooper, "Laminated Oject Manufacturing," in *Rapid prototyping technology selection and application* New York: Marcel Dekker, 2001, p. 9.

[8] K. G. Cooper, "Laser Engineered Net Shaping," in *Rapid prototyping technology selection and application* New York: Marcel Dekker, 2001.

[9] S. S. Crump, "Apparatus and method for creating three-dimensional objects," 1989.

[10] STRATASYS, "FORTUS 900mc."

[11] S. O. Onuh and K. K. B. Hon, "Optimising build parameters for improved surface finish in stereolithography," *International Journal of Machine Tools and Manufacture,* vol. 38, pp. 329-342, 1998.

[12] E. Sabourin, S. A. Houser, and J. H. Bohn, "Adaptive slicing using stepwise uniform refinement," *rapid Prototyping Journal,* vol. 2, pp. 20-26, 1996.

[13] C. S. Lee, S. G. Kim, H. J. Kim, and S. H. Ahn, "Measurement of anisotropic compressive strength of rapid prototyping parts," *Journal of Material Processing Technology,* vol. 187-188, pp. 627-630, 2007.

[14] R. Anitha, S. Arunachalam, and P. Radhakrishnan, "Critical parameters influencing the quality of prototypes in fused deposition modelling," *Journal of Material Processing Technology,* vol. 118, pp. 385-388, 2001.

[15] S. H. Choi and S. Samavedam, "Modelling and optimisation of Rapid Prototyping," *Computer in Industry,* vol. 47, pp. 39-53, 2002.

[16] M. Allahverdi, S. C. Danforth, M. Jafari, and A. Safari, "Processing of advanced electroceramic components by fused deposition technique," *Journal of the European Ceramic Society,* vol. 21, pp. 1485-1490, 2001.

[17] J. Mazumder, J. Choi, K. Nagarathnam, J. Koch, and D. Hetzner, "The direct metal deposition of H13 tool steel for 3-D components," *JOM Journal of the Minerals, Metals and Materials Society,* vol. 49, 1997.

[18] S. Khalil, J. Nam, and W. Sun, "Multi-nozzle deposition for construction of 3D biopolymer tissue scaffolds," *rapid Prototyping Journal,* vol. 11, pp. 9-17.

[19] F Xu, H. T. Loh, and Y. S. Wong, "Considerations and selection of optimal orientation for different rapid prototyping system," *rapid Prototyping Journal,* vol. 5, pp. 54-60, 1999.

[20] Z. Hu, K. Lee, and J. Hur, "Determination of optimal build orientation for hybrid rapid-prototyping," *Journal of Material Processing Technology,* vol. 130-131, pp. 378-383, 2002.

[21] M. K. Agarwala, V. R. Jamalabad, N. A. Langrana, A. Safari, P. J. Whalen, and S. C. Danforth, "Structural quality of parts processed by fused deposition," *rapid Prototyping Journal,* vol. 2, pp. 4-19, 1996.

[22] R. Jamieson and H. Hacker, "Direct Slicing of CAD Models for Rapid Prototyping," *Rapid Prototyping Journal,* vol. 1, 1995.

[23] P. Kulkarni and D. Dutta, "An accurate slicing procedure for layered manufacturing," *Computer Aided Design,* vol. 28, pp. 683-697, 1996.

[24] R. L. Hope, R. N. Roth, and P. A. Jacobs, "Adaptive slicing with sloping layer surfaces," *Rapid Prototyping Journal,* vol. 3, pp. 89-98, 1997.

[25] Y. Yang, J. Y. H. Fuh, H. T. Loh, and Y. G. Wang, "Equidistanct path generation for improving scanning effciency in layered manufacturing," *rapid Prototyping Journal,* vol. 8, pp. 30-37, 2002.

[26] R. C. Luo, P.-T. Yu, Y.-F. Lin, and H.-T. Leong, "Efficient 3D CAD Model Slicing for Rapid Prototyping Manufacturing System," *IEEE,* 1999.

[27] K. G. Cooper, "Fused Deposition Modeling," in *Rapid prototyping technology selection and application* New York: Marcel Dekker, 2001, pp. 68-88.

[28] M. K. Agarwal, R. V. Weeren, A. Bandyopadhyay, P. J. Whalen, A. Safari, and S. C. Danforth, "Fused deposition of ceramics and metals: An overview," in *Solid Freeform Fabrication Symposium*, The University of Texas, Austin, 1996, pp. 385-92.

[29] D. A. Klosterman, R. P. Chartoff, N. R. Osborne, G. A. Graves, A. Lightman, G. Han, A. Bezeredi, and S. Rodrigues, "Development of a curved layer LOM process for monolithic ceramics and ceramic matrix composites," *Rapid Prototyping Journal,* vol. 5, pp. 61-71, 1999.

[30] D. Chakraborty, B. A. Reddy, and R. Choudhury, "Extruder path generation for Curved Layer Fused Deposition Modeling," *Computer Aided Design,* vol. 40, pp. 235-243, 2008.

[31] F. W. LIOU, "Rapid Prototyping Processes," in *RAPID PROTOTYPING AND ENGINEERING APPLICATIONS: A Toolbox for Prototype Development*: CRC Press, 2007.

[32] G. Farin, "A History of Curves and Surfaces in CAGD," in *HANDBOOF OF COMPUTER AIDED GEOMETRIC DESIGN*, G. Farin, J. Hoschek, and M. S. Kim, Eds.

[33] P. N. RAO, "Geometric Modelling," in *CAD/CAM Principles and Applications* New Delhi: Tata McGraw-Hill Publishing Company Limited, 2002.

[34] D. F. Rogers and J. A. Adams, "Space Curves," in *Mathematical Elements for Computer Graphics*, 2nd ed New York: McGraw-Hill Publishing Company, 1990.

[35] C. K. Chua, K. F. Leong, and C. S. Lim, "Rapid Prototyping Data Formats," in *Rapid prototyping: Principle and Application*: World Scientific, 2003, pp. 237-294.

[36] "STL file format," Gesellschaft fur Optische MeBtechnik.

[37] R.-S. Lin, "Adaptive slicing for rapid prototyping," in *Software Solutions for Rapid Prototyping*, I. Gibson, Ed. London: Professional Engineering Publishing, 2002.

[38] B. Asiabanpour and B. Khoshnevis, "A new memory efficient tool path generation method for applying very large STL files in vector-by-vector rapid prototyping processes," in *the 31st International Conference on Computers and Industrial Engineering*, San Franciaco, California, US, 2005.

[39] D. Harlev, "stlread." vol. 07 Jan 2005, 04 Jan 2005 pp. This function reads a binary SPL file into X, Y, Z, C matrixes compatible with the MATLAB patch function.

[40] P. Hood-Daniel, "http://buildyourcnc.com/."

[41] CNC-Technik, "http://www.cnc-router-routers.com/."

[42] STRATASYS, "http://www.stratasys.com/."

[43] RepRap, "http://reprap.org/bin/view/Main/WebHome."

[44] Fab@Home, "http://www.fabathome.org/wiki/index.php?title=Main_Page."

[45] SILAFLEX, "http://www.everitts.co.nz/specsheets/silaflex-rtv.html."

[46] FabEpoxy, "http://www.kraftmark.biz/pdfs/Fabepoxy/FabEpoxy.infosheet.pdf."

List of Publications

[1] S. Singamneni, O. Diegel, B. Huang, I. Gibson, R. Chowdhury, Curved Layer Fused Deposition Modeling, Rapid Product Development Association of South Africa (RAPDASA) 2008, 9th Annual International Conference on Rapid Product Development, Bloemfontein, South Africa, 13-15 November 2008

[2] B. Huang, S. Singamneni, O. Diegel, Construction of a Curved Layer Rapid Prototyping System: Integrating Mechanical, Electronic and Software Engineering, 15th International Conference on Mechatronics and Machine Vision in Practice, 2008, Auckland, New Zealand, December 2-4, 2008.

[3] Curve Layer Fused Deposition Modeling presently being communicated to the Journal of Rapid Prototyping